

Linköping Studies in Science and Technology
Thesis No. 1488

Vehicle Level Diagnosis for Hybrid Powertrains

Christofer Sundström



Linköpings universitet
INSTITUTE OF TECHNOLOGY

Department of Electrical Engineering
Linköpings universitet, SE-581 83 Linköping, Sweden

Linköping 2011

Vehicle Level Diagnosis for Hybrid Powertrains

© 2011 Christofer Sundström

csu@isy.liu.se
<http://www.vehicular.isy.liu.se>
Department of Electrical Engineering,
Linköpings universitet,
SE-581 83 Linköping,
Sweden.

ISBN 978-91-7393-159-5

ISSN 0280-7971

LIU-TEK-LIC-2011:27

Printed by LiU-Tryck, Linköping, Sweden 2011

Abstract

There are possibilities to reduce the fuel consumption in trucks using hybrid technology. New components are added when hybridizing a vehicle, and these need to be monitored due to safety and legislative demands. Diagnosis aspects due to hybridization of the powertrain are investigated using a model of a long haulage truck. Such aspects are for example that there are more mode switches in the hybrid powertrain compared to a conventional vehicle, and there is a freedom in choosing operating points of the components in the powertrain via the energy management and still fulfill the torque request of the driver.

To investigate the influence of energy management and sensor configuration on the performance of the diagnosis system, three diagnosis systems on vehicle level are designed and implemented. The systems are based on different sensor configurations; one with a fairly typical sensor configuration, one with the same number of sensors but in model sense placed more closely to the components to be monitored, and one with the minimal number of sensors to ideally achieve full fault isolability. It is found that there is a connection between the design of the energy management and the diagnosis systems, and that this connection is of special relevance when the model used in the diagnosis is valid only for some operating modes of the powertrain.

In consistency based diagnosis it is investigated if there exists a solution to a set of equations with analytical redundancy, where the redundancy is obtained using measurements. The selection of sets of equations to be included in the diagnosis and how and in what order the unknown variables are to be computed affect the diagnosis performance. A simplified vehicle model is used to exemplify how an algebraic loop can be avoided for one computational sequence of the unknowns, but can not be avoided for a different computational sequence given the same overdetermined set of model equations. A vehicle level diagnosis system is designed using a systematic method to obtain unique residuals and that no signal is differentiated. The performance of the designed system is evaluated in a simulation study, and compared to a diagnosis system based on the same sets of equations, but where the residual generators are selected ad hoc. The results of the comparison are positive, which reinforces the idea of considering the properties of the residual generators in a systematic way.

A diagnosis system using a map based model of the electric machine is designed. The benefits of using map based models are that it is easy to construct the models if measurements are available, and that such models in general are accurate. As a consequence of the structure of the model, full fault isolability is not possible to achieve using only the model for fault free behavior of the machine. To achieve full fault isolability, fault models are added to the diagnosis system using a model with a different model structure. The system isolates the faults, even though the induced faults are small in the simulation study, and the size of the faults are accurately estimated using observers.

Acknowledgment

First of all I would like to express my gratitude to my supervisor Professor Lars Nielsen for letting me join his research group and for the support during these three years. It seems there is a never ending stream of ideas bubbling in you regarding everything from research topics to presentation techniques. My second supervisor Erik Frisk is acknowledged for the many discussions about diagnosis. This work had not been the same without your support.

The industrial involvement in the project is valuable and Tobias Axelsson, Marcus Stigsson, and Nils-Gunnar Vågstedt are acknowledged for this. Lars Eriksson and Richard Backman are acknowledged for convincing me to start as a Ph.D student in the first place. The colleges at vehicular systems are acknowledged for creating a nice and pleasant atmosphere to work in.

Emil Larsson and Oskar Leufvén are acknowledged for proofreading the manuscript. Emil is furthermore acknowledged for the interesting discussions about diagnosis in general. The very many discussions with Oskar during these years about everything you could possibly think about has brought lots of joy.

I will forever be in debt with my family for all their support and encouragement. Most importantly, thanks to you Therése and Tilda for always being at my side when I need you at the most!

CONTENTS

1	Introduction	1
1.1	Problem statement	2
1.2	Thesis outline and contributions	3
2	Vehicle Models from CAPSim	5
2.1	Vehicle concept	5
2.1.1	Concept_parallel_mild1	5
2.1.2	Concept_parallel_mild2	6
2.2	Vehicle driver	7
2.2.1	Vehicledriver_simple1	7
2.3	Controller and energy management	7
2.4	Environment_simple1	8
2.5	Buffer	8
2.5.1	Buffer_simple1	8
2.5.2	Buffer_simple2	9
2.5.3	Buffer_rint1	9
2.6	Electric machine	10
2.6.1	Electricmotor_quasistatic1	10
2.6.2	Electricmotor_quasistatic2	11
2.6.3	Electricmotor_simple1	12
2.6.4	Electricmotor_pmsm1	13
2.7	Fuel tank_simple1	13
2.8	Engine	13

2.8.1	Engine_simplemap1	13
2.8.2	Engine_scalable1	14
2.8.3	Engine_scalable2	14
2.9	Clutch_simple1	15
2.10	Mechanicaljoin_gear1	15
2.11	Gearbox_manual1	15
2.12	Chassis	16
2.12.1	Chassis_simple1	16
2.12.2	Chassis_simple4	17
3	Truck Model	19
3.1	Vehicle concept	19
3.2	Vehicle driver	20
3.3	Environment	20
3.4	Buffer	20
3.5	Electric machine	21
3.5.1	Electricmotor_quasistaic2	21
3.5.2	Map based permanent magnet synchronous machine	21
3.5.3	Parametrization of electricmotor_quasistatic2	22
3.5.4	Electricmotor_quasistatic3	24
3.6	Engine	26
3.7	Fuel tank	27
3.8	Clutch	27
3.9	Mechanical joint	27
3.10	Gearbox	27
3.11	Chassis	28
3.12	Controller and energy management	28
3.13	Driving cycles and simulation results	31
4	Diagnosis of the Truck Based on Models for Correct Behavior	35
4.1	Mathematical tools	35
4.1.1	Structural analysis	36
4.1.2	CUSUM	36
4.2	Components to monitor	37
4.3	Induced faults	38
4.4	Sensor noise and sample frequency	38
4.5	Sensor configurations	39
4.5.1	Diagnosis system 1	40
4.5.2	Diagnosis system 2	41
4.5.3	Diagnosis system 3	42
4.6	Design of diagnosis systems	43
4.6.1	Diagnosis system 1	43
4.6.2	Diagnosis system 2	47
4.6.3	Diagnosis system 3	54
4.7	Results and discussion	58

4.7.1	Diagnosis system 1	59
4.7.2	Diagnosis system 2	61
4.7.3	Diagnosis system 3	63
4.8	Conclusions	65
5	Residual Generator Selection	67
5.1	Background	68
5.1.1	Extended structural analysis	68
5.1.2	Dynamic equations	68
5.2	Algebraic loops	69
5.2.1	Series wound electric machine	71
5.3	Integral and derivative causality	71
5.3.1	MCDS and ICDS	72
5.3.2	Methodology to construct ICDS	72
5.4	Results and discussion	72
5.4.1	Selection of consistency relations used in ICDS	73
5.4.2	Simulation study	74
5.5	Conclusions	77
6	Diagnosis using a Map Based Model of the Electric Machine	79
6.1	Structure of the models	79
6.2	Introducing faulty behavior in the model	82
6.2.1	Finding an expression for ΔT_{em}	82
6.2.2	Finding an expression for $\Delta P_{em,l}$	83
6.3	Maximum fault isolability performance	84
6.3.1	Model for correct behavior	84
6.3.2	Model for correct and faulty behavior	85
6.4	Transforming the model from DAE to ODE	85
6.5	Design of residual generators	86
6.5.1	Observers	87
6.5.2	Residual generators and decision structure	88
6.6	Results	89
6.7	Conclusions	91
7	Conclusions	93
	References	95
A	Model Equations	99
A.1	Vehicle driver	100
A.2	Control and energy management	100
A.3	Vehicle	102
A.3.1	Fuel tank	102
A.3.2	Engine	102
A.3.3	Buffer	102

A.3.4	Electric Machine - <code>electricmotor_quasistatic2</code>	103
A.3.5	Electric Machine - Map based model	104
A.3.6	Clutch	104
A.3.7	Mechanical joint	104
A.3.8	Gearbox	105
A.3.9	Chassis	105
B	Residual Generators Used in Chapter 4	107
B.1	Diagnosis system 2 - Test 4	108
B.2	Diagnosis system 3 - Test 3	109
B.3	Diagnosis system 3 - Test 4	110
B.4	Diagnosis system 3 - Test 5	111
B.5	Diagnosis system 3 - Test 6	112

INTRODUCTION

There are possibilities to increase the efficiency of automotive powertrains using hybrid technology. The highest relative fuel saving can be obtained in city buses and garbage trucks with many start and stops, but also a small relative saving in the fuel consumption for long haulage trucks results in a large amount of fuel. When hybridizing a vehicle, new components are added compared to a conventional vehicle, e.g. electric machines, battery, and power electronics, and these components need to be monitored with the same accuracy as the components used in a conventional vehicle.

One reason for monitoring the system is safety. Faults in the electrical components may be fatal due to the high voltage in the system. Further, a fault in the vehicle may lead to that a torque is applied on the wheels by the electric machine when the truck is at stand still, and this possibly results in that the truck starts to move. It is also of relevance to protect components from breaking down if a fault occurs. It is especially important to protect the battery that is expensive and may degrade fast, if e.g. large power flows are used in the battery. High power in the electrical components may for example be caused by a fault in the power electronics or the electric machine.

The demands on the diagnosis systems in a conventional vehicle have been increased over a long period of time. Therefore such diagnosis systems have been developed and refined step by step to achieve the performance of today's systems. Monitoring the powertrain of a hybrid electric vehicle (HEV) leads to new challenges since there for example are many different operating modes in an HEV. These operating modes also offer possibilities to increase the performance of the diagnosis system, since there is a freedom in choosing operating points of

the components via the energy management. One example is that the required torque from the driver, can be achieved by combining the combustion engine and the electric machine in different ways.

Diagnosis

Diagnosis is used to detect and isolate faults in a system using measurements, and there are several approaches to be used. One of the more common is consistency based diagnosis (de Kleer et al., 1992), that can be based on a general diagnostic engine (de Kleer and Williams, 1987; Struss and Dressier, 1989), or residual generators (Blanke et al., 2006). The basic principle when constructing the residual generators are that a set of equations are used to compute the unknown variables, that are inserted in a redundant equation called consistency relation. This computation can be done by finding algebraic expressions for the variables or using numerical techniques, e.g. a differential algebraic system solver (DASSL) described in Brenan et al. (1996). One disadvantage using numerical solvers in nonlinear systems is that it is generally more computationally demanding compared to using algebraic expressions. The designed diagnosis systems are supposed to be able to be implemented in a truck with limited computational power, and therefore algebraic expressions are found for the variables in the residual generators in this study.

Vehicle level diagnosis

A hybrid electric vehicle powertrain consists of several components, such as combustion engine, electric machine, and energy buffer. The manufacturers of these components often deliver diagnosis systems for the specific component. When the components are connected in a hybrid powertrain it is possible to design a diagnosis system monitoring the entire powertrain. This type of overall diagnosis is here called vehicle level diagnosis, and is the main emphasis of this thesis. There are several possible benefits of using such a diagnosis system, e.g. that the performance of the diagnosis may increase, and that it may be possible to monitor the components by using fewer sensors, compared to using separate diagnosis systems for each component in the powertrain.

1.1 Problem statement

The aim of this work is to investigate aspects influencing diagnosis on vehicle level regarding performance, design complexity, and computational complexity. One example of an aspect is how the sensor configuration affects the diagnosis system. Another example is how the design of the energy management in combination with the driving mission and the driver, either can hide or attenuate a fault. This aspect is of higher relevance in hybrid vehicles compared to conventional vehicles, since there are more mode shifts in the hybrid system, and there

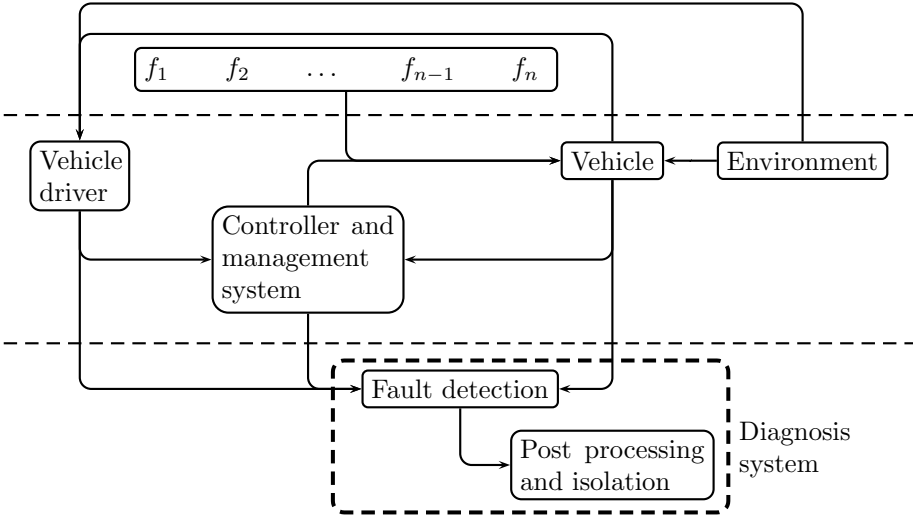


Figure 1.1: *The structure of the implemented simulation platform. The faults induced in the vehicle are modeled in the block above the top horizontal dashed line. The models for vehicle, driver, controller, and environment describing ambient parameters and the driving cycle, are included in the blocks between the dashed lines. This part includes the information needed to carry out a simulation of a vehicle to find the fuel consumption and the operating points of the components in the powertrain. The diagnosis system is included below the lower dashed line and uses information from sensors and control signals.*

is a freedom in selecting operating modes via the energy management. The understanding of such issues is crucial when constructing a diagnosis system on vehicle level for hybrid trucks.

1.2 Thesis outline and contributions

To study overall monitoring and diagnosis for hybrid vehicles a simulation platform has been developed. The platform contains models of the driver, environment, vehicle, controller and energy management, and faults, as well as the diagnosis system. The parts of the platform interact according to Figure 1.1, and most of the models used are obtained from an existing model library called Center for Automotive Propulsion Simulations (CAPSim, 2009). Some of the models in CAPSim being of interest in the model of a parallel hybrid truck are recalled in Chapter 2. The models used in the simulation platform are given in Chapter 3, where the modifications to the original models in CAPSim are stated. The energy management and a model of the electric machine are developed and also described in 3. Chapters 2 and 3 are based on Sundström et al. (2010b).

The simulation platform is used to study the vehicle level diagnosis aspects described in Section 1.1, and this is done in Chapters 4-6. First, the interaction between diagnosis performance, sensor configuration, and energy management design is investigated in Chapter 4, that is based on Sundström et al. (2010a). This is done by designing and implementing three model based diagnosis systems in the simulation environment. The systems are based on a model only describing the fault free behavior of the truck, i.e. how the faults affect the powertrain is not included in the diagnosis system. Three different sensor configurations are used in the diagnosis systems, and it is indicated that the diagnosis performance generally increases when several sensors are used and the sensor placement is selected so only a few model equations are required in the residual generators. The performance in the diagnosis system depends on the operating points of the components in the powertrain. Using a well designed energy management increases the diagnosis performance, especially for the system based on few sensors.

An investigation of the properties of the residual generators in one of the diagnosis system constructed in Chapter 4 is carried out in Chapter 5, that is based on Sundström et al. (2011). A systematic method is used to get proposals of residual generators that fulfills predefined constraints, such as that unique expressions for the residual generators are to be found, and how dynamic equations are to be evaluated in a computational sequence. It is shown that it is non-trivial to design a diagnosis system that fulfills predefined requirements in a complex system as a vehicle. The value of using systematic methods to design the diagnosis system is thereby reinforced.

In the diagnosis systems in Chapters 4 and 5, a model based on an equivalence circuit of the electric machine is used. In Chapter 6 a map based model of the machine is used in the diagnosis system to investigate difficulties and limitations using a map based model in a diagnosis system regarding fault isolability. To more clearly illustrate these aspects, only the electric machine is monitored in the diagnosis system, and not the entire powertrain as is the case in Chapters 4 and 5. The map based model is well suited for fault detection due to the high accuracy in the model, but the structure of the model leads to that fault models are required to achieve fault isolability, and not only use models for fault free behavior as is the case in the diagnosis systems in Chapters 4 and 5. To model how the faults affect the behavior of the machine a model based on an equivalence circuit is used, since it is easy to model the faults in this model. This leads to that the map based model is used to model the fault free behavior of the machine, while the equivalence circuit model handles the faults' impact. Full fault isolability is achieved using the two models of the machine in the diagnosis system, and the faults are accurately estimated using observers.

The overall conclusions are given in Chapter 7.

VEHICLE MODELS FROM CAPSIM

In the simulation platform, it has been a strategy to use models based on the model library called Center for Automotive Propulsion Simulations (CAPSim, 2009), where some models are based on the QSS library (Guzzella and Amstutz, 1999). This chapter recalls some of the models used in CAPSim, that are of interest modeling a powertrain of a parallel hybrid truck. For some components several models are described to investigate the differences between the models, and to select a suitable component model to be used in the vehicle model. The original documentation of the models can be found in the library of CAPSim. This chapter describes the models in a slightly different way, but the content is mainly the same.

2.1 Vehicle concept

There are different possible architectures of a hybrid vehicle powertrain. The models of the vehicle concept include information about which components that are used in the vehicle, and how these are connected. This states whether the vehicle is e.g. a conventional, parallel hybrid, or series hybrid vehicle.

In this section two parallel hybrid concepts are described. The difference between these concepts are where the electrical part of the driveline is connected to the conventional part. In both concepts the inertia in the components are summed, and used in the expression for the vehicle acceleration in the chassis.

2.1.1 `Concept_parallel_mild1`

The concept `concept_parallel_mild1` includes a fuel tank, internal combustion engine, clutch, gearbox, and chassis. In parallel to the combustion engine

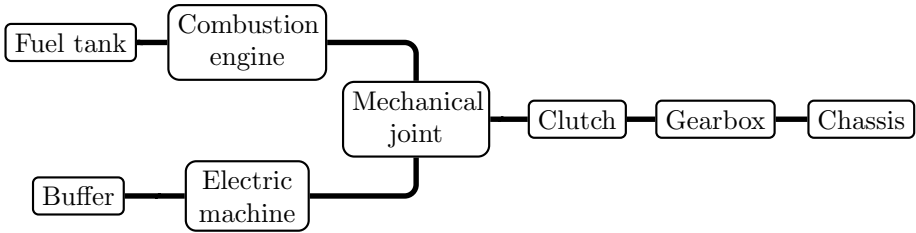


Figure 2.1: *The electrical part of the driveline is connected to the conventional part between the engine and the clutch in `concept_parallel_mild1`.*

there is an electric machine and an energy buffer, which are connected to the conventional part of the powertrain between the engine and the clutch (Figure 2.1). This concept thereby represents a vehicle with an integrated starter-alternator, or a pre-clutch parallel hybrid electric vehicle. Energy can be regenerated by braking using the electric machine, though the clutch has to be engaged for this to be possible.

2.1.2 `concept_parallel_mild2`

The concept `concept_parallel_mild2` consists of the same components as `concept_parallel_mild1`. The difference compared to the previous model is that the electric and mechanical parts of the powertrain are connected between the clutch and the gearbox in this concept, as can be seen in Figure 2.2. Energy can be regenerated using the electric machine, even when the clutch is disengaged and the engine is switched off. The disadvantage with this concept is that the electric machine cannot be used as a starter motor for the combustion engine, leading to increased cost and weight of the vehicle.

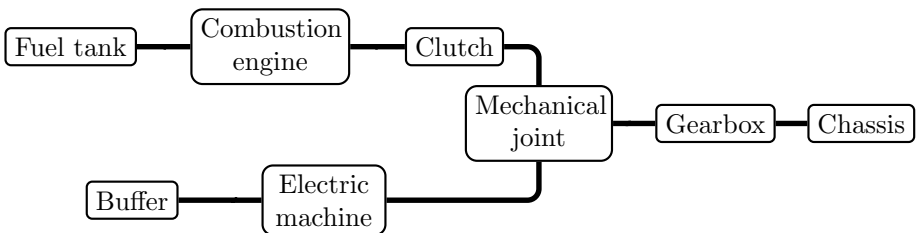


Figure 2.2: *The `concept_parallel_mild2` model. The difference compared to `concept_parallel_mild1` seen in Figure 2.1, is that the engine and electric machine are connected after the clutch in this model.*

2.2 Vehicle driver

The model representing the driver is described in the component vehicle driver. The positions of the accelerator, brake pedal, clutch, and gear selection are set in this component.

2.2.1 Vehicledriver_simple1

In the model `vehicledriver_simple1`, the vehicle follows a driving cycle using a PI-regulator

$$u_{vd} = \begin{cases} -1, & K_p e + K_i \int e dt < -1 \\ K_p e + K_i \int e dt, & -1 \leq K_p e + K_i \int e dt < 1 \\ 1, & K_p e + K_i \int e dt \geq 1 \end{cases} \quad (2.1a)$$

$$e = v_{ref} - v \quad (2.1b)$$

where v is the velocity of the vehicle, and v_{ref} the reference speed given by the driving cycle. There is no functionality for anti-wind-up included in the regulator. The pedal position for the accelerator is calculated as

$$\text{accPed} = \max \{u_{vd}, 0\} \quad (2.2)$$

and the brake pedal position as

$$\text{brakePed} = -\min \{u_{vd}, 0\} \quad (2.3)$$

The selection of gear depends on the velocity of the vehicle, except the selection of the first gear that is dependent on the reference velocity

$$\text{gear} = f(v, v_{ref}), \quad \text{gear} \in \{0, 1, \dots, 6\} \quad (2.4)$$

The clutch pedal is pressed down for a predefined time, Δ , during a gear shift

$$\text{clutchPed}(t) = \begin{cases} 0, & \text{gear}(t) \neq \text{gear}(t - \Delta) \\ 1, & \text{gear}(t) = \text{gear}(t - \Delta) \end{cases} \quad (2.5)$$

where `clutchPed` is zero when the clutch pedal is pressed down, and one when the pedal is released.

2.3 Controller and energy management

The controller sets the reference torques for the energy converters and the mechanical brakes. This is done based on information from sensors and outputs from the vehicle driver. Most of the controller is modified in the model used in the truck, and therefore no deeper investigation of the component implemented in `CAPSim` is of interest in this description.

2.4 Environment_simple1

The environment model sets parameters such as the ambient pressure and temperature. The component called `environment_simple1` sets values to the following parameters:

Reference velocity: of the vehicle is an output from the model, but is defined in the driving cycle.

Gear: is defined in the driving cycle. This signal is not used when the vehicle driver presented in Section 2.2.1 is used.

Slope: both longitudinal and lateral slopes are set.

Steering wheel position: may be used in the chassis to simulate the lateral forces acting on the vehicle.

Ambient pressure: is a constant value

Ambient temperature: is a constant value

The parameters, except the ambient pressure and temperature, can be set as a function of either time or distance.

2.5 Buffer

In this section three models of super capacitors and batteries are described.

2.5.1 Buffer_simple1

The model `buffer_simple1` models the buffer as an equivalent circuit, including a voltage source and a resistance, R_b , connected as a Thévenin circuit (Hambley, 2005) according to Figure 2.3. The voltage of the buffer, U_b , is proportional to the state of charge, SoC

$$U_b = K_v SoC \quad (2.6)$$

where K_v is the constant correlating the charge of the buffer with the voltage. This model represents a super capacitor since the voltage is proportional with SoC .

The power is integrated to find the SoC of the buffer

$$SoC = SoC_0 - \frac{1}{E_{max}} \int (R_b I_b^2 + U_b I_b) dt, \quad SoC \in [0, 1] \quad (2.7)$$

where E_{max} is the total energy that can be stored in the buffer, and SoC_0 the initial state of charge of the buffer. The current, I_b , is negative when the buffer is charged.

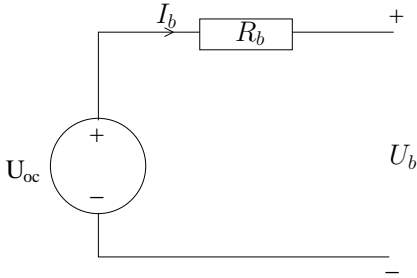


Figure 2.3: The equivalence circuit used in the buffer models.

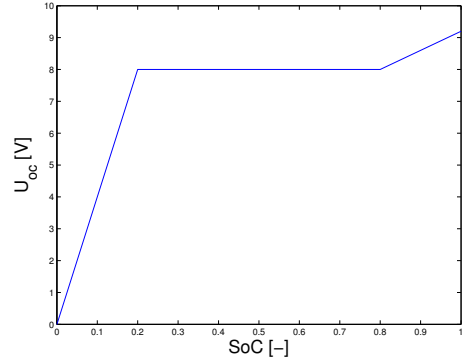


Figure 2.4: $U_{oc}(SoC)$ for one cell in `buffer_simple2`.

2.5.2 Buffer_simple2

In `buffer_simple2` the estimation of SoC is based on the current and not the power as is the case in `Buffer_simple1` in (2.7)

$$SoC = SoC_0 - \frac{1}{Q_b} \int I_b dt, \quad SoC \in [0, 1] \quad (2.8)$$

and the current is normalized with the capacity of the battery, Q_b .

A Thévenin equivalence circuit is used in `buffer_simple2` (see Figure 2.3), leading to

$$U_b = U_{oc} - R_b I_b \quad (2.9)$$

where U_{oc} is the open circuit voltage and is a function of (SoC). This voltage is given for one cell in Figure 2.4, and the model represents a battery using this parametrization.

2.5.3 Buffer_rint1

There is one model in CAPSim called `buffer_rint1` that is more detailed than the previously described buffer models. The parameters R_b and U_{oc} are dependent on SoC and the battery temperature, T_b

$$R_b = f(SoC, T_b) \quad (2.10)$$

$$U_{oc} = f(SoC, T_b) \quad (2.11)$$

and the state of charge is defined as in (2.8). In this model, the current used in the integration is reduced when the battery is being charged. This is due to the Coulombic efficiency, $\eta_{b,c}$, and the current that is integrated in (2.8) is

$$I_{b,eff} = \max(I_b, 0) + \min(I_b, 0)\eta_{b,c} \quad (2.12)$$

In the default parametrization in CAPSim the Coulombic efficiency is set to 90.5%. The Thévenin equivalent circuit is used as in `buffer_simple2`, and is shown in Figure 2.3. The battery voltage is based on $I_{b,eff}$

$$U_b = U_{oc} - R_b I_{b,eff} \quad (2.13)$$

The parameters R_b and U_{oc} are only given for two temperatures. This is a weakness in the parametrization of the model, especially since the temperatures used are 0°C and 25°C. Further, in the model implemented in CAPSim, the battery temperature is assumed to be constant. It is preferable to add a temperature model for the battery and extend the maps of U_{oc} and R_b .

2.6 Electric machine

An electric machine is able to operate in all 4 quadrants. This means that the machine is able to reverse in addition to forward operation, as well as deliver both positive and negative torques. Three models of direct current machines and one alternating current machine are presented in this section. In the models of the electric machine, an ideal model for the power electronics is included.

2.6.1 Electricmotor_quasistatic1

The basic idea in the model `electricmotor_quasistatic1` is that the torque, T_{em} , is proportional to the current I_{em}

$$T_{em} = k I_{em} \quad (2.14)$$

The parameter k is defined by $k = L_m I_{em,f}$, where L_m is the field mutual inductance, and $I_{em,f}$ is the field current (Guzzella and Sciarretta, 2007). This current is constant in the model, leading to that k is constant.

The current is calculated using the voltage, U_{em} , and the electromotive force (emf), that depends on the speed of the machine, ω_{em}

$$I_{em} = \frac{1}{R_{em}} (U_{em} - \underbrace{k\omega_{em}}_{emf}) \quad (2.15)$$

where R_{em} is the resistance in the electric machine. Combining (2.14) and (2.15) results in

$$T_{em} = \frac{k}{R_{em}} U_{em} - \frac{k^2}{R_{em}} \omega_{em} \quad (2.16)$$

The following expression for T_{em} is implemented in the CAPSim library

$$T_{em} = \frac{k}{R_{em}} U_{em} - \frac{k^2}{R_{em}} \omega_{em} \text{sign}(U_{em}) \quad (2.17)$$

The computed torques in (2.16) and (2.17) only differs when U_{em} is negative. The voltage is positive for a realistic parametrization of the machine, as long as the vehicle is driving forward. This is the case in the driving cycles used, and the difference between (2.16) and (2.17) does not affect the simulation results.

The electric power in the electric machine is equal to the input power to the power electronics since this component is assumed to be ideal. The battery current can be expressed as

$$I_b = \underbrace{\frac{T_{em}}{k}}_{I_{em}} \frac{U_{em}}{U_b} \quad (2.18)$$

In the implementation there is an absolute value of the voltage in the machine

$$I_b = \underbrace{\frac{T_{em}}{k}}_{I_{em}} \frac{|U_{em}|}{U_b} \quad (2.19)$$

that has no impact on the simulation results since $U_{em} \geq 0$ as stated above.

Local controller

The controller of the machine sets a requested voltage $U_{em,ctrl}$ to be applied on the machine by the power electronics. This is done using the model of the machine to calculate the voltage required to achieve a requested torque, $T_{em,req}$, set in the energy management

$$U_{em,ctrl} = \frac{R_{em}}{k} \left(T_{em,req} + \frac{k^2}{R_{em}} \omega_{em} \right) \quad (2.20)$$

The model for the power electronics supplies this voltage to the machine.

$$U_{em} = U_{em,ctrl} \quad (2.21)$$

2.6.2 Electricmotor_quasistatic2

Electricmotor_quasistatic2 is similar to electricmotor_quasistatic1. The differences between the models are:

- The input signal from the local controller, i.e. the voltage applied by the power electronics to the machine, is filtered with a time constant τ_{em} . This is to decrease the stiffness of the model.

$$\tilde{U}_{em} = \frac{1}{\tau_{em}s + 1} U_{em} \quad (2.22)$$

- The parameter k used in (2.14)-(2.19) is modeled as two constants in this model. The torque constant, k_a , replaces k in (2.14)

$$T_{em} = k_a I_{em} \quad (2.23)$$

and the speed constant, k_i , replaces k in (2.15)

$$I_{em} = \frac{1}{R_{em}} \left(\underbrace{k_i \omega_{em}}_{emf} - \tilde{U}_{em} \right) \quad (2.24)$$

This is one way to model the losses in the machine since $k_a < k_i$ in the model.

Corresponding equation to (2.16) is

$$T_{em} = \frac{\tilde{U}_{em} k_a}{R_{em}} - \frac{\omega_{em} k_a k_i}{R_{em}} \quad (2.25)$$

and the equation for I_b is the same as is given in (2.19), except from that U_{em} is replaced with the filtered voltage and the parameter k is replaced with k_a

$$I_b = \underbrace{\frac{T_{em}}{k_a}}_{I_{em}} \frac{|\tilde{U}_{em}|}{U_b} \quad (2.26)$$

A drawback with this model is that I_b is limited to $|I_b| \leq 300$ A in a non physical way, since I_{em} and T_{em} are not limited when $|I_b| > 300$ A. Therefore, when this constraint occurs all consumed energy from the machine is not taken from the battery, since the power from the battery is reduced. A better way to avoid large currents would be to reduce $U_{em,ctrl}$ in the local controller of the electric machine if the magnitude of I_b is too large.

2.6.3 Electricmotor_simple1

In `electricmotor_simple1` the back electromotive force is modeled in series with a resistor and an inductance. The losses in the wires are modeled with the resistor, and the inertia of the magnetic field in the machine is modeled with the inductance. The electromotive force is the voltage generated when the windings of the rotor moves in the magnetic field. This term is proportional to the angular speed of the machine

$$U_{em} - R_{em} I_{em} - L_{em} \frac{dI_{em}}{dt} - \underbrace{k_i \omega_{em}}_{emf} = 0 \quad (2.27)$$

As in the previous described models, the torque is proportional to the current

$$T_{em} = k_a I_{em} \quad (2.28)$$

and the torque and speed constants differ to model the losses, as is done in `Electricmotor_quasistatic2`.

2.6.4 `Electricmotor_pmsm1`

Permanent magnet synchronous machines (PMSM) have in general higher efficiency compared to other machine types (Zhu and Howe, 2007). Typical efficiency maps for an induction machine and a PMSM are shown in Mellor (1999). One disadvantage with permanent magnet machines is the higher cost, that is related to the permanent magnets. `Electricmotor_pmsm1` is a model of a PMSM implemented in CAPSim.

A PMSM consists of a stator with windings, and a rotor with permanent magnets. The magnets are either mounted on the outside of the rotor, or are integrated inside the rotor (Chau et al., 2008). By applying a voltage that results in a current in the stator, the rotor starts to move.

A PMSM is an AC machine and a transformation is used in the model that e.g. is called Park transformation (Wallmark, 2006), or direct and quadrature axis (dq0) transformation as in Fitzgerald et al. (2003). The benefit of using this transformation is that in a balanced three phase machine, the currents and torques can be described without any sinusoidal terms. The transformation is described in the documentation of the model in CAPSim (2009).

2.7 `Fueltank_simple1`

The model `fueltank_simple1` models the mass of the fuel in the tank, m_f , by integrating the fuel mass-flow, \dot{m}_f , to the engine. The integrator is initialized with the mass of the fuel at the beginning of the driving cycle, $m_{f,0}$.

$$m_f = \int -\max\{0, \dot{m}_f\} dt + m_{f,0} \quad (2.29)$$

The weight reduction of the vehicle when fuel is consumed is also computed

$$m_{f,r} = \int \max\{0, \dot{m}_f\} dt \quad (2.30)$$

2.8 Engine

2.8.1 `Engine_simplemap1`

The model `engine_simplemap1` is based on two look-up maps. The map including the delivered torque on the crank shaft takes the engine speed and the accelerator pedal position as inputs

$$T_e = f(\omega_e, \text{accPed}) \quad (2.31)$$

The specific fuel consumption [kg/kWh] is given in a map

$$\text{sfc} = f(\omega_e, T_e) \quad (2.32)$$

and the fuel consumption [kg/s] is calculated by

$$\dot{m}_f = \frac{1}{3600} T_e \omega_e \text{sfc} \quad (2.33)$$

2.8.2 Engine_scalable1

`Engine_scalable1` is based on a model in QSS (Guzzella and Amstutz, 1999). The model computes the mean brake effective pressure, p_{me} , of the engine to calculate the torque delivered by the engine. The mean effective pressure is defined as

$$p_{me} = \frac{4\pi T_e}{V_d} \quad (2.34)$$

where V_d is the displacement of the engine. The pressure p_{me} is calculated using Willans approximation (Guzzella and Sciarretta, 2007)

$$p_{me} = \eta_{e,i} p_{m\phi} - p_{me0} \quad (2.35)$$

where $\eta_{e,i}$ is the indicated engine efficiency, i.e the efficiency of the transformation from chemical energy to pressure inside the cylinders, p_{me0} is the pumping and friction losses, and $p_{m\phi}$ the fuel mean effective pressure. The constant losses are modeled as

$$p_{me,0} = p_{me0,f} + p_{me0,g} \quad (2.36)$$

where the pumping losses, $p_{me0,g}$, are assumed to be constant. The friction losses are modeled using the ETH friction model given in Guzzella and Onder (2004), that is a simplified model of Inhelder (1996)

$$p_{me0,f} = k_1 (k_2 + k_3 S^2 \omega_e^2) \Pi_{bl} \sqrt{\frac{k_4}{B}} \quad (2.37)$$

In the expression, $k_{\{1,2,3,4\}}$ are constants, B and S the bore and stroke, and Π_{bl} the boost layout of the engine that affects the dimensioning of e.g. bearings. The efficiency of the engine is approximated to only be dependent on the delivered torque.

2.8.3 Engine_scalable2

`Engine_scalable2` is similar to `engine_scalable1`. The difference between the models is that dynamics in the delivered torque is included in this model. This is done using

$$\ddot{\tilde{T}}_e = c_1 (T_e - \tilde{T}_e) \omega_e^2 - c_2 \omega_e \dot{\tilde{T}}_{e,req} \quad (2.38)$$

where T_e is calculated using (2.34), and \tilde{T}_e is the delivered torque from the engine. The constants c_1 and c_2 are designed with the approximation that it takes about two crank shafts for a four stroke engine to reach a stationary operating point.

2.9 Clutch_simple1

The model of the clutch is called `clutch_simple1`. The clutch pedal position is an input signal, that is zero when the clutch pedal is pressed down and the clutch is disengaged. A flywheel is included in the model and the difference in angular speed between the flywheel, $\omega_{c, fly}$, and the outgoing shaft, ω_c , is calculated by

$$\Delta\omega_c = \omega_{c, fly} - \omega_c \quad (2.39)$$

There is a variable called `disengaged` in the model. The value of the variable is zero when $|\Delta\omega_c| < 1^{\text{rad/s}}$ and `clutchPed` ≥ 0.1 . If not both these conditions are fulfilled, the value of `disengaged` is one.

When `disengaged` = 0, the torque from the clutch is equal to the torque from the engine

$$T_c = T_e, \quad \text{disengaged} = 0 \quad (2.40)$$

When `disengaged` = 1, T_c is set to a constant value, $T_{c, max}$, that changes sign depending on the sign of $\Delta\omega_c$

$$T_c = T_{c, max} \cdot \text{clutchPed} \cdot \text{sign}(\Delta\omega_c), \quad \text{disengaged}=1 \quad (2.41)$$

2.10 Mechanicaljoin_gear1

The model of the component that mechanically joins three components of the driveline is `Mechanicaljoin_gear1`. In this component a gear ratio, u_{em} , is applied between the shaft the electric motor is connected to, and the other two shafts. The torque delivered from the component is calculated using

$$T_{mj} = T_e + T_{em}u_{em} \quad (2.42)$$

if the vehicle has the configuration as in Figure 2.2. The inertia is calculated using

$$J_{mj} = J_e + J_{em}u_{em}^2 \quad (2.43)$$

where J_e and J_{em} are the inertia of the engine and electric machine.

2.11 Gearbox_manual1

`Gearbox_manual1` is a model of a fix step manual gearbox. The used gear is an input signal to the gearbox and is set in the vehicle driver model. Based on this signal the gear ratio, u_{gb} , is achieved. The losses in the gearbox are modeled using an affine dependency between the input and output torques. The torque consumed at idle is denoted $T_{gb, l}$, and the proportional coefficient, η_{gb} , is multiplied with the torque from the mechanical joint. The delivered torque from the gearbox is

$$T_{gb} = \begin{cases} u_{gb} (T_{mj} - T_{gb, l}) \eta_{gb} & T_{mj} - T_{gb, l} \geq 0 \\ u_{gb} (T_{mj} - T_{gb, l}) \frac{1}{\eta_{gb}} & T_{mj} - T_{gb, l} < 0 \end{cases} \quad (2.44)$$

where η_{gb} depends on the selected gear, and $T_{gb,l}$ depends on the ingoing speed and the selected gear. The inertia from the input shaft is compensated for the gear ratio when the inertia of the vehicle is calculated

$$J_{tot} = J_{gb} + u_{gb}^2 J_{mj} \quad (2.45)$$

2.12 Chassis

In the chassis the output shaft from the gearbox is connected to the final gear, and finally to the wheels. The losses according to e.g. drag and rolling resistance are modeled, as well as the change in potential energy of the vehicle due to the slope of the road. The acceleration of the vehicle is calculated based on the resulting torque acting on the wheels.

2.12.1 Chassis_simple1

The first described model of the chassis is `Chassis_simple1`. The drag and rolling resistance forces, F_d and F_r , are modeled by

$$F_d = \frac{1}{2} \rho C_d A_f v^2 \quad (2.46)$$

$$F_r = C_r m_v g \left(1 - \frac{1}{2.81^{(0.5v)}} \right) \quad (2.47)$$

and the force due to the slope of the road by

$$F_g = m_v g \sin \alpha \quad (2.48)$$

where ρ is the air density, C_d and C_r the air drag and rolling resistance constants, A_f the frontal area of the vehicle, v the vehicle velocity, m_v the mass of the vehicle, and α the slope of the road. The sum of these forces are

$$F_w = F_r + F_d + F_g \quad (2.49)$$

The net torque is used to calculate the velocity of the vehicle

$$v = v_0 + \frac{1}{m_v} \int (T_{gb} u_f - T_b) \frac{1}{r_w} - F_w dt \quad (2.50)$$

by multiplying the gear ratio in the final gear, u_f , with T_{gb} and subtract the torque from the mechanical brakes, T_b , and the forces included in F_w . The initial velocity is denoted v_0 , and the wheel radius r_w .

The chassis model includes functionality to handle the slip between the tires and the road, but the model equations for this is not included here.

2.12.2 Chassis_simple4

In the model called `Chassis_simple4`, the road slope is used to calculate the change in potential energy, but is not used in the expression for the rolling resistance. The rolling resistance is modeled as

$$F_r = m_v g C_r \quad (2.51)$$

To be able to handle low velocities and stand still, the torque due to the rolling resistance, T_r , is proportional to the angular speed of the wheels, ω_w , at low speeds. If the vehicle is reversing, T_r changes sign in the model

$$T_r = \begin{cases} m_v g C_r r_w, & 1000\omega_w > m_v g C_r r_w \\ 1000\omega_w, & -m_v g C_r r_w \leq 1000\omega_w < m_v g C_r r_w \\ -m_v g C_r r_w, & 1000\omega_w \leq -m_v g C_r r_w \end{cases} \quad (2.52)$$

The torques due to drag and potential energy of the vehicle are modeled as in (2.46) and (2.48)

$$T_d = \frac{1}{2} \rho C_d A_f \omega_w^2 r_w^3 \quad (2.53)$$

$$T_g = m_v g r_w \sin \alpha \quad (2.54)$$

and the net torque acting on the wheels are

$$T_{net} = T_{gb} u_f - T_d - T_b - T_r - T_g \quad (2.55)$$

The effective inertia and the mass of the vehicle are used to calculate the angular acceleration of the wheels

$$\dot{\omega}_w = \frac{T_{net}}{J_{tot} u_f^2 + m_v r_w^2} \quad (2.56)$$

where the mass of the vehicle is

$$m_v = m_{v,0} - m_{f,r} \quad (2.57)$$

where $m_{v,0}$ is the initial weight of the vehicle when the simulation starts and $m_{f,r}$ is calculated in (2.30). The velocity and distance travelled are calculated by

$$v = \omega_w r_w \quad (2.58)$$

$$s = r_w \int \omega_w dt \quad (2.59)$$

and the angular velocity of the shaft between the gearbox and the final gear is

$$\omega_{gb} = \omega_w u_f \quad (2.60)$$

The implementation of the chassis does not fully support negative velocities. The rolling resistance handles this, but the mechanical brakes do not, since the torque applied by the brakes on the wheels does not change sign with the velocity. This could lead to problems at stand still, since if the vehicle is slightly reversing nothing is forcing the vehicle to stand still except the rolling resistance.

TRUCK MODEL

To make quantitative investigations in the following chapters, a model of a truck is implemented in the simulation environment in Figure 1.1. The vehicle is assumed to be a long haulage truck with a mass of 40 tons and otherwise parametrized with realistic values. The configuration of the powertrain is a parallel hybrid, and the added components compared to a conventional powertrain are an electric machine and a battery package. As mentioned in Section 2.6, there is no separate component for the power electronics in the model. Instead this functionality is included in the model for the electric machine.

The vehicle model is implemented mainly using component models included in CAPSim presented in Chapter 2. Compared to the models in CAPSim there are some modifications and additions to achieve the vehicle model, and these are described in this chapter. Notably, there are several models of the electric machine discussed in this chapter, one based on a CAPSim model, but also two other models of electric machines. The models of the machine are used in the diagnosis systems in Chapters 4-6, to investigate how the diagnosis performance is affected by the model used.

The complete set of model equations used is summarized in Appendix A.

3.1 Vehicle concept

The model for the vehicle concept of the truck is `concept_parallel_mild2`. In this model the electric machine is connected to the conventional part of the powertrain between the clutch and the gearbox (see Figure 2.2). No changes are made in the concept compared to the model in CAPSim.

Table 3.1: *Vehicle speeds where gear shifts occur.*

Gear	Change up speed [m/s]	Change down speed [m/s]
1	ε	0
2	1.5	0.5
3	2.5	1.5
4	4	3
5	6	4
6	8	6
7	10.5	8
8	13	10
9	15	12
10	17	14
11	19	16
12	22	20

3.2 Vehicle driver

`VehicleDriver_simple1` is used to model the driver. This model is slightly modified to be able to handle a 12 speed gearbox. In Table 3.1 the gear selection is given as a function of the vehicle speed. The change up speed is the velocity of the vehicle when a gear is selected from a lower gear, and the change down velocity when a down shift is to occur. For example, if fourth gear is used, fifth gear will be selected if $v > 6$ m/s and third gear if $v < 3$ m/s. The velocity of the vehicle is compared to the values in the table except in first gear, where the reference velocity from the driving cycle is used instead. This is to be able to select the first gear at stand still, and the reference speed is not zero since the vehicle is to take off. The parameter ε in the table is set to value close to zero, resulting in that a gear is selected at take off.

3.3 Environment

The model for the environment in the truck model is `environment_simple1`. No changes are made in the environment model.

3.4 Buffer

The vehicle modeled uses `buffer_simple2` as the buffer, and this can be seen as a model of lithium-ion batteries. The advantage of this model compared to `buffer_rint1` is that there are less parameters to tune. The disadvantage is that the inner resistance and voltage are not dependent on the temperature, as they are in `buffer_rint1`. The chosen model does not include the Coulombic

efficiency. This loss is assumed to be negligible since the Coulombic efficiency is close to one in lithium-ion batteries (Valøen and Shoesmith, 2007).

The capacity of each cell in the battery is increased from 5.8 Ah to 34.8 Ah compared to the original parametrization in CAPSim. The voltage of each cell is unchanged and is presented in Figure 2.4. The weight of each cell is scaled proportionally to the increase in the capacity to 6 kg from 1 kg. There are 32 cells connected in series in the battery, resulting in a total weight of 192 kg, a storage capacity of approximately 9 kWh, and a nominal battery voltage of 256 V.

3.5 Electric machine

Three models of the electric machine are used and compared in the diagnosis systems. One model is based on CAPSim, one model uses a different assumption when the losses are modeled compared to the CAPSim model, and one model describes the losses by using a map. The model from CAPSim is `electricmotor_quasistaic2`. This model is chosen since it has the ability of modeling the losses in one more way than `electricmotor_quasistaic1`. At the same time the model is not too complex, and therefore gives the possibility to e.g. analyze the impact on the operating modes of the electric machine if the power electronics is broken. The map based model represents a permanent magnet synchronous machine (PMSM), and is used since the model is based on measurements, and the machine type is common in HEVs (Chau et al., 2008).

3.5.1 Electricmotor_quasistaic2

The model `electricmotor_quasistatic2` is a model of a DC-machine. The model and the parameters are unchanged except from the time constant in the filter of the voltage in (2.22) that is increased to 0.1 seconds from 0.01 seconds, to decrease the stiffness of the model. The model is parametrized as a 33 kW DC machine with constant magnetic flux. The parameter values of the resistance, R_{em} , torque constant, k_a , and speed constant, k_i , are set to 0.044 Ω , 0.50 Nm/A , and 0.51 Vs/rad , respectively. The functionality for limiting the current to the battery described in Section 2.6.2 is not used in this model.

3.5.2 Map based permanent magnet synchronous machine

A PMSM is modeled using a map describing the power losses. There is a map describing the power losses in the power electronics, in addition to the map describing the losses in the machine. The sum of these two power losses is used and is called $P_{em,l}$. The map of the total losses is three dimensional taking the delivered torque, motor speed, and battery voltage as inputs

$$P_{em,l} = f(T_{em}, \omega_{em}, U_b) \quad (3.1)$$

There are limitations in the delivered torque from the machine, denoted $T_{em,min}$ in generator mode and $T_{em,max}$ in motor mode, that are functions of ω_{em} and U_b . The limited torque, $T_{em,lim}$ is equal to the requested torque, $T_{em,req}$, if the requested torque is within the limitations of what the machine is able to deliver

$$T_{em,lim} = \begin{cases} T_{em,min}, & T_{em,req} < T_{em,min} \\ T_{em,req}, & T_{em,min} \leq T_{em,req} < T_{em,max} \\ T_{em,max}, & T_{em,req} \geq T_{em,max} \end{cases} \quad (3.2)$$

The delivered torque is computed by filtering $T_{em,lim}$

$$T_{em} = \frac{1}{\tau_{em}s + 1} T_{em,lim} \quad (3.3)$$

and the mechanical power delivered by the machine

$$P_{em,m} = T_{em}\omega_{em} \quad (3.4)$$

is used to calculate the electrical power

$$P_{em,e} = P_{em,m} + P_{em,l} \quad (3.5)$$

The battery current is finally computed using

$$I_b = \frac{P_{em,e}}{U_b} \quad (3.6)$$

Figure 3.1 shows the efficiency of the electric machine when the battery voltage is 220 V. There are small variations in the efficiencies due to U_b , while the maximum torque line is significantly dependent on the battery voltage. When the voltage is low, the maximum torque line is shifted down. In the figure the operating points for the electric machine is shown when the truck follows the driving cycle FTP75. At high load the battery voltage is lower than 220 V, which is the reason why there are no operating points on the maximum torque line in the figure, but slightly below.

3.5.3 Parametrization of `electricmotor_quasistatic2`

The torque generation is equal in the permanent magnet synchronous machine and brushless DC machines (BLDC) (Fitzgerald et al., 2003). The difference between the machines is that the PMSM is supplied with AC voltage, while the power electronics creates a varying voltage that is used in the BLDC. Historically, BLDCs are often modeled as separately excited DC motors with constant field, while PMSMs are modeled as a synchronous AC machine using the d-q transformation (Guzzella and Sciarretta, 2007). In this section `electricmotor_quasistaic2`, that is a model of a separately excited DC motor with constant field, is parametrized to represent the PMSM described in Section 3.5.2.

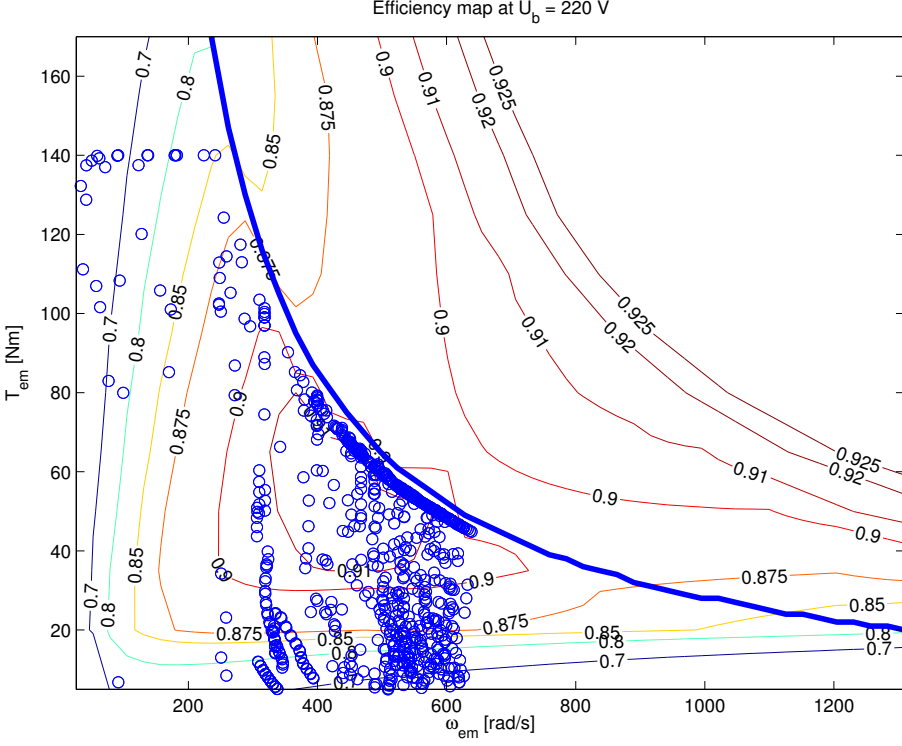


Figure 3.1: The efficiency of the permanent magnet synchronous machine for $U_b=220$ V. In the figure the motor mode is shown, but not generator mode. The efficiency of the machine in generator mode is almost the same as in motor mode. The circles indicate the operating points of the machine when the driving cycle FTP75 is used.

To be able to do the parametrization of k_a , k_i , and R_{em} , the electrical power and the mechanical power are compared to find the expression for the losses in the `electricmotor_quasistaic2` model

$$P_{em,l}^{eq2} = I_{em} \tilde{U}_{em} - T_{em} \omega_{em} \quad (3.7)$$

Substituting U_{em} and I_{em} using (2.23) and (2.24) results in

$$P_{em,l}^{eq2} = \underbrace{\frac{T_{em}^2}{k_a^2}}_{I_{em}^2} R_{em} + \left(\frac{k_i}{k_a} - 1 \right) T_{em} \omega_{em} \quad (3.8)$$

There are three parameters to be identified. These are only included in two terms in the expression, leading to that all parameters cannot be identified.

Using

$$k_{em,1} = \frac{R_{em}}{k_i^2} \quad (3.9)$$

$$k_{em,2} = \frac{k_i}{k_a} \quad (3.10)$$

instead gives

$$P_{em,l}^{eq2} = T_{em}^2 k_{em,1} + (k_{em,2} - 1) T_{em} \omega_{em} \quad (3.11)$$

where the values of the introduced parameters $k_{em,1}$ and $k_{em,2}$, are identified. This is done using least squares to (3.11) and the data from the map described in Section 3.5.2. The battery voltage is not included in (3.11), but is required in the map based model. In the parametrization of the model, the battery voltage is assumed to its open circuit voltage, i.e. 256 V. The values of the parameters found are $k_{em,1} = 0.27 \text{ } \Omega\text{A}/\text{N}^2\text{m}^2$ and $k_{em,2} = 0.99$. The losses in the electric machine in the map and the parametrized equation (3.11) are shown in Figure 3.2. It can be seen in the figure that the `electricmotor_quasistaic2` does not model the losses well, since the dashed lines do not even capture the qualitative behavior of the solid lines.

For comparison to the parameters used in the model described in Section 3.5.1, k_a is set to $0.5 \text{ Nm}/\text{A}$, which is the same value as in the parametrization of `electricmotor_quasistaic2`. Based on this assumption $k_i = 0.495 \text{ Vs}/\text{rad}$ and $R_{em} = 0.067 \text{ } \Omega$ are computed. Note that $k_a > k_i$ and not $k_a < k_i$ as expected.

The unsatisfactory agreement between this model and map data motivates the development of a new model, which is the topic of the next section.

3.5.4 Electricmotor_quasistatic3

A new model of the electric machine called `electricmotor_quasistatic3` is developed, where the losses are modeled differently compared to the models included in `CAPSim`. The resistive losses are modeled in the same way as in `electricmotor_quasistatic1` and `electricmotor_quasistatic2`. Other losses are lumped in `electricmotor_quasistatic2` and modeled by using two constants for the speed and torque constants (see Section 2.6.2 for details). In this model the friction losses are instead modeled, and the combined torque and speed constant k used in `electricmotor_quasistatic1` is used. The friction losses are modeled to be proportional to ω_{em} (Zhu et al., 2000)

$$T_f = c_{em,f} \omega_{em} \quad (3.12)$$

where $c_{em,f}$ is a friction constant. The output torque from the machine is

$$T_{em} = k I_{em} - c_{em,f} \omega_{em} \quad (3.13)$$

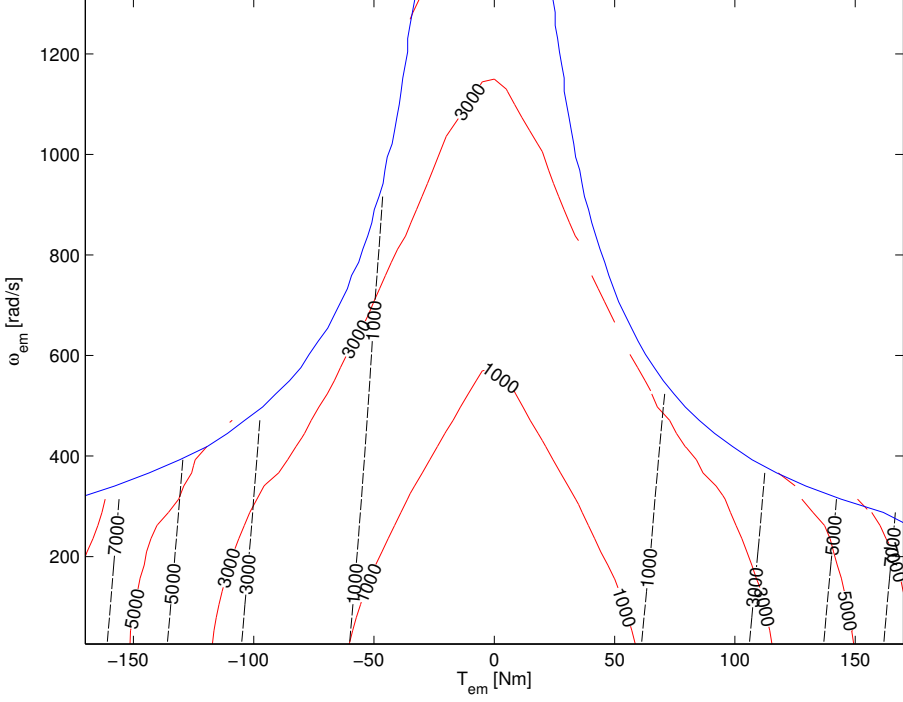


Figure 3.2: The power losses [W] of the electric machine. The dashed lines are the parametrized CAPSim model `electricmotor_quasistatic2`, and the solid lines the losses in the map.

using (2.15), the torque can be expressed as

$$T_{em} = k \left(\frac{U_{em}}{R_{em}} - \frac{k}{R_{em}} \omega_{em} \right) - c_{em,f} \omega_{em} \quad (3.14)$$

The power losses in the machine are computed using

$$P_{em,l}^{eq3} = U_{em} I_{em} - T_{em} \omega_{em} \quad (3.15)$$

By rewriting (2.15) an expression for U_{em} is achieved

$$U_{em} = k \omega_{em} + R_{em} I_{em} \quad (3.16)$$

Using this equation and the expression for I_{em} based on (3.13) results in the following expression for $P_{em,l}$

$$P_{em,l}^{eq3} = R_{em} \left(\frac{T_{em}^2}{k^2} + \frac{2c_{em,f}}{k^2} \omega_{em} T_{em} + \frac{c_{em,f}^2}{k^2} \omega_{em}^2 \right) + c_{f,em} \omega_{em}^2 \quad (3.17)$$

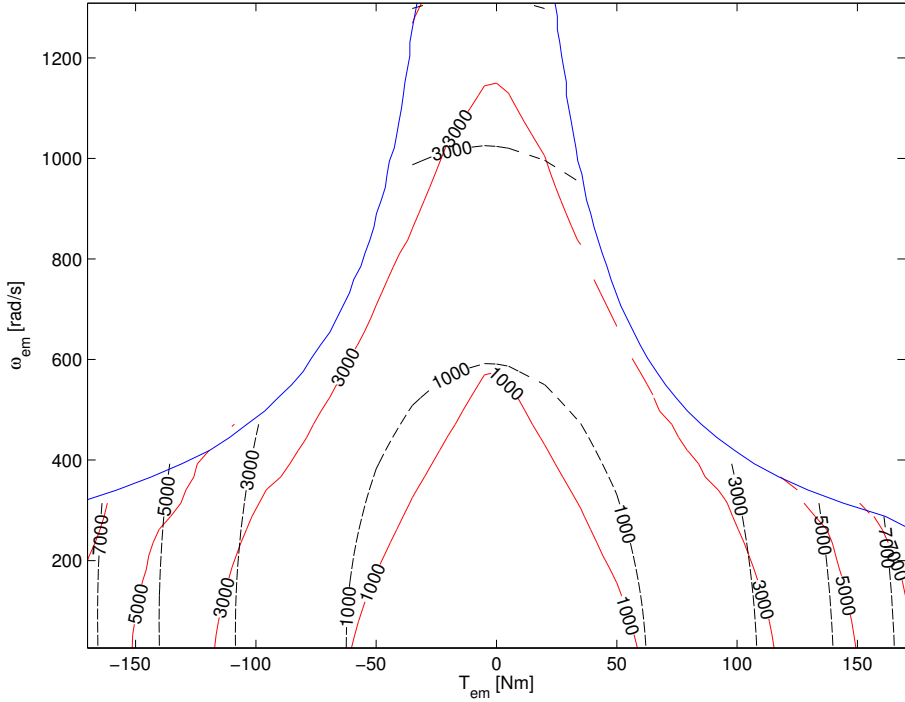


Figure 3.3: *The power losses [W] of the electric machine. The dashed lines illustrate the parametrized model described in Section 3.5.4, and the solid lines the losses in the map described in Section 3.5.2.*

This model is parametrized to fit the data of the losses given in Section 3.5.2. Using least squares of (3.17) results in that the parameters k , R_{em} , and $c_{em,f}$ are found to be 0.495 Nm/A , $0.13 \text{ } \Omega$, and 0.0029 Nm/s , respectively. The battery voltage is assumed to be the open circuit voltage, i.e. 256 V , when using the map to find the losses. The power losses computed in (3.17) are compared with the measured losses in Figure 3.3, and even though the fit is not complete the main qualities are captured.

3.6 Engine

`Engine_scalable1` is used to model the engine. `Engine_gasoline1` is not used since there is a diesel engine in the truck, and `engine_simplemap1` is not used since not enough engine data to parametrize a map is available. `Engine_scalable2` is similar to `engine_scalable1` with the difference that the former includes dynamics with a time constant of approximately two engine cycles. Fast dynamics is not an issue in this investigation, and therefore

Table 3.2: *Some key parameters used in the combustion engine*

Parameter	Value	Unit
Number of cylinders	6	[-]
Stroke	0.165	[m]
Bore	0.144	[m]
Indicated efficiency	0.50	[-]
Max torque (speed)	3150 (1250)	[Nm (rpm)]
Max power (speed)	515 (1700)	[kW (rpm)]
Mass	800	[kg]

`engine_scalable1` is used. There are no changes made in the model compared to the one described in Section 2.8.2. The parameters are based on Volvo's D16 that produces 700 hp. General parameters in the Willans approximation such as the indicated efficiency are the same that are used for a diesel engine in QSS (Guzzella and Amstutz, 1999). Some of the parameters used are presented in Table 3.2.

3.7 Fuel tank

The model for the fuel tank in the truck model is `fueltank_simple1`, and no changes are made in the model.

3.8 Clutch

The model of the clutch is `clutch_simple1`. The maximum torque the clutch is able to transfer is increased to 5000 Nm.

3.9 Mechanical joint

`Mechanicaljoin_gear1` is used to model the connection between the electric machine, clutch and gearbox. The gear ratio between the electric machine and the combustion engine is one when `electricmotor_quasistatic2` is used, and three when the map based model for the electric machine is used.

3.10 Gearbox

The gearbox used in the model is `gearbox_manual1` and is supposed to represent Volvo's Ishift. The gearbox is modeled as a conventional 12 gear manual gearbox with gear ratios between 11.73 (1st gear) and 0.78 (12th gear). The weight of the component is 277 kg and the efficiency is increased to 0.975.

Table 3.3: *The parameters used in the model of the chassis.*

Parameter	Value	Unit
Vehicle total mass	40000	[kg]
Tire specification	315/80R22.5	[-]
Rolling resistance	0.007	[-]
Drag coefficient	0.8	[-]
Vehicle frontal area	10	[m ²]
Final gear	3.21	[-]

3.11 Chassis

The model of the chassis is `chassis_simple4`. The total mass of the vehicle is given as a parameter, instead of being calculated by the sums of the masses of the components in the vehicle, as is the case in the original model. The parameters used are given in Table 3.3.

3.12 Controller and energy management

There are several approaches to energy management, e.g. the global optimal solution (Lin et al., 2003) using dynamic programming, model predictive control (Borhan et al., 2009), or finding equivalent-consumption minimization strategies (ECMS) (Sciarretta and Guzzella, 2007; Sivertsson et al., 2011). In this study a heuristic design is used since it is less complex than the above mentioned methodologies, and the focus is here on the design of the diagnosis systems.

One input signal to the controller is the required torque, T_{req} , from the driver. This torque is to be delivered by the electric machine and the combustion engine, and the SoC of the battery is not to decrease below a certain level, SoC_{ref} . When energy is recuperated, the energy stored in the battery is increased. It is however not possible to increase SoC above a predefined value, $SoC_{UpperLimit}$, in order not to wear the battery, as indicated in Peterson et al. (2010). When $SoC > SoC_{ref}$, energy is primarily taken from the battery, and when $SoC < SoC_{ref}$ the electric machine will never be part of the propulsion of the vehicle. To be more robust to faults in the electrical components, a braking torque is requested from the electric machine if SoC is below a threshold, here set to 5 % below SoC_{ref} . This will lead to that the battery will be charged.

To describe the controller in detail, the implemented controller is given below, where the following parameters and variables are used:

maxEMTorqueLocal: is a parameter that includes information about the maximum torque the electric machine is allowed to deliver. The parameter is dependent on SoC accordingly to Figure 3.4, when SoC_{ref} is set to 0.50.

maxEMTorque: The value of this parameter is set to 200 Nm and gives the maximum value of `maxEMTorqueLocal` when the vehicle is in traction.

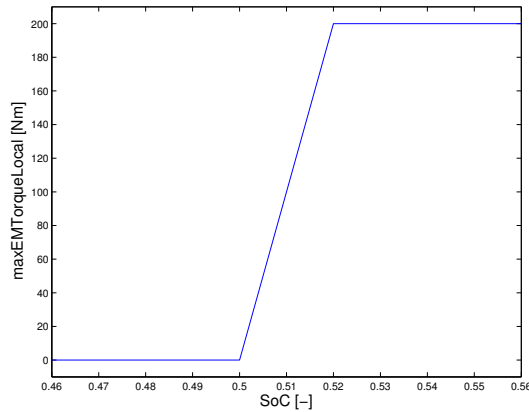


Figure 3.4: The maximum requested torque from the electric machine as a function of SoC. The value of `maxEMTorqueLocal` is found from this function when the vehicle is in traction.

maxEMBrakeTorque: is the maximum brake torque of the electric machine. The value of the parameter is 200 Nm.

connected: is a signal stating if the combustion engine is connected to the wheels or not. The signal is one if the clutch is disengaged and a gear is selected. If any of these conditions are not fulfilled, the signal is zero.

socDiff: is defined as $SoC - SoC_{ref}$.

Gr: is the gear ratio in the gearbox.

The controller is implemented in m-code, that is given here:

```

if Treq < 0
    if soc > socUpperLimit
        Tem = 0;
        Tbrake = Treq;
    else
        if -maxEMBrakeTorque < Treq
            if gear == 0
                Tem=0;
                Tbrake = Treq*Gr;
            else
                Tem = Treq/uem;
                Tbrake = 0;
            end
        else
            if gear == 0
                Tem = 0;
                Tbrake = Treq;
            else

```

```

        Tem = -maxEMBrakeTorque;
        Tbrake = (Treq + maxEMBrakeTorque)*Gr;
    end
end
end
else
    if socDiff > 0
        if socDiff < 0.02
            maxEMTorqueLocal = 50*(socDiff)*maxEMTorque;
        else
            maxEMTorqueLocal = maxEMTorque;
        end
    elseif socDiff < -0.05
        if socDiff > -0.07
            maxEMTorqueLocal = 50*(socDiff+0.05)*maxEMTorque;
        else
            maxEMTorqueLocal = -maxEMTorque;
        end
    else
        maxEMTorqueLocal = 0;
    end

    if connected == 0
        if gear == 0
            Tem = 0;
            Tice = 0;
        else
            if Treq < maxEMTorqueLocal
                Tem = Treq;
                Tice = 0;
            else
                Tem = maxEMTorqueLocal;
                Tice = 0;
            end
        end
    else
        if gear == 0
            Tem = 0;
            Tice = 0;
        else
            if Treq < 0.7*maxEMTorqueLocal
                Tem = Treq*1/uem;
                Tice = 0;
            else
                Tem = 0.7*maxEMTorqueLocal;
                Tice = Treq - Tem*uem;
            end
        end
    end
end
end
end

TeReq1 = Tice;
TemReq1 = Tem;
TbReq1 = Tbrake;

```

When the required torque is positive, it is checked if the torque the electric machine is able to deliver is enough to fulfill the demanded torque. If not, the combustion engine delivers the torque the electric machine was not able to deliver. In order to not add tension to the battery, the maximum torque delivered by the electric machine (see Figure 3.4) is multiplied by 0.7 if the torque requested is positive. This results in that the maximum torque the electric machine is able to deliver is 140 Nm. During regenerative braking the machine is able to apply a negative torque of 200 Nm. The requested torques of the components are filtered and are given by

$$T_{e,req} = \frac{1}{\tau_{ctrls} + 1} T_{e,req1} \quad (3.18a)$$

$$T_{em,req} = \frac{1}{\tau_{ctrls} + 1} T_{em,req1} \quad (3.18b)$$

$$T_{b,req} = \frac{1}{\tau_{ctrls} + 1} T_{b,req1} \quad (3.18c)$$

where τ_{ctrl} is set to 0.1 seconds.

3.13 Driving cycles and simulation results

Simulations of the vehicle are carried out to verify the model. Two driving cycles are used, FTP75 and a velocity profile collected from real driving between Linköping and Jönköping. FTP75 is a driving cycle including many starts and stops (see Figure 3.5), while the collected data represents highway driving. As seen in Figure 3.6, the truck is driving at constant speed at highway driving during most of the time, but at a few times the vehicle decreases the velocity. The slope of the road is such that the vehicle brakes a few times to keep constant speed. When this occurs the battery is charged, which can be seen in the figure. The fuel consumption is 39 l/100km when driving from Linköping to Jönköping, which is a reasonable fuel consumption for a fully loaded long haulage truck.

Diagnosis of the electrical parts of the powertrain is of high interest in this thesis and is handled in Chapters 4-6. With the designed energy management, these components are only active if there are some energy to recuperate, or there are energy stored in the batteries. The electrical components are frequently active when FTP75 is used, since this driving cycle includes many starts and stops. When diagnosis systems are evaluated using the simulation model, it may be preferable to use a driving cycle that frequently excites the components that are to be monitored, and FTP75 is mainly used for this purpose. To verify that these results are valid for a long haulage truck in more standard highway driving, the recorded data from Linköping to Jönköping is used in some cases.

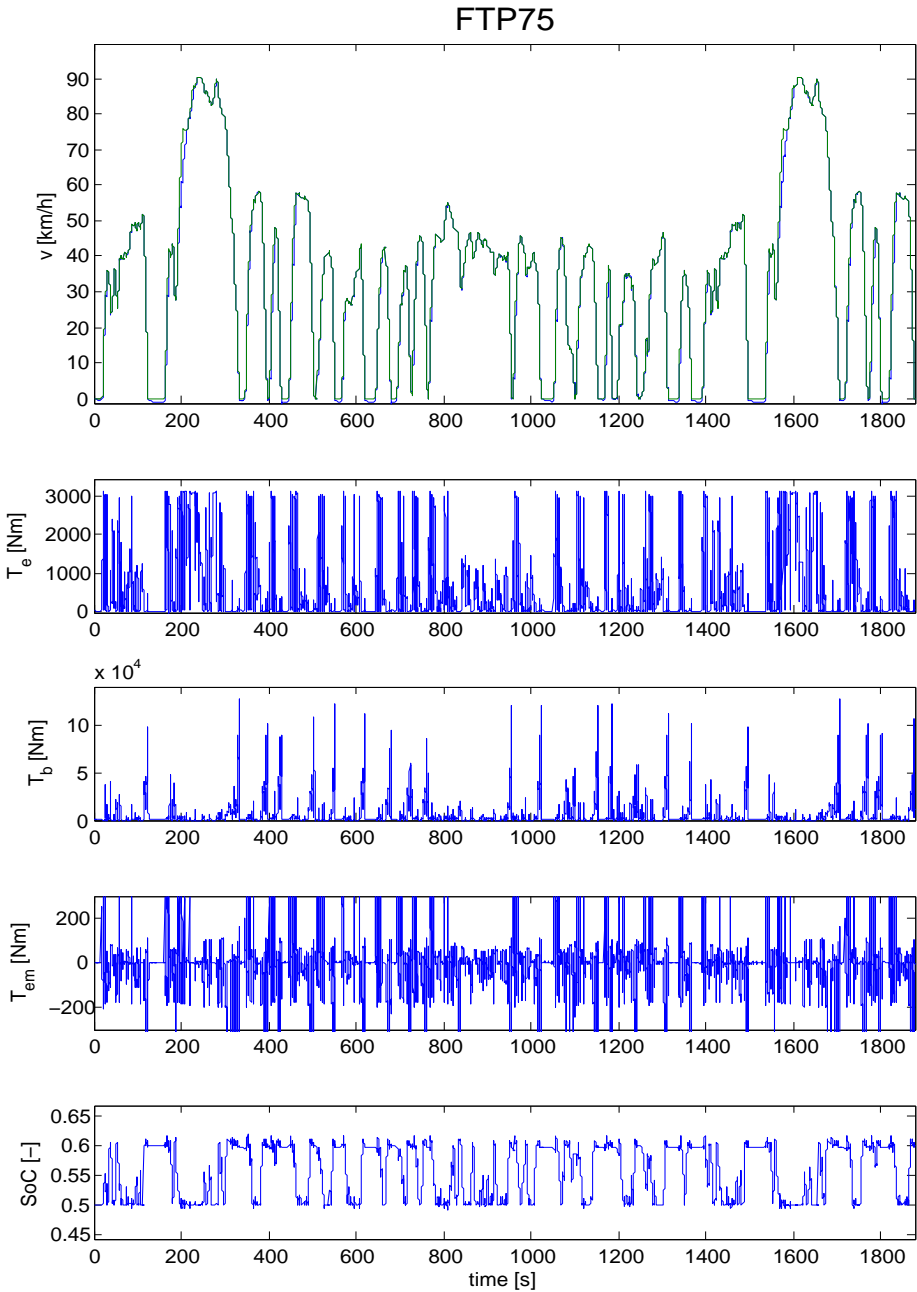


Figure 3.5: The reference velocity and the velocity of the vehicle when FTP75 is used, are given in the first plot. The engine, brake, and electric machine torques, as well as the SoC of the battery are also presented.

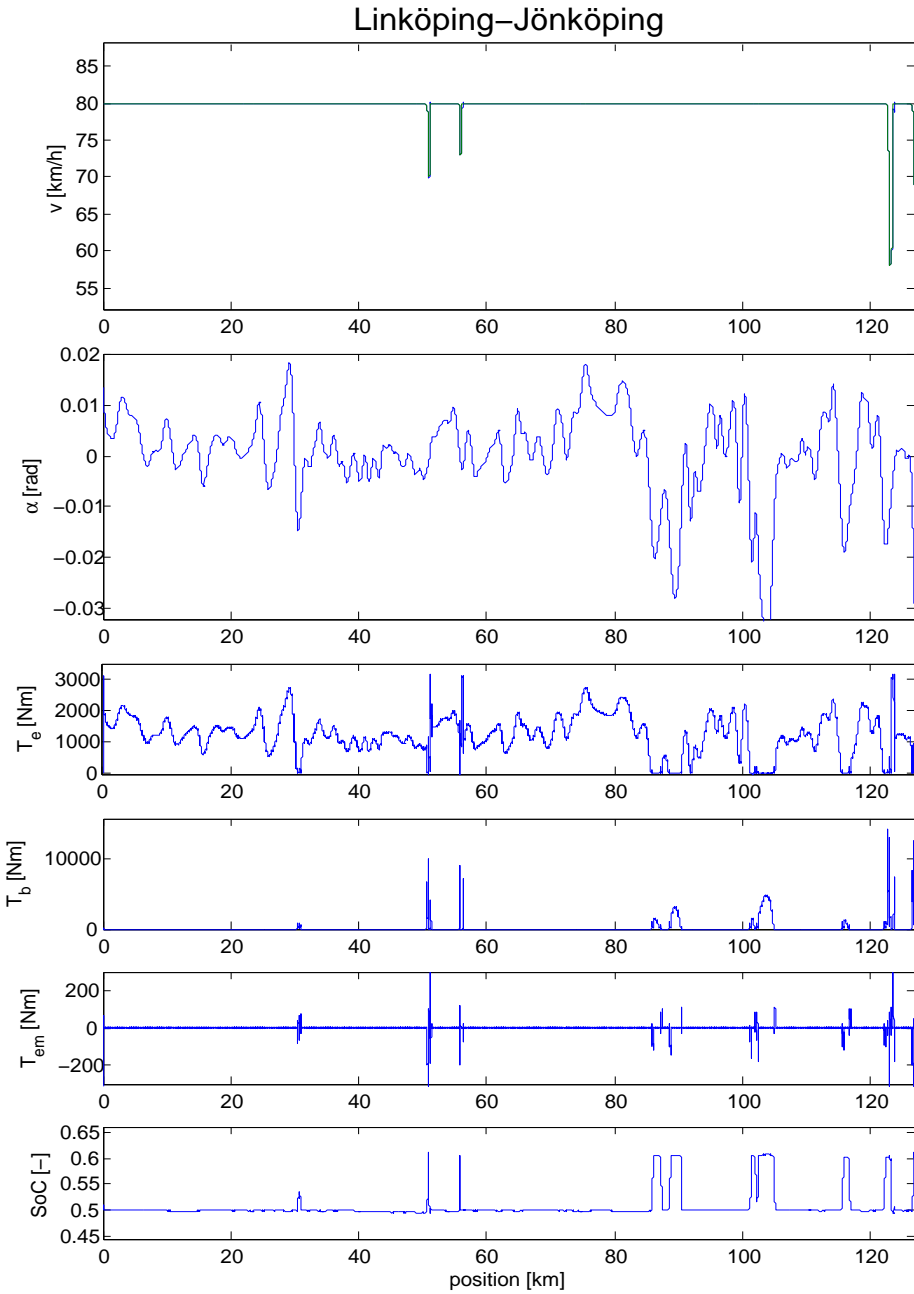


Figure 3.6: The velocity of the truck and road slope when driving from Linköping to Jönköping are presented in the upper plots. The engine, brake, and electric machine torques, as well as SoC are also shown. The electric machine is not used during long periods in this driving scenario.

DIAGNOSIS OF THE TRUCK BASED ON MODELS FOR CORRECT BEHAVIOR

The objective of this chapter is to study topics for monitoring and diagnosis of hybrid vehicle powertrains on vehicle level, i.e. when several components are monitored in the same diagnosis system and these components are connected in a hybrid vehicle architecture. In this chapter it is examined e.g. how the selection of the sensor configuration affects the performance of the diagnosis system. Other issues are how the design of the energy management affects the diagnosis performance, as well as the design and computational complexity of the diagnosis systems. For this purpose, three model based diagnosis systems for the truck are derived, evaluated and compared. The diagnosis systems use different sensor configurations to analyze the implications the sensor configuration has on the diagnosis performance. In the diagnosis systems, only models describing the fault free behavior of the components are used. This means that no information about the faults' impact on the supervised component is used, which saves significant engineering effort in the design of the diagnosis systems.

The model of the truck described in Chapter 3 is used including the electric machine based on an equivalence circuit described in Section 3.5.1. The scope is generic for parallel hybrids, even though the study is based on a specific truck model.

4.1 Mathematical tools

This section consists of two parts. First, when designing the diagnosis systems described in Section 4.6, a well known method called structural analysis is used. There are several different approaches and notations in the field, which are briefly described in Section 4.1.1. Secondly, post processing of the residuals

used in the diagnosis systems are required, and is done in the CUSUM algorithm described in Section 4.1.2.

4.1.1 Structural analysis

Given a model and a set of sensors it is possible to determine what detectability and isolability of the faults that are ideally possible to achieve. In Krysander and Frisk (2008) this is done by a structural analysis (Dustegör et al., 2006; Blanke et al., 2006) of the model. The method is based on that all variables that are used in every equation are listed. How the variables are included (e.g. linear, exponential, differentiated) is not of importance in this analysis.

Structural analysis is based on a bipartite graph, including information about the variables that are included in each model equation. Based on this graph a Dulmage-Mendelsohn decomposition (Dulmage and Mendelsohn, 1958) gives information about what part of the model that is overdetermined and thereby can be monitored. There are several efficient tools available to find subsets of the model with analytical redundancy, and some of these are discussed and compared in Armengol et al. (2009).

Minimal structurally overdetermined sets

Overdetermined sets of model equations are of special interest since they are used to construct residuals, and are denoted e.g. ARRs (Cassar and Staroswiecki, 1997), possible conflicts (Pulido and Gonzalez, 2004), and MSOs (Krysander et al., 2008).

A set of equations, \mathcal{M} , is structurally overdetermined if there are more equations than unknowns in \mathcal{M} . The set \mathcal{M} is a Minimal Structurally Overdetermined (MSO) set if there is no subset of \mathcal{M} that is structurally overdetermined. The structural method used when designing the diagnosis systems in Chapters 4-6 are described in Krysander et al. (2008); Krysander and Frisk (2008).

4.1.2 CUSUM

A residual, r , indicates that a fault has occurred if $r \neq 0$. To handle noise and model uncertainties in the residuals, post processing is necessary. Residual generators are used to construct tests, that are supposed to react if there is a fault in the monitored system. A well known algorithm calculating test quantities is CUSUM (Page, 1954). The basis in the algorithm is to construct a signal, s , that has a negative expectation value in a fault free case, and positive when a fault has occurred. The trend of the cumulative sum, g , of s will contain information about the status of the monitored system

$$s(t) = |r(t)| - \nu \quad (4.1a)$$

$$g(t+1) = g(t) + s(t) \quad (4.1b)$$

where ν is an offset parameter to ensure that $E\{s(t)\} < 0$ in the fault free case.

A test quantity is calculated in the algorithm and is given by

$$T(t) = g(t) - \min_{0 \leq i < t} g(i) \quad (4.2)$$

The test alarms if $T(t)$ is larger than a threshold J .

In the algorithm ν and J are design parameters, and are set to avoid false alarms. The first step to decide the design parameters is to study the residual in the fault free case. The offset parameter ν is set to be large enough to ensure that the demand $E\{s(t)\} < 0$ is fulfilled and thereby avoid false alarms in the tests. If ν is set too large, the fault detection will take longer time and smaller faults in the vehicle will possibly not be detected. This has to be considered in the design of the parameters in the algorithm. After ν is decided, T is studied. The threshold, J , is set to achieve a system that does not alarm when the system is fault free. Tests are carried out where faults are induced in the system. If the diagnosis system lacks in performance, the parameters described above are modified. The fault free case is then analyzed again till a satisfactory performance is achieved.

4.2 Components to monitor

The components monitored in the vehicle level diagnosis systems are the electrical components in the powertrain, i.e. the electric machine, power electronics, and the battery. The model used in the diagnosis systems only describes the fault free behavior of the truck, which is beneficial since the diagnosis systems are more generic and easier to design compared to a system including fault models.

The power electronics delivers a requested voltage to the electric machine by transforming the battery voltage. A fault in the power electronics is assumed to result in that $U_{em} \neq U_{em,ctrl}$. Except from that it is not known how the fault will affect U_{em} in the diagnosis systems.

In some cases it is of interest to detect what part of a component that is broken. To represent this, variations in both the inner resistance and the torque constant in the electric machine are fault modes that are to be monitored and isolated from each other. The component is broken if at least one of these parameters has drifted from its nominal value.

The fault in the battery that is monitored is a short circuit. This will affect the battery voltage, since the number of cells that is used in the battery is reduced when a short circuit occurs. In the diagnosis system, the knowledge that the number of cells used never can be more than there are physical cells, is never used.

There is a possibility to add the functionality to monitor the sensors used in the model. This means that a fault in the sensor should be detected and isolated from the other fault modes by the diagnosis system. The sensors that are monitored differ from each system and are stated in the description of the diagnosis systems in Section 4.6.

Table 4.1: Values of faults induced in the model. The voltage U_{em} varies in the range $0 - 200$ V, $U_b \approx 250$ V, and $\omega_{gb} < 50$ rad/s.

Faults	Value
$f_{em,ka}$	-0.5
$f_{em,R}$	-0.5
f_{pe}	-0.5
$f_{b,sc}$	-0.5
$f_{b,U,sens}$	20 V
$f_{em,U,sens}$	20 V
$f_{gb,\omega,sens}$	20 rad/s

4.3 Induced faults

The induced faults in the model affects the same parameters that are affected in the fault modes in the components that are to be monitored (see Section 4.2). To model that the battery, power electronics, or the electric machine may break down, two parameter values and two voltages in these models have the possibility to be modified. Note that these faults are only examples of how a fault in these components can be represented in the model. The following modifications of the signals are introduced to model the faults, where the nominal signals are denoted by the superscript *nom*:

$$f_{em,ka} : k_a = (1 + f_{em,ka}) k_a^{nom} \quad (4.3a)$$

$$f_{em,R} : R = (1 + f_{em,R}) R_{em}^{nom} \quad (4.3b)$$

$$f_{pe} : U_{em,ctrl} = (1 + f_{pe}) U_{em,ctrl}^{nom} \quad (4.3c)$$

$$f_{b,sc} : U_b = (1 + f_{b,sc}) U_b^{nom} \quad (4.3d)$$

where $f_{b,sc}$ models that not all cells in the battery are used due to an internal short circuit, f_{pe} is a fault in the power electronics, and $f_{em,ka}$ and $f_{em,R}$ are two fault modes in the electric machine.

Sensor faults are modeled as an offset fault, e.g. for the voltage sensor in the electric machine

$$U_{em,sens} = U_{em} + f_{em,U,sens} \quad (4.4)$$

When a fault is induced in the model, the value of the fault is given in Table 4.1.

4.4 Sensor noise and sample frequency

In order to get a more realistic simulation, noise \tilde{v} is included in the sensor signals. The block used in Simulink to produce the noise signals is called **Band-Limited White Noise**, and the power of the noise added to the sensors

Table 4.2: *The intensity of the noise added to the sensor signals in the model according to (4.5).*

Sensor	Noise Power
$U_{b,sens}$	0.01
$I_{b,sens}$	0.01
$I_{em,sens}$	0.01
$U_{em,sens}$	0.01
$T_{em,sens}$	0.01
$\omega_{em,sens}$	0.005
$\omega_e,sens$	0.005
$\omega_{gb,sens}$	0.005
$\omega_w,sens$	0.005

used in the model is given in Table 4.2. The measurement signal y is given by the noise free signal y^* added with \tilde{v}

$$y = y^* + \tilde{v} \quad (4.5)$$

The sensors measure the signals at 80 Hz and the diagnosis system is updated at the same frequency, while the vehicle model is simulated using a variable step length solver.

4.5 Sensor configurations

One way to investigate the properties of the diagnosis systems regarding detectability and isolability is to use structural analysis. The basic idea is to, as stated in Section 4.1.1, tabulate the variables and faults each equation in the model is dependent on. The result from the analysis depends on what sensors that are used in the diagnosis system. The outcome from the analysis is examples of how to combine parts of the model to achieve over determined parts that may be used in the diagnosis. Some of these parts are used to produce tests that alarm if the over determined equation system does not have any solution. The overdetermined parts used in the tests are selected to achieve as good fault isolability as possible without using fault models in the diagnosis systems.

The three designed diagnosis systems use different sensor configurations. One system has a sensor configuration resulting in a diagnosis system where the tests are based on a small part of the vehicle model. This system uses a torque sensor in the electric machine that is not used in the second system. The third system is based on a sensor configuration using as few sensors as possible to structurally achieve full fault isolability. The sensor configurations used in the systems are described one by one below.

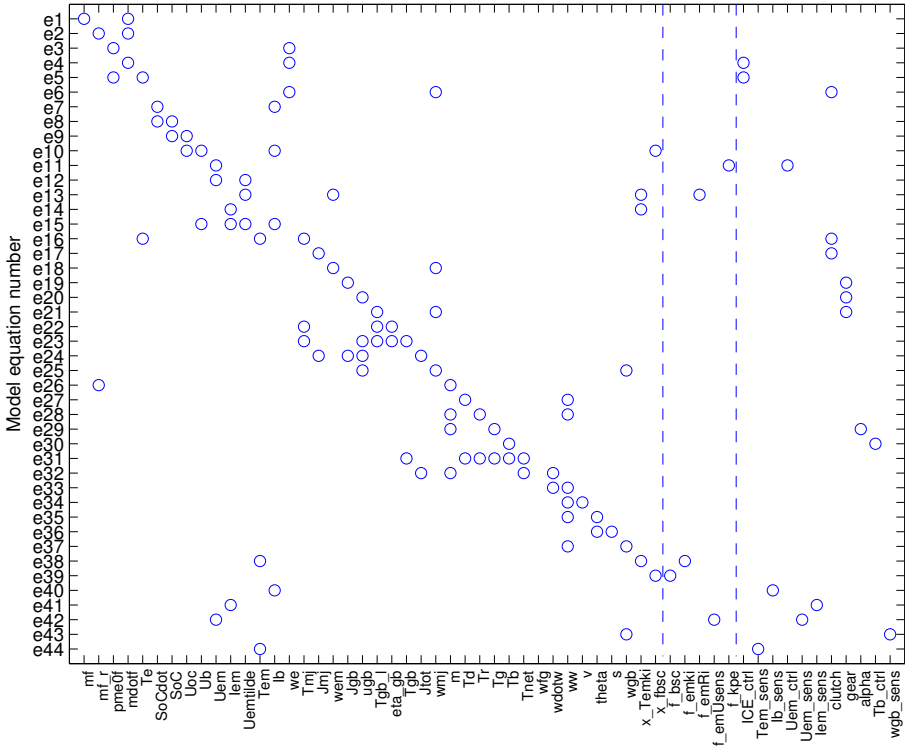


Figure 4.1: The structural model of the truck using the sensor configuration Diagnosis system 1 is based on. Each row represents an equation, each column a variable, fault or known signal, and the circles indicate the variables, faults, and known signals included in each equation. The variables to the left of the dashed lines are unknown variables, between the lines are possible faults, and to the right the known signals, such as sensor signals and signals from the controllers.

4.5.1 Diagnosis system 1

The following sensors are used in the first diagnosis system:

- $\omega_{gb,sens}$ - outgoing speed of the gear box
- $I_{b,sens}$ - battery current
- $I_{em,sens}$ - electric machine current
- $U_{em,sens}$ - electric machine voltage
- $T_{em,sens}$ - torque delivered by the electric machine. This sensor is not common in series production

The structural model using this sensor configuration is shown in Figure 4.1. The last five equations represent the sensor equations and are modified if a different

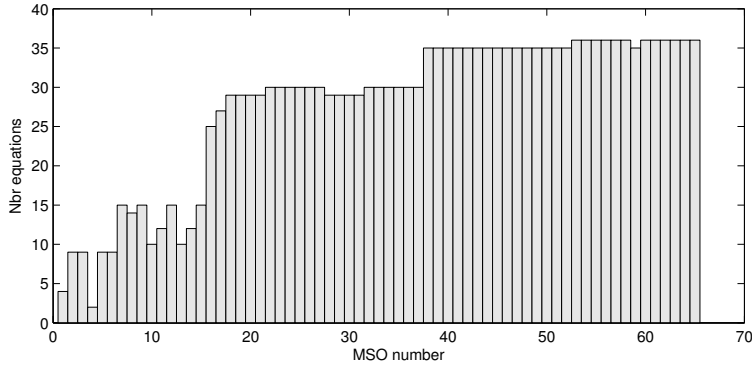


Figure 4.2: *The number of equations used in each MSO for the sensor placement in Diagnosis system 1. As seen in the figure there are a few MSOs based on few equations, but most of the MSOs are based on a larger part of the entire model, that includes 44 equations.*

sensor configuration is used. In the figure the unknowns are in the left part, the faults in the middle, and the known variables at the right. On the vertical axis all equations in the model are given. In this example there are 44 equations.

For this sensor configuration it is possible to construct 65 MSOs, and the number of model equations each MSO consists of is shown in Figure 4.2. The number of MSOs, that here are used to construct tests, increases when more sensors are used. This is due to that there are more possibilities to create overdetermined sets of equations when many sensors are used. Observe that not all MSOs are used to construct tests that are the basis in the diagnosis system. In general, many equations in a test leads to that higher computational effort is required, as well as increased sensitivity for noise and model uncertainties. Some of the equations are trivial relationships such as sensor equations. If the sensor is not to be monitored by the diagnosis system (4.5) is used as the sensor equation, otherwise a combination of (4.4) and (4.5) is used resulting in

$$y = y^* + \tilde{v} + f_{sens}$$

where f_{sens} is a fault in the sensor.

4.5.2 Diagnosis system 2

In this diagnosis system the sensors used are similar to the previous system. The difference is that the torque sensor in the electric machine is replaced with an engine speed sensor. This results in that the following sensors are used in this system:

- $\omega_{e,sens}$ - engine speed
- $\omega_{gb,sens}$ - outgoing speed of the gear box

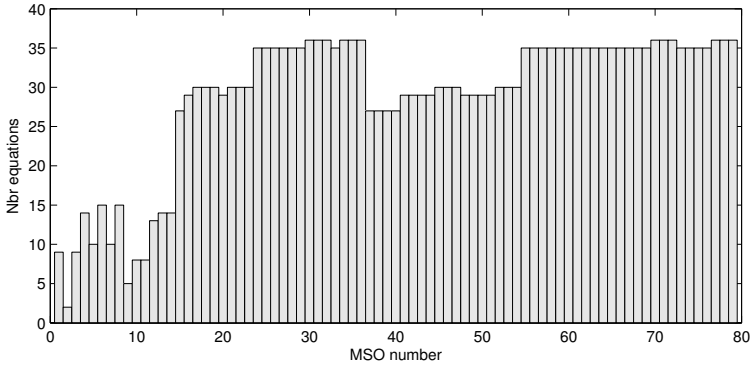


Figure 4.3: The number of equations used in each MSO for the sensor placement used in Diagnosis system 2.

- $I_{b,sens}$ - battery current
- $I_{em,sens}$ - electric machine current
- $U_{em,sens}$ - electric machine voltage

The number of equations included in the MSOs for this sensor configuration are shown in Figure 4.3. There is no major difference in the size of the MSOs using the sensor configurations in Diagnosis system 1 and Diagnosis system 2.

4.5.3 Diagnosis system 3

In this diagnosis system a minimal set of sensors are used to achieve full fault isolability. To achieve this, structural analysis is used to propose sensor configurations that fulfill the demand on full fault isolability in the system (Krysanter and Frisk, 2008). It can be shown that two sensors are sufficient to isolate the four fault modes in the electrical components described in Section 4.2. To be able to also isolate faults from all sensors in the system, three sensors are required. There are several sensor configurations that manage this, but in this specific system the following sensor configuration is used:

- $\omega_{gb,sens}$ - outgoing speed of gearbox
- $U_{b,sens,a}$ - battery voltage
- $U_{b,sens,b}$ - battery voltage

If only one battery voltage sensor is used, a fault in this sensor cannot be isolated from other faults. Therefore two voltage sensors are required.

The number of equations included in the MSOs for this sensor configuration are shown in Figure 4.4. There are not as many over determined parts using this sensor configuration compared to Diagnosis system 1 and Diagnosis system 2. This is due to that fewer sensors are used in this system. The number of tests based on smaller parts of the model are also fewer in this system.

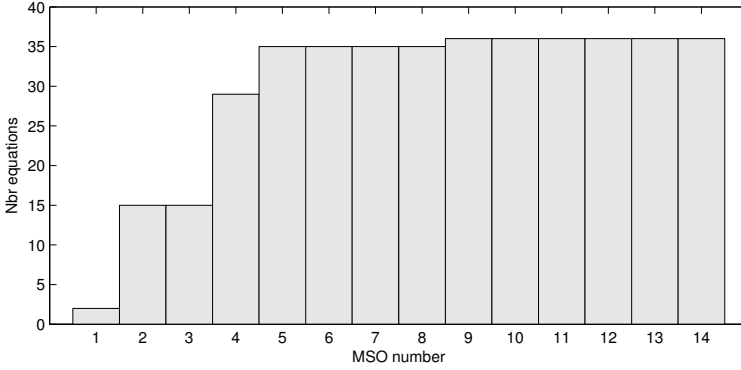


Figure 4.4: *The number of equations used in each test for the sensor placement used in Diagnosis system 3. There are not as many MSOs that include few equations as in the previous diagnosis systems. There are also fewer minimal structural overdetermined parts in the system since there are less sensors used.*

4.6 Design of diagnosis systems

The results from the structural analysis states what the performance of the diagnosis system ideally will be, but this analysis does not give any information about e.g. robustness to noise and model uncertainties. Further, there is no guarantee that every fault is detectable in all driving modes. A fault in the electric machine that only influences the system when there is a torque delivered by the component will e.g. not be detected if the vehicle does not use the electric machine. To investigate such issues the diagnosis systems are implemented in the simulation platform according to Figure 1.1, and the design of the diagnosis systems are described in this section. Simulations are carried out and the results are presented in Section 4.7.

4.6.1 Diagnosis system 1

The first diagnosis system uses the engine torque T_{em} as a measured signal, and series production vehicles are usually not equipped with torque sensors. However, this diagnosis system is of interest since it is used to investigate how the diagnosis performance is affected when many signals are measured in the components to be monitored. In addition to the faults listed in (4.3), the voltage sensor in the electric machine is monitored in the diagnosis system.

The diagnosis system is based on model equations from the battery, electric machine, mechanical joint, and the gearbox. There are four tests that use subsets of equations from these models, in order to only be sensitive to some of the fault modes. This is the basis to isolate the faults and not only detect that the system is faulty. Full isolability is achieved using these four tests according to the structural analysis. The tests that are included in the diagnosis system are described below.

Test 1

The first test in this diagnosis system uses the model for the power electronics to detect a fault in this component. The voltage sensor in the electric machine is used in Test 1

$$- U_{em,sens}$$

and the faults the test reacts on according to the structural analysis are

$$- f_{pe}$$

$$- f_{em,U,sens}$$

The residual generator is given below and will ideally react on these two faults

$$r = U_{em,sens} - U_{em}$$

where

$$U_{em} = U_{em,ctrl}$$

Test 2

Test 2 includes parts of the model of the electric machine, and is sensitive for the two faults in the machine. The sensors used in the test are

$$- T_{em,sens}$$

$$- \omega_{gb,sens}$$

and the faults the test reacts on according to the structural analysis are

$$- f_{em,ka}$$

$$- f_{em,R}$$

$$- f_{pe}$$

The residual generator is

$$r = T_{em,sens} - T_{em}$$

where T_{em} is calculated using the substitution chain

$$T_{em} = \frac{\tilde{U}_{em}k_a}{R_{em}} - \frac{\omega_{em}k_a k_i}{R_{em}}$$

$$\tilde{U}_{em} = \frac{1}{\tau_{em}s + 1} U_{em}$$

$$U_{em} = U_{em,ctrl}$$

$$\omega_{em} = u_{em}\omega_{mj}$$

$$\omega_{mj} = u_{gb}\omega_{gb}$$

$$u_{gb} = f(\text{gear})$$

$$\omega_{gb} = \omega_{gb,sens}$$

The angular speed in the electric machine is calculated using the speed sensor at the outgoing shaft of the gearbox and the gear ratios in the gearbox, u_{gb} , and the mechanical joint, u_{em} , according to

$$\omega_{em} = u_{em}u_{gb}\omega_{gb,sens}$$

The noise in $\omega_{gb,sens}$ is amplified with the gear ratios when ω_{em} is computed, and this signal is later used in the residual generator. To get equal test significance for all gears, varying parameters in the post processing of the residuals need to be considered. Here a simple approach is adopted where the test is not valid for gears 1-4, and the test quantity thereby is not updated since u_{gb} is large for low gears.

Test 3

Test 3 monitors the battery and parts of the electric machine using the following sensors

- $I_{b,sens}$
- $I_{em,sens}$
- $\omega_{gb,sens}$

and the faults the test reacts on according to the structural analysis are

- $f_{em,R}$
- $f_{b,sc}$

The residual generator is

$$r = I_b - I_{b,sens}$$

where

$$\begin{aligned} I_b &= I_{em} \frac{\tilde{U}_{em}}{U_b} \\ \tilde{U}_{em} &= I_{em}R_{em} + \omega_{em}k_i \\ \omega_{em} &= u_{em}\omega_{mj} \\ \omega_{mj} &= u_{gb}\omega_{gb} \\ u_{gb} &= f(\text{gear}) \\ U_b &= nU_{oc} - nR_bI_b \\ U_{oc} &= f(\text{SoC}) \\ \text{SoC} &= \int \text{SoC} dt \\ \text{SoC} &= -\frac{I_b}{Q_b} \\ I_{em} &= I_{em,sens} \\ \omega_{gb} &= \omega_{gb,sens} \end{aligned}$$

This expression contains an integration to compute SoC . In most cases it is troublesome to integrate signals, since a small bias in the model causes drift in the integrated signal. In this case the state of charge is used only to calculate U_{oc} , that is modeled to be constant for large variations in SoC (see Figure 2.4). In the diagnosis systems that are not updated at all times, drift is a problem if longer driving cycles are used. This is not the case with the actual parameter configuration of the vehicle and the driving cycles used. Therefore the issue about drift in the integrator is not handled in this investigation.

Test 4

The sensors used in Test 4 are

- $I_{b,sens}$
- $U_{em,sens}$
- $T_{em,sens}$

and the faults the test reacts on according to the structural analysis are

- $f_{em,ka}$
- $f_{b,sc}$
- $f_{em,U,sens}$

The residual generator is

$$r = T_{em}\tilde{U}_{em} - I_b U_b k_a$$

where

$$\begin{aligned}\tilde{U}_{em} &= \frac{1}{\tau_{em}s + 1} U_{em} \\ U_b &= nU_{oc} - nR_b I_b \\ U_{oc} &= f(SoC) \\ SoC &= \int SoC dt \\ \dot{SoC} &= -\frac{I_b}{Q_b} \\ I_b &= I_{b,sens} \\ U_{em} &= U_{em,sens} \\ T_{em} &= T_{em,sens}\end{aligned}$$

Thresholds in tests

Table 4.3 shows the parameter values used in the CUSUM algorithm described in Section 4.1.2 for this diagnosis system.

Table 4.3: Offsets, ν , and thresholds, J , used in the CUSUM algorithm in the tests in Diagnosis system 1.

	offset	threshold
$T1$	2	100
$T2$	20	1000
$T3$	10	100
$T4$	400	5000

Decision structure

Full isolability is achieved as long as the tests reacts on the faults as given in the structural analysis. This can be seen in the decision structure in Table 4.4. The table indicates what tests that are supposed to react on each fault mode. If only one test alarms, a fault may have occurred in any of the faults the test is expected to react on. If two or more tests alarm, the possible faults explaining this behavior are the faults that should get all tests that are triggered to alarm. Single faults are assumed in this study, leading to that the possible fault modes are given by the intersection of the fault modes in the tests that have reacted.

The diagnosis system is according to Table 4.4 able to decide which fault that has occurred, and not only detect that the system is faulty. Fault isolability is achieved since there is a unique set of tests that ideally alarm for each fault.

Table 4.4: Decision structure for Diagnosis system 1.

	$f_{em,ka}$	$f_{em,R}$	f_{pe}	$f_{b,sc}$	$f_{em,U,sens}$
$T1$			X		X
$T2$	X	X	X		
$T3$		X		X	
$T4$	X			X	X

4.6.2 Diagnosis system 2

The faults that are to be monitored in Diagnosis system 2 are the same as in the previous diagnosis system, which means that $U_{em,sens}$ is monitored in addition to the components given in Section 4.2. This diagnosis system is based on four tests, which achieves full isolability of the fault modes according to the structural analysis. Model equations from all components in the vehicle given in Figure 2.2 are used in this diagnosis system. The combustion engine and the clutch are used since the control signal to the engine is used to calculate the torque delivered from the engine. This torque is used to calculate the net torque on the wheels. The model for the clutch is required to do this, but modeling the clutch accurately during slip is a well known problem. Therefore, the model of the clutch used in the vehicle model is assumed not to be known in the diagnosis

systems. The clutch model used in the diagnosis system is valid only when the clutch is fully disengaged or engaged, and is assumed to be an ideal component. When there is a slip in the clutch, the model is not valid and the test quantities based on this model in the diagnosis system are not updated. The four tests implemented in the diagnosis system are described below.

Test 1

The first test is the same as Test 1 in Diagnosis system 1. The voltage sensor in the electric machine is used

$$- U_{em,sens}$$

and the faults the test reacts on according to the structural analysis are

$$\begin{aligned} &- f_{pe} \\ &- f_{em,U,sens} \end{aligned}$$

The residual generator is

$$r = U_{em} - U_{em,sens}$$

where

$$U_{em} = U_{em,ctrl}$$

Test 2

The second test consists of parts of the models of the electric machine, battery and gear box. The sensors used are

$$\begin{aligned} &- I_{b,sens} \\ &- I_{em,sens} \\ &- \omega_{gb,sens} \end{aligned}$$

and the faults the test reacts on according to the structural analysis are

$$\begin{aligned} &- f_{b,sc} \\ &- f_{em,R} \end{aligned}$$

The residual generator is

$$r = I_{b,sens} - I_b$$

where

$$\begin{aligned}
 I_b &= I_{em} \frac{\tilde{U}_{em}}{nU_{oc} - nR_b I_b} \\
 \tilde{U}_{em} &= I_{em} R_{em} + \omega_{em} k_i \\
 \omega_{em} &= u_{em} \omega_{mj} \\
 \omega_{mj} &= u_{gb} \omega_{gb} \\
 u_{gb} &= f(\text{gear}) \\
 U_{oc} &= f(\text{SoC}) \\
 \text{SoC} &= \int S\dot{o}C \, dt \\
 S\dot{o}C &= -\frac{I_b}{Q_b} \\
 I_b &= I_{b,sens} \\
 I_{em} &= I_{em,sens} \\
 \omega_{gb} &= \omega_{gb,sens}
 \end{aligned}$$

Test 3

Test 3 uses most of the model of the vehicle and the following sensors are used in the test

- $\omega_{e,sens}$
- $\omega_{gb,sens}$

and the faults the test reacts on according to the structural analysis are

- f_{pe}
- $f_{em,R}$
- $f_{em,ka}$

The residual generator is

$$\begin{aligned}
 \tilde{r} &= \underbrace{\frac{1}{u_{em}} \left(J_{tot} + \frac{1}{u_f^2} m_v r_w^2 \right)}_a \dot{\omega}_{gb} + \\
 &+ \underbrace{\frac{1}{u_{em} u_f} (T_d + T_r + T_b) + \frac{u_{gb} \eta_{gb}}{u_{em}} (T_{gb,l} - T_e) - (u_{gb} \eta_{gb}) T_{em}}_b \quad (4.6)
 \end{aligned}$$

where

$$\begin{aligned}
u_{gb} &= f(\text{gear}) \\
\dot{m}_f &= \text{ice}_{ctrl} \frac{\omega_e}{4\pi q_{LHV}} \\
m_{f,r} &= \int \dot{m}_f dt \\
m_v &= m_{v,0} - m_{f,r} \\
\eta_{gb} &= \begin{cases} \eta_{pos}, & T_{mj} > T_{gb,l} \\ \eta_{neg}, & T_{mj} \leq T_{gb,l} \end{cases} \\
T_{mj} &= u_{em} T_{em} + T_c \\
T_c &= T_e, \text{ when clutch engaged} \\
J_{tot} &= (J_{gb} + J_{mj}) u_{gb}^2 \\
J_{gb} &= f(\text{gear}) \\
J_{mj} &= J_{em} u_{em}^2 + J_c + J_e \\
T_d &= \frac{1}{2} \rho C_d A_f \omega_w^2 r_w^3 \\
T_r &= \begin{cases} m_v g C_r r_w, & 1000 \omega_w > m_v g C_r r_w \\ 1000 \omega_w, & -m_v g C_r r_w \leq 1000 \omega_w < m_v g C_r r_w \\ -m_v g C_r r_w, & 1000 \omega_w \leq -m_v g C_r r_w \end{cases} \\
T_b &= T_{b,ctrl} \\
T_{gb,l} &= f(\text{gear}, \omega_e) \\
\omega_w &= \frac{\omega_{gb}}{u_f} \\
T_e &= \left(\text{ice}_{ctrl} \frac{4\eta_{e,i}}{N_{cyl} \pi S B^2} - p_{me0,f} - p_{me0,g} \right) N_{cyl} \frac{S B^2}{16} \\
p_{me0,f} &= k_1 (k_2 + k_3 S^2 \omega_e^2) \Pi \sqrt{\frac{k_4}{B}} \\
T_g &= m_v g r_w \sin \alpha \\
T_{em} &= \frac{\tilde{U}_{em} k_a}{R_{em}} - \frac{\omega_{em} k_a k_i}{R_{em}} \\
\tilde{U}_{em} &= \frac{1}{\tau_{em} s + 1} U_{em} \\
U_{em} &= U_{em,ctrl} \\
\omega_e &= \omega_{e,sens} \\
\omega_{gb} &= \omega_{gb,sens}
\end{aligned}$$

In the expression for \tilde{r} above, $\dot{\omega}_{gb}$ is needed. The signal ω_{gb} is a sensor signal including noise and it is thereby unwanted to differentiate this signal. One solution is to integrate (4.6). The problem doing this is that a small modeling

fault results in drift in the integrated signal. Instead the residual in (4.6) is filtered to obtain the residual r

$$r = \frac{\alpha}{p + \alpha} \underbrace{(a\dot{\omega}_{gb} + b)}_{\tilde{r}} \quad (4.7a)$$

Now, it is possible to compute r in (4.7a), without calculating a differentiated signal using a variable transformation. Conditions for this to be possible is that the residual generator can be written on the form $\tilde{r} = a\dot{\omega}_{gb} + b$, where a is a constant and b a function of known signals, and the residual is filtered as in (4.7a) (Frisk and Nyberg, 2001). For \tilde{r} in (4.6), a is almost constant. The mass of the vehicle is decreased when fuel is consumed affecting a , though this is assumed not to influence the solution since the change is slow. The inertia is dependent on selected gear, but this is not a problem since the model is only valid when the clutch is engaged, and therefore the inertia is constant when the model is valid. by introducing the state Γ , the variable transformation is

$$\Gamma = r - \alpha a \omega_{gb} \quad (4.7b)$$

We obtain that the residual generator in (4.7a) can be expressed as

$$\dot{\Gamma} = -\alpha \Gamma - \alpha^2 a \omega_{gb} + \alpha b \quad (4.7c)$$

$$r = \Gamma + \alpha a \omega_{gb} \quad (4.7d)$$

The filter parameter α can be modified in the design of the low pass filter of the residual, where a smaller α filters the signal more. The disadvantage with this is that if there is an error in the initialization of the signal, it will take longer time before the error has faded out. On the other hand, it may be difficult to detect faults using a faster filter, due to the noise in \tilde{r} is more apparent in r in such a case.

When no gear is selected or the clutch is not engaged, the residual as well as the test quantity are not updated in this test. When the model in the diagnosis system is getting valid, Γ is reinitialized. This is needed since the state probably has drifted during the time the model was invalid. When Γ is initialized, it is always assumed that the vehicle is fault free. The expression for Γ when the model is getting valid at time t_0 is therefore

$$\Gamma(t_0) = -\alpha a \omega_{gb}(t_0) \quad (4.8)$$

Using this expression in the initialization is not a good idea, since it is sensitive to noise in $\omega_{gb, sens}$ at one sample. This can lead to a significant offset in the residual before the fault has faded out. To reduce the problem, the right hand side of (4.8) is filtered. It is possible to filter the sensor signal since $\omega_{gb} = \omega_{gb, sens}$ is valid even when the entire model used in the residual generator is not valid. Figure 4.5 shows the signal of $\alpha a \omega_{gb}$ in addition to this signal filtered with different time constants. The filter reduces the above described

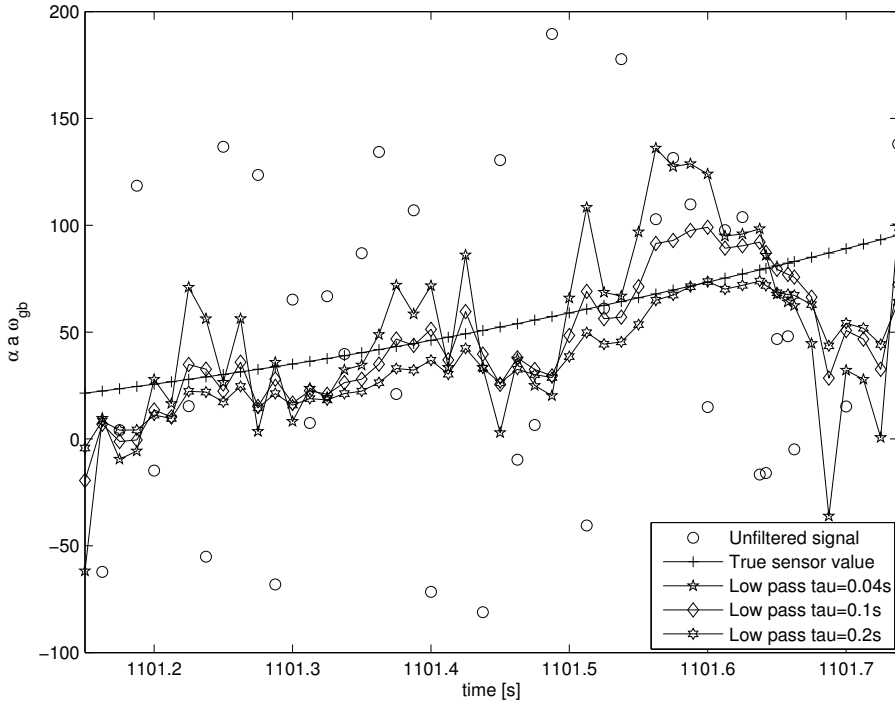


Figure 4.5: Three time constants in the filter of $\alpha\omega_{gb}$, in addition to the unfiltered signal, are included in the figure. The filter with small time constant is more noisy than the others, while the filter with large time constant has a time delay during the transient. The time constant is set to 0.1 seconds in the diagnosis systems.

problem in the initialization of the state. The signal is still noisy, but if it is more filtered there are significant errors during transients. The chosen time constant for all tests in this chapter using the filter is 0.1 seconds. One way to possibly increase the performance of the diagnosis system is to use the last valid value of the residual in (4.8) instead of assuming that the system is fault free. This possibly increases the performance of the diagnosis system when there e.g. are many gear changes, making the diagnosis system valid only for short periods.

To further reduce the issues when reinitializing the state in the residual generator, the CUSUM algorithm is not updated for the first 10 seconds after the model is getting valid. During this time, most of the error in the initialization of Γ will fade out. The drawback with this is that the test may be inactive a significant part of the time, and thereby reducing the performance of the system.

Test 4

This test is similar to the previous test. The same consistency relation is used in both tests, but some of the variables are calculated in different ways. The battery model is e.g. included in this test, but not in Test 3. The same transformation of the residual generators described in (4.7) is used in both tests. The following four sensors are used in this test

- $\omega_{e,sens}$
- $\omega_{gb,sens}$
- $U_{em,sens}$
- $I_{b,sens}$

and the faults the test reacts on according to the structural analysis are

- $f_{em,ka}$
- $f_{b,sc}$
- $f_{em,U,sens}$

In the residual generator, that is given in Appendix B.1, I_{em} is calculated by

$$I_{em} = \frac{I_b U_b}{\tilde{U}_{em}} \quad (4.9)$$

according to (B.1). The residual is not calculated when $|\tilde{U}_{em}| < 1$ V, in order to avoid division by a small number in the expression for I_{em} . Therefore, when $|\tilde{U}_{em}| < 1$ V, the test is not valid and the test quantity is not updated. This is also the case when the clutch is engaged or no gear is selected. The residual generator starts to update three seconds after the clutch has been disengaged. When any of these three cases occurs, the residual and the test quantity is not updated. As in Test 3, the test quantity starts to be updated 10 seconds after the residual is updated, to be less sensitive to errors in the initialization of Γ in (4.7).

Thresholds in tests

Table 4.5 shows the parameter values used in the CUSUM algorithm for this system.

Table 4.5: *Offsets, ν , and thresholds, J , used in the CUSUM algorithm in the tests in Diagnosis system 2.*

	offset	threshold
$T1$	2	500
$T2$	12	4000
$T3$	60	30000
$T4$	60	30000

Decision structure

In Table 4.6 the decision structure for this diagnosis system is shown. Full fault isolability is achieved according to the decision structure that is based on the structural analysis.

Table 4.6: *Decision structure for Diagnosis system 2.*

	$f_{em,ka}$	$f_{em,R}$	f_{pe}	$f_{b,sc}$	$f_{em,U,sens}$
T1			X		X
T2		X		X	
T3	X	X	X		
T4	X			X	X

4.6.3 Diagnosis system 3

A minimal set of sensors is used in Diagnosis system 3 to still achieve full fault isolability. In addition to the faults given in Section 4.2, all sensors are monitored in Diagnosis system 3. If the sensors are not monitored, two sensors manage the task detecting and isolating the given faults. To be able to isolate the faults in the sensors, two sensors measure the voltage in the battery in the used sensor configuration.

Tests 3-6 uses the filter and variable transformation of the residual generators described in (4.7) since $\dot{\omega}_{gb}$ is used in the consistency relations. The residuals used in Tests 2-6 are not updated when no gear is selected or the clutch is disengaged. The system starts to calculate the residuals 3 seconds after the clutch has been engaged. In Tests 5 and 6 the residuals are not updated when $|\tilde{U}_{em}| < 1$ V to avoid division by a small number. After a test including $\dot{\omega}_{gb}$ has not been updated and becomes valid again, the test quantity is not updated for 10 seconds. This is to decrease the problems when Γ in (4.7) is reinitialized, as described in the previous diagnosis system. There are 6 tests used in this system and each test is described below.

Test 1

The first test in this diagnosis system compares the sensors measuring the voltage in the battery. The following sensors are thereby used

- $U_{b,sens,a}$
- $U_{b,sens,b}$

and the faults the test reacts on according to the structural analysis are

- $f_{b,U,sens,a}$
- $f_{b,U,sens,b}$

The residual generator is

$$r = U_{b,sens,a} - U_{b,sens,b}$$

Test 2

Test 2 is based on models of the battery, electric machine and the gear box. The following sensors are used in this test

- $\omega_{gb,sens}$
- $U_{b,sens,b}$

and the faults the test reacts on according to the structural analysis are

- $f_{em,R}$
- f_{pe}
- $f_{b,sc}$
- $f_{gb,\omega,sens}$
- $f_{b,U,sens,b}$

The residual generator is

$$r = U_{b,sens,b} - U_b$$

where

$$U_b = nU_{oc} - nR_b I_b$$

$$U_{oc} = f(SoC)$$

$$SoC = \int \dot{SoC} dt$$

$$\dot{SoC} = -\frac{I_b}{Q_b}$$

$$I_b = I_{em} \frac{\tilde{U}_{em}}{U_{b,sens,b}}$$

$$I_{em} = \frac{\tilde{U}_{em} - \omega_{em} k_i}{R_{em}}$$

$$\tilde{U}_{em} = \frac{1}{\tau_{em}s + 1} U_{em}$$

$$\omega_{em} = u_{em} \omega_{mj}$$

$$\omega_{mj} = u_{gb} \omega_{gb,sens}$$

$$u_{gb} = f(\text{gear})$$

$$U_{em} = U_{em,ctrl}$$

$$\omega_{gb} = \omega_{gb,sens}$$

Test 3

Test 3 includes most parts of the model of the vehicle. The sensor used is

- $\omega_{gb,sens}$

and the faults the test reacts on according to the structural analysis are

- $f_{em,ka}$
- $f_{em,R}$
- f_{pe}
- $f_{gb,\omega,sens}$

The residual generator includes dynamics, and the consistency relation in this test is the same as the consistency relation used in Test 3 in Diagnosis system 2 given in (4.6). The residual generator is given in Appendix B.2.

Test 4

The sensors used in test 4 are

- $\omega_{gb,sens}$
- $U_{b,sens,a}$

and the faults the test reacts on according to the structural analysis are

- $f_{em,ka}$
- $f_{em,R}$
- $f_{b,sc}$
- $f_{b,U,sens,a}$
- $f_{gb,\omega,sens}$

The residual generator includes dynamics, and the consistency relation in this test is the same as the consistency relation used in Test 3 in Diagnosis system 2 given in (4.6). The residual generator is given in Appendix B.3.

In the residual generator I_{em} and \tilde{U}_{em} are calculated by

$$I_{em} = \frac{\tilde{U}_{em} - \omega_{em}k_i}{R_{em}} \quad (4.10a)$$

$$\tilde{U}_{em} = \frac{I_b U_b}{I_{em}} \quad (4.10b)$$

according to (B.2) and (B.3). These equations form an equation system that has to be solved. A second order equation is found for I_{em} when substituting (4.10b) into (4.10a). This leads to that there are two solutions for I_{em} , and these are expressed by

$$I_{em} = -\frac{\omega_{em}k_i}{2R_{em}} \pm \sqrt{\left(\frac{\omega_{em}k_i}{2R_{em}}\right)^2 + \frac{I_b U_b}{R_{em}}} \quad (4.11)$$

In most operating points it is possible to find a unique solution for I_{em} using the sign of $I_b U_b$, and the model for the power electronics, i.e. $I_b U_b = \tilde{U}_{em} I_{em}$. This requires that the sign of \tilde{U}_{em} is known. The voltage is often positive when the vehicle is driving forward. However, if a negative torque is applied at low speeds, the voltage may be negative. The sign of the voltage is also dependent on the

parameters of the machine according to (2.20). Due to the uncertainty about the sign of \tilde{U}_{em} , the information about the sign of $I_b U_b$ is not used. Residuals based on both expressions for the current are therefore used. The residual with the smallest amplitude is used as the residual in the test.

Each residual is filtered accordingly to (4.7). This is made for both residuals and before one residual is chosen in the test. The disadvantage doing this is that the solution is based on a faulty estimation of I_{em} after a mode change in the solution of I_{em} occurs. The alternative to this is to filter the residual after the residual with smallest magnitude is chosen.

Test 5

The sensors used in Test 5 are

- $\omega_{gb,sens}$
- $U_{b,sens,b}$

and the faults the test reacts on according to the structural analysis are

- $f_{em,ka}$
- f_{pe}
- $f_{b,sc}$
- $f_{b,U,sens,b}$
- $f_{gb,\omega,sens}$

The consistency relation in this test is the same as the consistency relation used in Test 3 in Diagnosis system 2 given in (4.6). The residual generator is given in Appendix B.4.

Test 6

The sensor used in Test 6 is

- $U_{b,sens,b}$

and the faults the test reacts on according to the structural analysis are

- $f_{em,ka}$
- $f_{em,R}$
- f_{pe}
- $f_{b,sc}$
- $f_{b,U,sens,b}$

The consistency relation in this test is the same as the consistency relation used in Test 3 in Diagnosis system 2 given in (4.6). The residual generator is given in Appendix B.5.

Thresholds in tests

Table 4.7 shows the parameter values used in the CUSUM algorithm for this system. The parameter α used in the filter described in (4.7) is set to 0.1 in the tests that use the filter, i.e. Tests 3-6.

Table 4.7: *Offsets, ν , and thresholds, J , used in the CUSUM algorithm in the tests in Diagnosis system 3.*

	offset	threshold
$T1$	2	30
$T2$	4	500
$T3$	70	3000
$T4$	60	18000
$T5$	65	4000
$T6$	300	7500

Decision structure

The decision structure for this diagnosis system is shown in Table 4.8. Full isolability is achieved according to the structural analysis. To isolate all faults, four tests have to react, except from when $U_{b,sens,a}$ breaks down and only two tests are supposed to be affected. This can be explained by that most of the vehicle model is used in four of the tests, and thereby more tests react on the faults in this diagnosis system compared to Diagnosis system 1 and Diagnosis system 2. This results in that if one test is not working properly in this system, the probability for detecting the fault is increased since more tests are sensitive for the fault. The probability for full isolability generally decreases when the number of tests that are required to react to separate the faults increases.

Table 4.8: *Decision structure for Diagnosis system 3.*

	$f_{em,ka}$	$f_{em,R}$	f_{pe}	$f_{b,sc}$	$f_{b,U,sens,a}$	$f_{b,U,sens,b}$	$f_{\omega,gb,sens}$
$T1$					X	X	
$T2$		X	X	X		X	X
$T3$	X	X	X				X
$T4$	X	X		X	X		X
$T5$	X		X	X		X	X
$T6$	X	X	X	X		X	

4.7 Results and discussion

The designed diagnosis systems achieve full fault isolability according to the structural analysis. To evaluate the performance of the diagnosis systems when noise is added to the sensor signals, simulations of a long haulage truck are

carried out. The type of issues handled are e.g. the impact of the number of sensors on the performance of the diagnosis, and the interplay between diagnosis and the energy management. These issues are of interest, since they will also occur in reality when developing diagnosis systems. In the simulations, the faults listed in Section 4.3 are induced one by one to evaluate the diagnosis performance. The size of the induced faults are given in Table 4.1, and noise is added according to Table 4.2.

The test quantities achieved from the simulations of the diagnosis systems are normalized with the threshold used in CUSUM (Section 4.1.2)

$$T_{\text{norm}} = \frac{T}{J} \quad (4.12)$$

and the test alarms if $T_{\text{norm}} > 1$.

4.7.1 Diagnosis system 1

The diagnosis systems based on five sensors including the torque sensor, detects and isolates all faults in a few seconds. As an illustration, Figure 4.6 shows T_{norm} when $f_{em,R}$ is induced in the model after 400 seconds and the driving cycle used is FTP75. Test 2 and Test 3 react on this fault, as expected according to the decision structure in Table 4.4. The performance of the system detecting $f_{em,R}$, is representative for all faults that are to be detected.

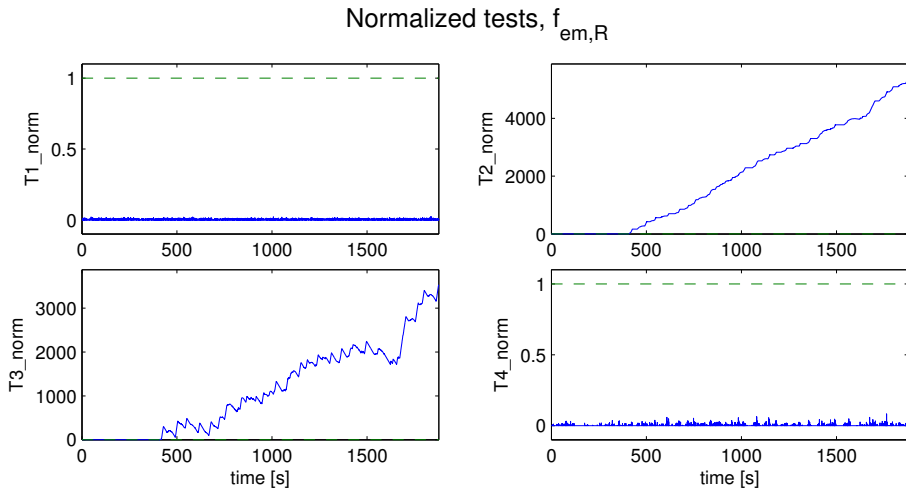


Figure 4.6: Normalized test quantities in Diagnosis system 1 when R_{em} is halved at 400 seconds and the driving cycle used is FTP75. The tests alarm if the normalized test quantity is larger than one, and Test 2 and Test 3 react on the fault as expected.

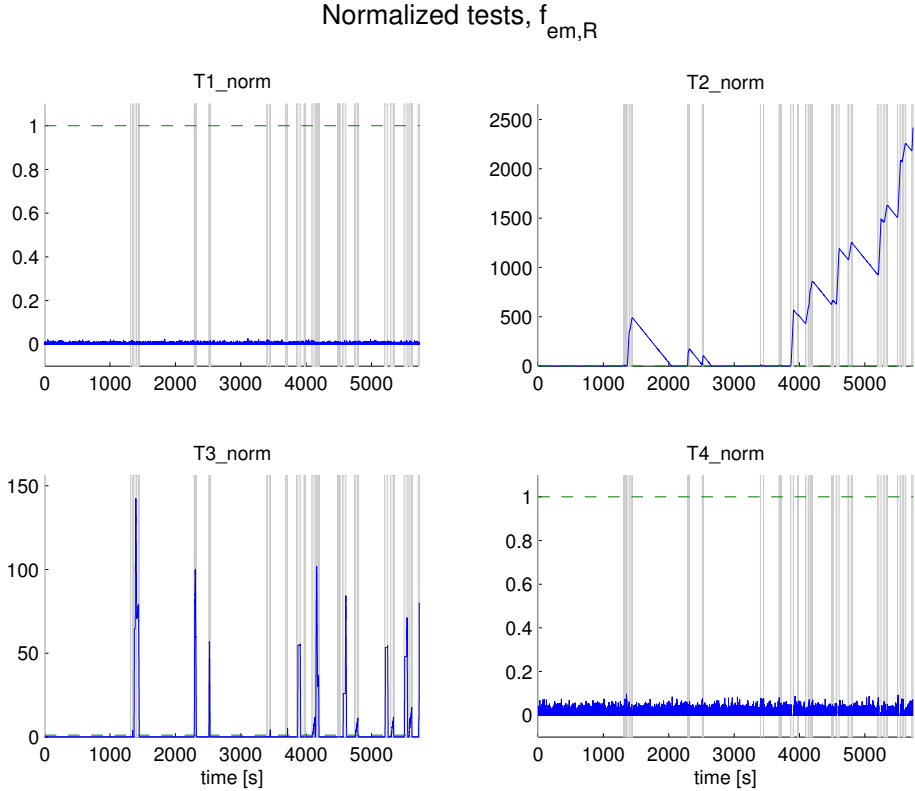


Figure 4.7: Normalized test quantities in Diagnosis system 1 when R_{em} is halved at 400 seconds and the route used is Linköping to Jönköping. The shaded fields indicate when $|I_{em}| > 40A$, which approximately is 20 Nm for the nominal value of k_a . It is clearly shown that the performance in the diagnosis system is dependent on the operating points in the electric machine. Both Tests 2 and 3 react on the fault as expected.

A simulation is carried out when the driving profile from Linköping to Jönköping is used and the resistance in the electric machine is modified after 400 seconds, and the result from the simulation is given in Figure 4.7. Test 2 and Test 3 react and isolate the fault in this realistic driving scenario. The reason for that the tests do not react at all times on the fault, is that the electric machine is not used during long periods. The shaded areas in the figure states when $|I_{em}| > 40A$, which approximately leads to a torque of 20 Nm for the nominal value of k_a . This condition is not used in the diagnosis system. If the tests were only to be updated if $|I_{em}| > 40A$, Test 2 and Test 3 would be increasing after the fault is induced.

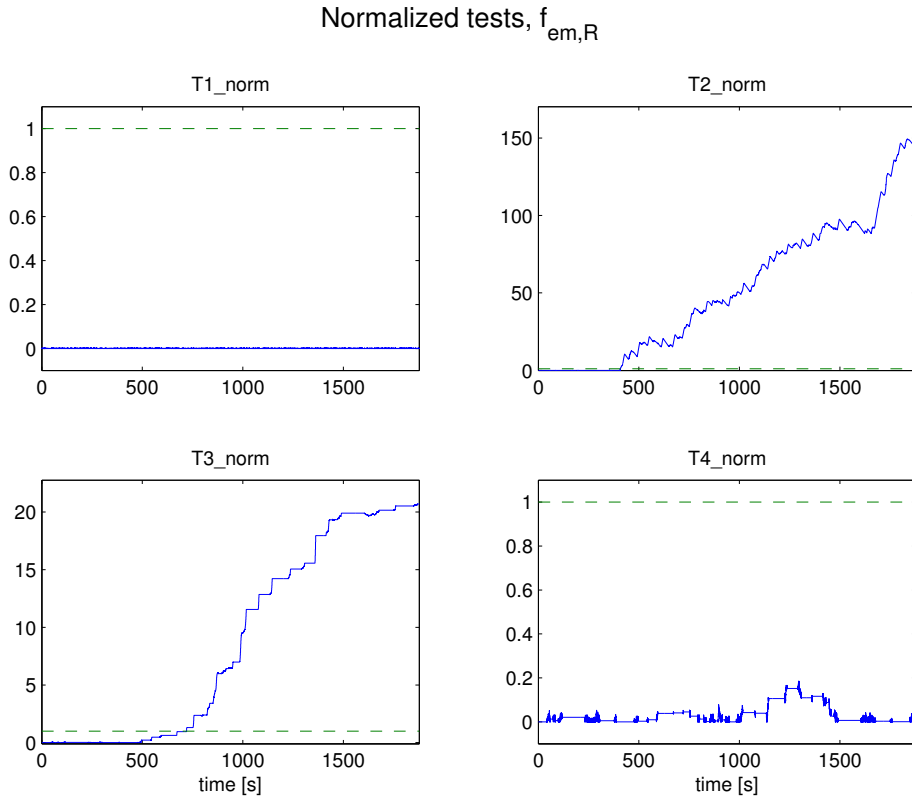


Figure 4.8: The tests alarm if the normalized test quantity is larger than one. The fault $f_{em,R}$ is induced in the model after 400 seconds, and Test 2 and Test 3 in Diagnosis system 2 react as expected.

4.7.2 Diagnosis system 2

All faults are detected and isolated in Diagnosis system 2, that is based on five sensors. The normalized test quantities are in general smaller after the fault is induced in the vehicle model, compared to Diagnosis system 1. Figure 4.8 shows the test quantities when the fault in the resistance of the electric machine is induced at 400 seconds and FTP75 is used.

The results when the fault in the power electronics is induced in the model is presented in Figure 4.9. Test 4 reacts on the fault after 870 seconds, even if this is not expected according to the decision structure. The reason for this is that SoC of the battery is used to calculate U_{oc} in the diagnosis system. The model used in Test 4 is not consistent with the vehicle model in all driving modes, and when this occurs the test quantity as well as the states in the test is not updated. This leads to that there will be a discrepancy between the

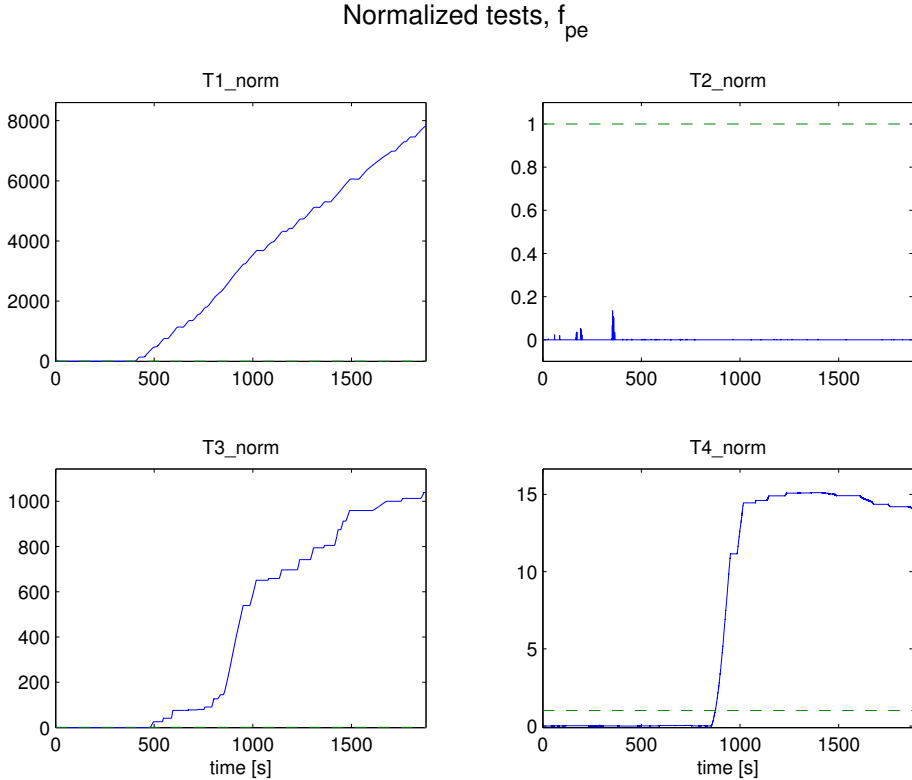


Figure 4.9: The tests alarm if the normalized test quantity is larger than one. The fault f_{pe} is induced in the model after 400 seconds, and Test 2 and Test 3 in Diagnosis system 2 react as expected. Test 4 is not supposed to react on the fault, but does so after 870 seconds. The reason is that there is drift in the computation of SoC of the battery in the diagnosis system, leading to that the computed U_{oc} is not correct at some parts of the simulation.

computed SoC in the diagnosis system and the actual SoC in the battery (see Figure 4.10). This has no influence in the fault free case in the driving situations studied here, as stated in Section 4.6.1. But when there is a fault in the power electronics, the applied voltage on the electric machine is assumed to be half of the requested voltage. This may result in that even if a positive torque from the electric machine is requested by the energy management, the machine will apply a braking torque on the powertrain. The SoC of the battery will therefore increase above the levels specified in the energy management in Section 3.12. Due to that U_{oc} is not constant when $SoC > 0.8$ according to Figure 2.4, the U_{oc} used in Test 4 will be different compared to the U_{oc} of the battery (see Figure 4.10). This example illustrates the importance of handling drift in the

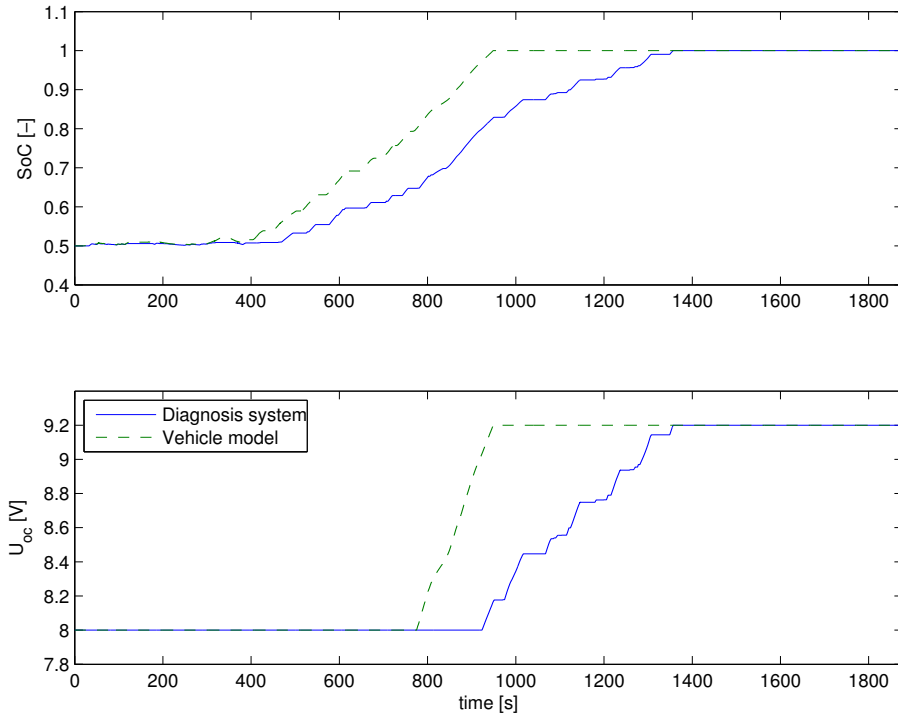


Figure 4.10: *The upper plot shows the SoC in the battery and the computed SoC in Test 4 in Diagnosis system 2, when a fault in the power electronics is induced after 400 seconds. The model in the residual generator is not valid in all operating points and the state is therefore not always updated. This leads to that the computed open circuit voltage significantly differs from the actual U_{oc} of the battery, and this is the reason why Test 4 reacts on f_{pe} even if this is not expected.*

states used in the diagnosis systems. The need of fault tolerant control to, in this case, avoid over charging of the battery and thereby damage the energy storage is also exemplified.

4.7.3 Diagnosis system 3

All faults are detected in Diagnosis system 3. However, only five of the seven faults are fully isolated when the driving cycle FTP75 is used. The reasons are as follows. When the torque constant in the electric machine has changed, i.e. the fault $f_{em,ka}$, Test 6 does not react as expected from the structural analysis and the decision structure in Table 4.8. This means that this fault can not be isolated from $f_{gb,\omega,sens}$. Further, when the resistance in the electric machine has changed, i.e. $f_{em,R}$, Test 4 is not affected as expected. This is the case in both

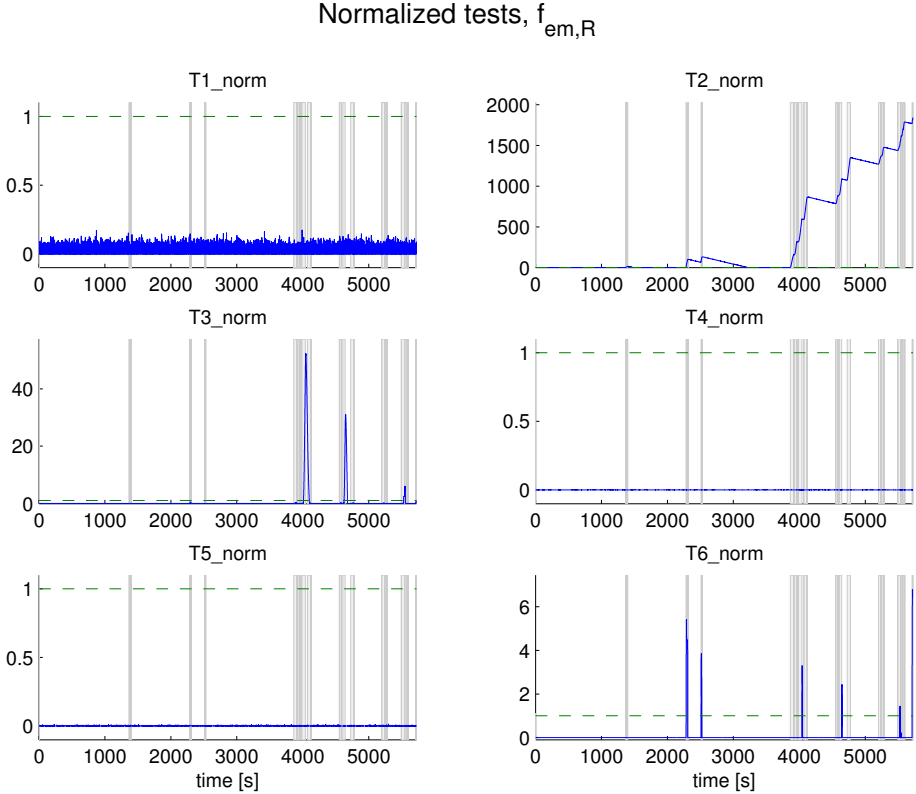


Figure 4.11: The figure shows the normalized tests when there is a fault in the resistance in the electric machine using Diagnosis system 3 and the driving profile from Linköping to Jönköping. Test 4 does not react on the fault as it should according to the structural analysis. The shaded fields indicate when $|I_{em}| > 40A$, which approximately is 20 Nm for the nominal value of k_a .

FTP75 and Linköping-Jönköping, and is shown in Figure 4.11 for Linköping-Jönköping. Due to that Test 4 does not react on the fault, $f_{em,R}$ can not be isolated from f_{pe} . Improvements can be sought by using variable parameters in the CUSUM algorithm, that changes with the operating points of the vehicle to adapt to the varying fault sensitivity.

For the five faults that are fully isolable, the result is obtained within 100 seconds. There are a number of reasons that it takes longer than for especially Diagnosis system 1, but also Diagnosis system 2. One reason is that an algebraic loop is not uniquely solved in one of the tests in this diagnosis system. Another reason is that more of the tests are not valid at all times, here because the model of the clutch is not valid in all operating modes, $|U_{em}|$ is small, or that no gear is selected. A test based on a dynamic residual generator that

includes the limitation $|U_{em}| > 1$ V, is e.g. only updated during 30% of the simulation time when FTP75 is used.

In the four tests based on dynamic residual generators, the states in the filters are reinitialized when the system is reactivated. The assumption that the system is fault free is used in the reinitialization of the state. An alternative to this, which possibly increases the performance of the diagnosis, is to instead use the previous valid value of the residual in the initialization of the state.

4.8 Conclusions

In hybrid vehicles there are new features compared to conventional vehicles, like e.g. mode switches. The influence of these properties on diagnosis has been studied by designing and implementing three diagnosis systems on vehicle level. The three diagnosis systems were chosen for their principal interest; one with a fairly typical sensor configuration, one with the same number of sensors but in model sense placed more closely to the components to be monitored, and one with the minimal number of sensors to structurally achieve full fault isolability. The diagnosis systems are based on a model only describing the fault free behavior of the truck.

According to the structural analysis of the model, full fault isolability is achieved using the three sensor configurations. In two of the implemented diagnosis systems full isolability is achieved in the simulations, but not in the third system. The discrepancy between the model analysis and the performance of the implemented diagnosis system, stems from the influence of the faults on the system in relation to the noise level.

The driving cycle used is mainly FTP75. The realistic driving scenario driving from Linköping to Jönköping, is used to verify that the results from FTP75 are relevant. The performance of the diagnosis systems is similar for these two driving scenarios.

There is no major complexity difference in the design and implementation between the three diagnosis systems. Due to the sensor configuration in the system based on few sensors, the tests are larger and therefore slightly more computational demanding than the other two systems. For the same reason, Diagnosis system 2 is more computational demanding than Diagnosis system 1. Both Diagnosis system 1 and Diagnosis system 2 are based on five sensors, but the sensors used in the first system are placed closer to the components to be monitored, in the sense that fewer model equations are needed to calculate the signals used in the consistency relations in the first system.

It is shown that the diagnosis performance is affected of the operating points of the vehicle. This interaction is of special interest in the dynamic residual generators, since the test quantities are not updated for some time after the model has become valid, to reduce the impact of an error in the initialization of the states used in the filters of the residuals. Therefore it is preferable to avoid many deactivations and activations of the tests, and this can be achieved in a well designed energy management.

RESIDUAL GENERATOR SELECTION

A diagnosis system consists here of residual generators that are constructed from minimal sets of equations with analytical redundancy. These sets are called minimal structurally overdetermined (MSO) sets, and are described in Section 4.1.1. To construct residual generators based on the MSOs, one of the equations in the MSO is selected as the consistency relation, i.e. the equation where the consistency of the model and measurements is analyzed. There are in general many sets of MSOs that achieve as good fault isolability as possible in a diagnosis system. The selection of the sets of equations to be used in the diagnosis system, as well as the selection of consistency relations, may significantly affect the diagnosis performance due to non-linearities in the model. In Chapter 4, the consistency relations and the sets of MSOs were selected ad hoc from the sets of MSOs that structurally achieve full fault isolability, but here a more systematic method is used.

The unknown variables in a residual generator are computed using all equations except the selected consistency relation in the MSO. The properties of the computational sequence of the variables vary with the selected consistency relation. Dynamic equations e.g. results in that a signal either is differentiated or integrated. It is in general not possible to state that either differentiation or integration in the computational sequence is preferable, but the designer of the system may prefer one of these due to the knowledge of the system to be monitored regarding model accuracy and measurement noise levels. In this chapter a methodology is used to select a set of MSOs and the consistency relations to find residual generators that fulfill predefined conditions on the computational sequence of the variables. The conditions used are that unique expressions for

the variables used in the residual generator is to be found, and that dynamic equations in the computational sequence is to be integrated. The investigation is made by first studying a simplified model to illustrate how the selection of consistency relation affect the possibility to find a unique residual generator. Secondly a simulation study using the entire vehicle model the is carried out.

5.1 Background

This section consists of two parts. First, the methodology for designing the diagnosis systems in this thesis is based on structural analysis and is described in Section 4.1.1. An extended version of the structural analysis including the algebraic expressions is described in Section 5.1.1. Secondly, a dynamic equation can in a computational sequence either be integrated or differentiated, and the notation used for this is given in Section 5.1.2.

5.1.1 Extended structural analysis

The first developed algorithms to find minimal sets of equations with analytical redundancy one (MSOs) using structural analysis, do not consider how to find the algebraic expressions for the residual generators. Recent algorithms that consider invertibility and how differential equations are solved in the residual generators have been developed, see e.g. de Flaugergues et al. (2009). These algorithms investigate the properties of the MSOs, but do not provide the user information about which consistency relations that are possible to use to achieve wanted properties of the residual generators. Svärd and Nyberg (2010) analyzes the characteristics of the system for every possible consistency relation. This is done by first using structural analysis to find the overdetermined sets, and the computational order of the unknowns is found using Dulmage-Mendelsohn decomposition. The algebraic expressions are then used in the algorithm to analyze if predefined constraints of the residual generators are fulfilled. Such constraints may e.g. be that differential equations only can be solved by differentiating or integrating a signal, and that a unique residual generator is to be found. These properties may vary depending on the selection of the consistency relation in a set of equations, and therefore all possible residual generators are to be investigated. This methodology is used in this investigation.

5.1.2 Dynamic equations

The system used in this investigation is based on model equations, g , including dynamics

$$g(x_1, \dot{x}_1, x_2, z) = 0 \quad (5.1)$$

where x_1 is a vector of unknown dynamic variables, x_2 is a vector of unknown algebraic variables, and z is a vector of known signals. The relation between a

variable $x_{1,i} \in x_1$ and $\dot{x}_{1,i}$ is given in the dynamic equation

$$\frac{d}{dt}x_{1,i} = \dot{x}_{1,i} \quad (5.2)$$

that can be used in a computational sequence using two different methods or computational causalities, here causality is used for short (Frisk et al., 2010):

derivative causality is when $x_{1,i}$ is differentiated to obtain $\dot{x}_{1,i}$, i.e.

$$\dot{x}_{1,i} := \frac{d}{dt}x_{1,i}$$

integral causality is when $\dot{x}_{1,i}$ is integrated to obtain $x_{1,i}$, i.e.

$$x_{1,i} := \int \dot{x}_{1,i} dt + C, \text{ where } C \text{ is the initial value of } x_{1,i}.$$

mixed causality is when a system can be solved using both derivative and integral causality

5.2 Algebraic loops

The MSO algorithm used in Chapter 4 (Krysander et al., 2008) does not consider how the unknown variables are computed. Algebraic loops, as well as that the unknown variables are not invertible, may occur in the just-determined parts of the MSOs. There are several numerical and analytical solving methods available to solve algebraic loops. Linear algebraic loops are e.g. easily solved, but other algebraic loops may demand a large computational effort and a solution is not always obtained.

The possibility to find a unique residual generator given a set of equations in an MSO varies with the chosen consistency relation. This is exemplified using a reduced and simplified set of the model equations used in Test 4 in Diagnosis system 3, given in Section 4.7.3 and Appendix B.3

$$\begin{aligned} e_1 : & T_e + \underbrace{k_a I_{em}}_{T_{em}} - T_l(\omega) - J_{tot}\dot{\omega} = 0 \\ e_2 : & \frac{U_{em} - \omega k_i}{R_{em}} - I_{em} = 0 \\ e_3 : & I_b U_b - I_{em} U_{em} = 0 \\ e_4 : & U_{oc} - U_b - R_b I_b = 0 \\ e_5 : & \frac{d}{dt}\omega - \dot{\omega} = 0 \\ e_6 : & U_b - y_1 = 0 \\ e_7 : & \omega - y_2 = 0 \end{aligned} \quad (5.3)$$

where ω is an angular speed, J_{tot} the inertia of the vehicle, U_{oc} and R_b the open source voltage and the inner resistance in the battery, T_l the lumped torque due

Table 5.1: *Permuted structural model of the system given in (5.3) except e_1 that is chosen to the consistency relation. Equations e_2 and e_3 form an algebraic loop for I_{em} and U_{em} .*

	ω	U_b	$\dot{\omega}$	I_b	U_{em}	I_{em}
e_7	X					
e_6		X				
e_5	X		X			
e_4		X		X		
e_3		X		X	X	X
e_2	X				X	X

to losses in the vehicle, T_e the torque from the engine, and y_1 and y_2 are sensor signals. The torques T_e and T_l are in this example assumed to be known.

If e_1 is selected as the consistency relation, the permuted structural model of the just-determined part, i.e. $\{e_2 - e_7\}$, is given in Table 5.1. The corresponding computational order would be:

$$\mathcal{C} = (\{\omega\}, \{e_7\}), (\{U_b\}, \{e_6\}), (\{\dot{\omega}\}, \{e_5\}), \\ (\{I_b\}, \{e_4\}), (\{I_{em}, U_{em}\}, \{e_2, e_3\}) \quad (5.4)$$

indicating that ω is computed from e_7 , U_b is computed from e_6 and so forth. The pair $(\{I_{em}, U_{em}\}, \{e_2, e_3\})$ indicates that there is an algebraic loop, that also can be seen in Table 5.1. This loop has the non unique solution

$$I_{em} = -\frac{\omega k_i}{2R_{em}} \pm \sqrt{\left(\frac{\omega k_i}{2R_{em}}\right)^2 + \frac{I_b U_b}{R_{em}}} \quad (5.5)$$

If one of e_2 or e_3 is used as consistency relation instead of e_1 , there is no algebraic loop in the just-determined part. Since the variables in the substitution chain are invertible, a unique residual generator can therefore be expressed. The computational order of the unknown variables if e.g. e_2 is used as the consistency relation will be

$$\mathcal{C} = (\{\omega\}, \{e_7\}), (\{U_b\}, \{e_6\}), (\{\dot{\omega}\}, \{e_5\}), \\ (\{I_b\}, \{e_4\}), (\{I_{em}\}, \{e_1\}), (\{U_{em}\}, \{e_3\}) \quad (5.6)$$

Note that since consistency based diagnosis is used, it is possible to construct a test that is based on a residual generator with several solutions. As long as at least one of the possible residuals is close to zero, the test will not react

$$|r(t_k)| = \min\{|r_1(t_k)|, |r_2(t_k)|, \dots, |r_i(t_k)|\}, i \geq 2$$

However, the computational complexity of the system increases if more than one residual are to be evaluated in a test.

5.2.1 Series wound electric machine

In the example above the magnetic field, ϕ , in the electric machine is assumed to be constant. This is the case in PMSMs that is the machine type mainly used for vehicle propulsion in hybrid electric vehicles. However, if a series wound machine is used instead, that e.g. is used in starter motors (Gerhardsson, 2010; Hambley, 2005), e_1 and e_2 in (5.3) are modified to

$$e_1 : T_e + \underbrace{k_a I_{em}^2}_{T_{em}} - T_l(\omega) - J_{tot} \dot{\omega} = 0 \quad (5.7a)$$

$$e_2 : \frac{U_{em}}{R_{em} + \omega k_i} - I_{em} = 0 \quad (5.7b)$$

due to that ϕ increases linearly with the current in the rotor and stator according to

$$\phi = k I_{em} \quad (5.8)$$

The same variables are included in each equation in (5.3) and (5.7), and therefore the structural models are the same for the two systems. It is however not possible to chose a consistency relation that results in a unique expression for the residual generator in the later system. This is due to that the algebraic loop in e_2 and e_3 adds the constraint that one of these equations is to be used as consistency relation. The current I_{em} is then to be calculated using e_1 , but since I_{em} is not longer invertible in e_1 , it is not possible to find a unique residual generator.

5.3 Integral and derivative causality

In this section differential equations are considered. It is not possible to state that one of integral, derivative, or mixed causality always performs best and therefore is preferable. In general it is not preferable to differentiate a noisy signal, and not to integrate a signal in a diagnosis system where an offset occurs since this will lead to drift in the integrator.

In this investigation two diagnosis systems are compared, one based on mixed causality and one on integral causality. The basis for these diagnosis systems is Diagnosis system 2 described in Section 4.7.2. Test 3 and Test 4 used in the system include dynamics and are therefore handled here. In the original system, mixed causality is used in these two tests. The mass of the fuel consumed, m_f , is solved by using integral causality

$$m_f = \int \dot{m}_f dt \quad (5.9)$$

Equation (2.56), that is similar to e_1 in (5.3), is used as consistency relation (see (4.6) for the entire residual generator) and is recalled

$$\dot{\omega}_w = \frac{T_{net}}{J_{tot} u_f^2 + m_v r_w^2} \quad (5.10)$$

In this expression \dot{w}_w is used, that is computed from $\omega_w = \frac{1}{u_f}\omega_{gb}$, leading to that derivative causality is used. For the computation the reformulation in (4.7) is used.

5.3.1 MCDS and ICDS

The diagnosis system described above where two of the tests are based on mixed causality, is denoted **mixed causality diagnosis system**, or MCDS for short. The MCDS is to be compared with a system where the following constraints are to be fulfilled

- integral causality is used
- The set of equations in the just-determined parts of the MSOs are globally invertible. Maple is used to investigate this constraint

This diagnosis system is denoted **integral causality diagnosis system**, or ICDS for short. The methodology described in Section 5.3.2 is used to find such a system.

5.3.2 Methodology to construct ICDS

The algorithm used to find the ICDS is based on the algorithm described in Svård and Nyberg (2010) and briefly recalled in Section 5.1.1. In the original algorithm only the just-determined part of the residual generator is considered, i.e. the consistency relation is not included in the analysis determining the properties of the residual generator. When designing ICDS also the consistency relation is included in the analysis. This only affects the constraint on how differential equations are to be solved, since all unknowns are computed in the just-determined part and therefore invertibility is not an issue in the consistency relation. The constraint in Section 5.3.1 regarding differential equations states that derivative causality is not to be used in ICDS. One of the constraints on the analyzed set of equations is that, without loss of generality, a differentiated variable may only occur once in the system. Therefore, if a differentiated signal is included in the consistency relation, the output from the original algorithm might be that only integrating causality is used. However, if there is a differentiated variable in the consistency relation, a signal must be differentiated since it is only known in its undifferentiated form from the just-determined set of equations. Therefore derivative causality is used in the residual generator in such a case.

5.4 Results and discussion

One result from this study is the outcome from the analysis of the diagnosis systems regarding algebraic loops and different ways of computing differential

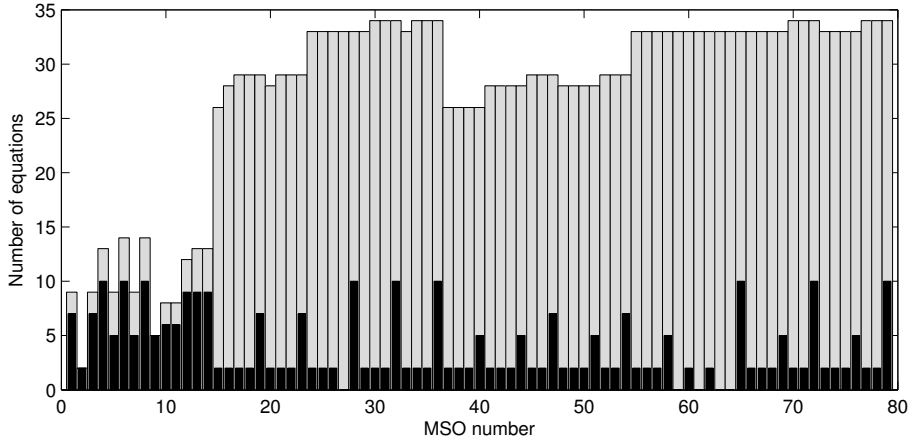


Figure 5.1: *The gray bars indicate the number of equations in the MSOs that can be constructed given the sensor configuration used in the diagnosis systems. The black bars indicate the number of equations that can be selected to consistency relations in each MSO to fulfill the constraints in the ICDS. The number of MSOs and equations in MCDS and ICDS are the same, since the same vehicle model and sensor configuration is used.*

equations. The other main result is a simulation study comparing the performance in the mixed causality diagnosis system and the integral causality diagnosis system with constraints defined in Section 5.3.1.

5.4.1 Selection of consistency relations used in ICDS

Given the five sensors available in the diagnosis systems used in the study about how differential equations are solved, 79 MSOs are found. Each equation in an overdetermined part can potentially be selected as the consistency relation used to construct the residual generator for that set of equations. For all MSOs there are 2162 residuals generators to be investigated. In Figure 5.1 the number of model equations in each MSO is shown, but also how many equations that can be selected as consistency relation to fulfill the requirements in ICDS, i.e. integral causality and global invertibility. In MSOs 15-79 there is only a small fraction of the equations that can be used as consistency relations in the ICDS in order to fulfill these constraints. These MSOs include (5.10) that uses the torque acting on the wheels to compute ω_w , but computes the torques and angular speeds in different ways. There are five MSOs that do not have any consistency relation that fulfills the requirements.

The four tests used in the diagnosis system based on mixed causality, are included in the set of 74 MSOs that fulfills the constraints for ICDS given in Section 5.3, for at least one selection of consistency relation. The residual

generators used in Test 1 and Test 2 in the MCDS fulfills the constraints for ICDS using the selected consistency relation, and are therefore used unchanged in the new diagnosis system. In the MSOs used in Test 3 and Test 4 in MCDS (see Section 4.6.2 and Appendix B.1 for the equations included in the MSOs), there are two equations that can be selected as the consistency relation in ICDS. These are

$$\omega_{gb} = \omega_{gb,sens} \quad (5.11)$$

$$\omega_w = \frac{\omega_{gb}}{u_f} \quad (5.12)$$

for both tests, where ω_w and ω_{gb} are the angular speeds at the wheels and the outgoing shaft of the gearbox, and u_f is the gear ratio in the final gear. When using one of these consistency relations, $\dot{\omega}_w$ is calculated using (5.10). The angular velocity ω_w is calculated by integrating this signal

$$\omega_w = \int \dot{\omega}_w dt \quad (5.13)$$

to be used in the consistency relation. In the two residual generators, (5.11) is used as consistency relation and ω_w in (5.13) is multiplied with the final gear to calculate ω_{gb} .

The algebraic loop for I_{em} and U_{em} that is considered in Section 5.2 is not an issue in these two residual generators since U_{em} is known without using any of e_2 and e_3 in (5.3). The required voltage from the power electronics is known in Test 3, and the sensor measuring U_{em} is available in Test 4.

5.4.2 Simulation study

To evaluate how the performance of the diagnosis systems is affected when dynamic equations are computed in different ways, simulations of a long haulage truck are carried out. The faults are induced one by one in the simulations, and the driving cycle used is FTP75. Since Test 1 and Test 2 do not differ in the two diagnosis systems, the simulation results for these tests are not presented. The noise in the sensor signals are increased in the angular speed sensors in this study compared to what is given in Table 4.2, and the noise power used in all sensors is 0.01.

Initialization of states

The state in the transformation used in MCDS is reinitialized when the model used in the diagnosis system is getting valid, as described in Section 4.6.2. The state w_w calculated from (5.13) is reinitialized in the residual generators used in ICDS. This is done by using a filtered sensor signal scaled with the final gear

$$\omega_w(t_0) = \frac{1}{\tau_w s + 1} \frac{\omega_{gb,sens}(t_0)}{u_f} \quad (5.14)$$

where t_0 is the time when the residual generator is getting valid.

In the initialization in the states in both MCDS and ICDS, it is assumed that the monitored system is fault free and the residual is zero. If the equations used in the expression for the signal to be integrated are inconsistent with the monitored system, the integrated signal will drift from the true value. The test quantity is therefore not updated during the first 10 seconds after a test has been valid to be able to detect the fault, and not use a residual that is close to zero even though the estimation of the signal to be integrated is inconsistent with the fault free vehicle model.

Simulation results

In Figure 5.2, the normalized test quantities, T_{norm} , (see Section 4.7 for details) from the simulations in the fault free case for both diagnosis systems are presented. All test quantities are well below one, and no false alarm occurs in the simulations.

The normalized test quantities for Tests 4 (both MCDS and ICDS) when $f_{em,U,sens}$ occurs are given in Figure 5.3. Tests 3 do not react on this fault, as expected, and the simulation results for these tests are not included. Figure 5.4 shows T_{norm} for Tests 3 when the resistance in the electric machine is modified.

All five fault modes are fully isolated in the ICDS, and all except the fault in the voltage sensor in the electric machine in the MCDS. The reason that $f_{em,U,sens}$ is not isolated from a fault in the power electronics, is that Test 4 does not react as expected in the MCDS on this fault (see Figure 5.3 and the decision structure in Table 4.6). The normalized test quantity when there is a

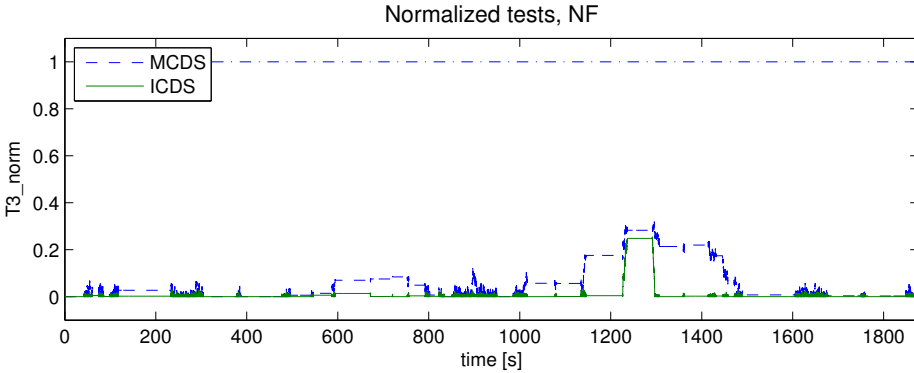


Figure 5.2: *The normalized test quantities in the two diagnosis systems based on mixed and integral causality when the system is fault free. The tests react if the signal is above one. No false detection occurs in the diagnosis systems and the test quantities are well below the thresholds. Similar results are achieved in Tests 4.*

fault in the voltage sensor is almost one, and a different selection of parameters in the CUSUM algorithm possibly achieves full isolability for the MCDS.

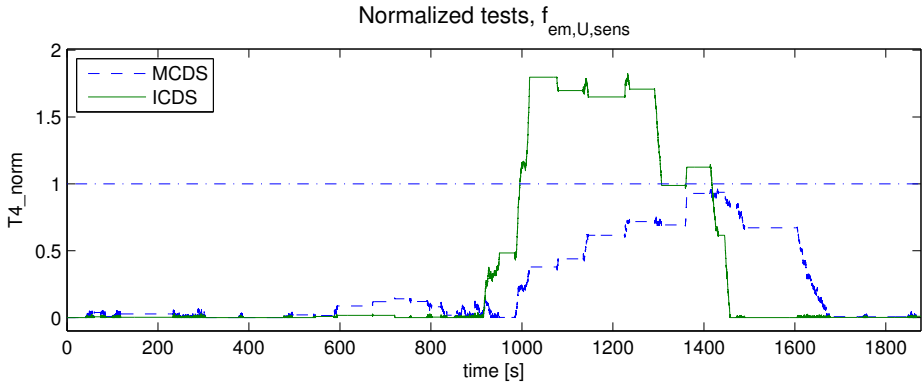


Figure 5.3: The normalized test quantities when a fault is induced in the voltage sensor in the electric machine after 400 seconds. The test quantity in the mixed causality diagnosis system is almost above the threshold, but the test does not alarm. The test in the integral causality diagnosis system reacts approximately 600 seconds after the fault is induced.

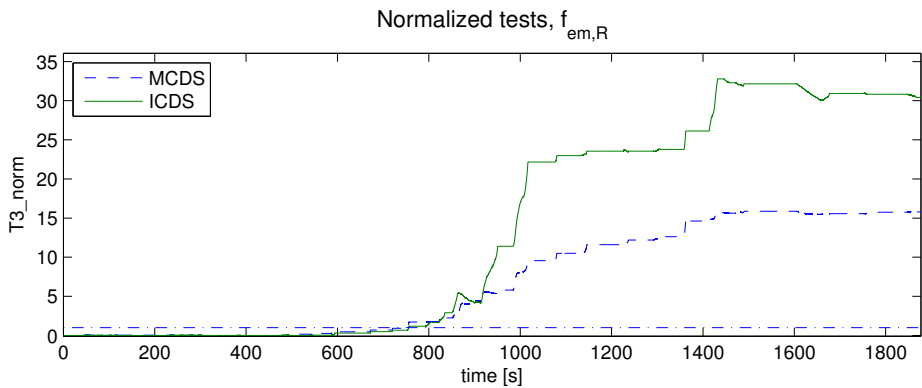


Figure 5.4: The normalized test quantities when $f_{em,R}$ is induced in the model after 400 seconds. Both diagnosis systems react about 350 seconds after the fault is induced in the vehicle model. The magnitude of the test quantity in the integral causality diagnosis system is almost twice that of the mixed causality diagnosis system at the end of the simulation.

5.5 Conclusions

The selection of consistency relations affects the performance of the diagnosis system. There are many possible residual generators in a physical system, since there are many possible MSOs, and within each MSO every equation is a potential residual generator. It is not obvious how to make these selections to achieve as good performance as possible in the diagnosis system. Here a systematic approach is sought for in the selection of the residual generators, and the method is to investigate the properties of the computational sequences in the residual generators.

Analyzing model characteristics, it was shown by using a simplified set of equations included in an MSO used in Diagnosis system 2 in Chapter 4, that algebraic loops in residual generators can be avoided for certain selections of consistency relations, but not for others. When the electric machine type was changed from permanent magnet to series wound, it was no longer possible to find a unique residual generator. This is due to that all variables are no longer globally invertible if the algebraic loop is to be avoided.

To find good alternatives among all possible choices of residual generators, the approach is to use an extended version of structural analysis that is able to handle the issues posed in the model analysis in the previous paragraph. The structural analysis used in Chapter 4 resulted in a diagnosis system based on mixed causality (MCDS), but here the extended version of the structural analysis is used to design a diagnosis system (ICDS). It is based on the entire vehicle model with constraints on the computational sequence, and by including the consistency relation in the analysis of the properties of the residual generators, it was possible to find a residual generator without differentiating any signal. In the two MSOs used in ICDS, there are only two of approximately 30 equations that can be selected as consistency relations to fulfill the constraints on the computational sequence defined for ICDS. These equations are similar and one of these was selected as consistency relation in the tests in ICDS. Since in general only a few equations can be selected, here two of 30, as consistency relations to fulfill the constraints, it can be stated that it is non-trivial to find consistency relations that fulfill predefined constraints on the computational sequence in the residual generators for large systems. Thus the idea to use systematic methods in the selection of residual generators is reinforced.

A simulation study is carried out to compare MCDS and ICDS. The parameters used in the model are the same as those used in the vehicle model, but sensor noise is included in the models of the sensors. Therefore it is reasonable to assume that integral causality is preferable, and this is verified in this case, since when a fault is induced in the vehicle model the test quantities generally react better in the system based on integral causality compared to the system based on mixed causality. Thus, the improvement compared to Chapter 4 shows that this is a promising path of development.

DIAGNOSIS USING A MAP BASED MODEL OF THE ELECTRIC MACHINE

Models are developed for different purposes and to different level of detail. A common approach is map based models, since it is easy to design the models using measurements. A map based model often consists of few equations or maps, that describe the observations rather than the physical behavior of the component. Fault detection is straightforward in a diagnosis system based on such a model since the consistency of the entire machine model and the physical machine is investigated using measurements. However, the use of map based models leads to that it may be troublesome to isolate different fault modes within the component to be monitored, since several faults may affect the same equations or maps in the model.

Since map based models are common in automotive systems, the difficulties and limitations of using such a model in a diagnosis system regarding fault isolability are investigated in this chapter. This is done using the map based model for the electric machine and power electronics, described in Section 3.5.2, where the map of the power losses is based on accurate measured values. The diagnosis systems designed in Chapters 4 and 5 include models for the entire powertrain, but to more clearly illustrate the impact on the diagnosis system of using a map based model of a component, only the electric machine and the power electronics is treated here.

6.1 Structure of the models

The models `electricmotor_quasistatic2` and `electricmotor_quasistatic3`, described in Sections 2.6.2 and 3.5.4 respectively, are well suited for diagnosis

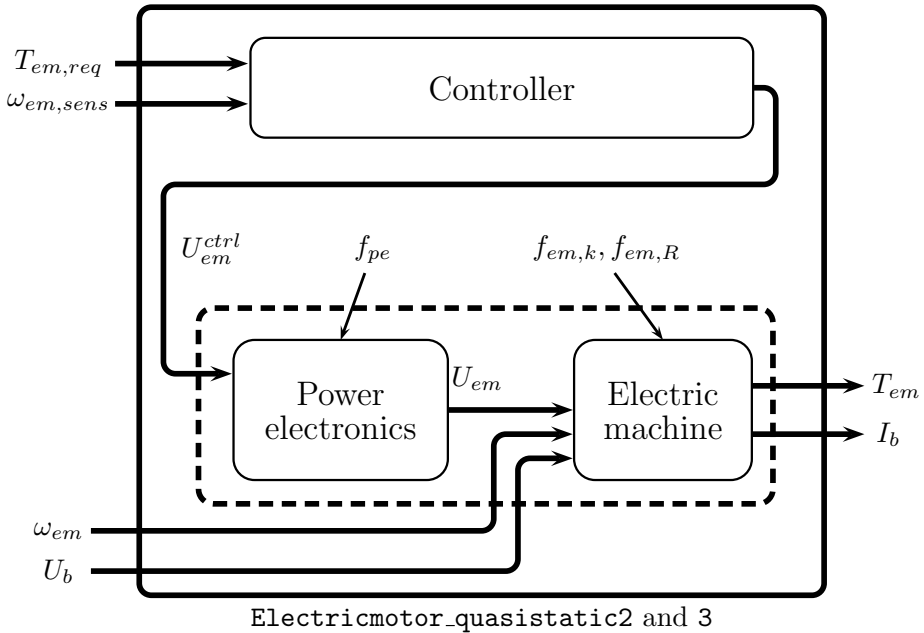


Figure 6.1: A requested voltage is calculated in the controller based on the requested torque in the models for *electricmotor_quasistatic2* and *electricmotor_quasistatic3*. If the system is fault free, the requested voltage is delivered by the power electronics, and the electric machine delivers the requested torque. The parts inside the dashed line are models of physical components.

on vehicle level. The models are based on several physical relations containing parameters to be monitored, and it is thereby possible to isolate several fault modes in the component using only the fault free model of the machine. The schematic structures of the two above mentioned models are identical and are shown in Figure 6.1. A requested torque, $T_{em,req}$, from the electric machine is set by the energy management and is used as a control signal to the model. The controller sets a requested voltage, U_{em}^{ctrl} , the power electronics is expected to deliver. Open loop control is used that is based on the inverse of the electric machine model as stated in Section 2.6.1. This control strategy may work well if the system is fault free, but if there is a fault in the system a closed loop controller is valuable. The power electronics delivers the requested voltage if the component is fault free, i.e. $U_{em} = U_{em}^{ctrl}$, and the models of the electric machine calculate the delivered torque and the current used from the battery. The delivered torque, T_{em} , is equal to the requested torque if the machine is able to deliver the requested torque, and the machine and power electronics are fault free.

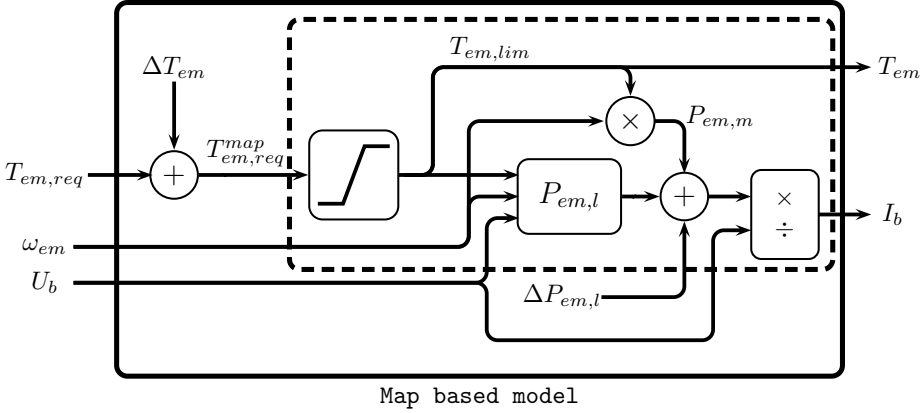


Figure 6.2: The input and output signals are identical in the map based model and the models described in Figure 6.1, except the sensor signal for ω_{em} that is used in the controller in Figure 6.1. The map based model includes a limitation in the torque signal, since the machine has limitations in the torque it is capable to deliver. The battery current is calculated from the mechanical power and the power losses. The modifications in the operating modes and the efficiency of the machine due to faults in the component are modeled with ΔT_{em} and $\Delta P_{em,l}$. The part inside the dashed line is the nominal model with no functionality for fault modeling.

The schematic structure of the map based model can be seen in Figure 6.2. This model has the same input and output signals as the models described in Figure 6.1, except for $\omega_{em,sens}$ that is used in the controller in Figure 6.1. In the fault free case, the map based model of the machine is modeled to deliver the requested torque, as long as the machine is capable of delivering the torque. The battery current, I_b , is calculated using the mechanical power, $P_{em,m}$, and the power losses, $P_{em,l}$, that is a map and depends on the operating points of the machine, as described in Section 3.5.2.

One way to model faults in the map based model is to modify the input signals used in the map and to modify the output of the map. Functionality is here added to modify the delivered torque from the machine by modifying the requested torque using ΔT_{em} according to Figure 6.2. This results in that the power losses of the machine changes when there is a fault affecting the delivered torque. A fault affecting the power losses of the machine affect the current to the battery, and is modeled using $\Delta P_{em,l}$. A schematic expression for the power losses in the machine are found using ΔT_{em} and $\Delta P_{em,l}$

$$\tilde{P}_{em,l}^{map} = P_{em,l}(T_{em,req} + \Delta T_{em}(f), \omega_{em}, U_b) + \Delta P_{em,l}(f) \quad (6.1)$$

where f are the faults.

6.2 Introducing faulty behavior in the model

Three fault modes are modeled in this section to be used in the design of the diagnosis system as described in Section 6.5, and to be able to evaluate the diagnosis system using the simulation environment described in Figure 1.1 and Chapter 3. The faults to be modeled in the electric machine are similar to the faults modeled in (4.3) that are used to evaluate the diagnosis systems designed in the previous chapters. The faults affect the resistance of the machine, and the lumped torque and speed constant k used in `electricmotor_quasistatic3` and described in Sections 2.6.1 and 3.5.4. When the power electronics is broken, the applied voltage on the electric machine is not the requested voltage. The faults are modeled as

$$k = k^{nom}(1 + f_{em,k}) \quad (6.2a)$$

$$R_{em} = R_{em}^{nom}(1 + f_{em,R}) \quad (6.2b)$$

$$U_{em} = U_{em}^{NF}(1 + f_{pe}) \quad (6.2c)$$

where k^{nom} and R_{em}^{nom} are the nominal values of the parameters, and U_{em}^{NF} the delivered voltage from the power electronics in the fault free case. These faults are relevant to monitor since they affect the delivered torque from the electric machine, as can be seen in (3.14) and recalled here

$$T_{em}^{eq3} = k \left(\frac{U_{em}}{R_{em}} - \frac{k}{R_{em}} \omega_{em} \right) - c_{em,f} \omega_{em} \quad (6.3)$$

The map based model is beneficial to use since it has high accuracy, but the model has the disadvantage that the parameters affected when a fault has occurred are not included in the model. In the other models of the electric machine described in Section 3.5, it is possible to easily induce the faults described in (6.2) since these parameters are included in the models. The accuracy is however generally lower in these models compared to the map based model. Therefore, the map based model is used to model the fault free case, and another model is used to model the influence of the faults on the electrical machine. In section 6.1 it is stated that functionality is added to the map based model to modify the requested torque using ΔT_{em} and the power losses using $\Delta P_{em,l}$, when there is a fault in the component. Expressions for ΔT_{em} and $\Delta P_{em,l}$ as functions of the fault modes in (6.2) are derived below.

6.2.1 Finding an expression for ΔT_{em}

An expression for ΔT_{em} is derived using `electricmotor_quasistatic3`, that includes a model for the friction losses and is described in Section 3.5.4. This model is used since the losses are better described in this model compared to for example `electricmotor_quasistatic2`. The losses for these two models are compared with the map describing the losses of the machine in Figures 3.2 and 3.3.

Based on (6.3) it can be stated that all three fault modes in (6.2) affect the delivered torque of the electric machine. This is modeled by modifying the requested torque to the fault free map based model according to

$$T_{em,req}^{map} = T_{em,req} + \Delta T_{em} \quad (6.4)$$

where $T_{em,req}$ is the requested torque from the energy management, and ΔT_{em} is the difference between T_{em} and $T_{em,req}$ due to a fault in the system. To find an expression for ΔT_{em} , `electricmotor_quasistatic3` given in Section 3.5.4 is used

$$\begin{aligned} \Delta T_{em} &= T_{em}^{eq3} - T_{em}^{eq3,NF} \\ &= \frac{k}{R_{em}} (U_{em} - k\omega_{em}) - \frac{k^{nom}}{R_{em}^{nom}} (U_{em}^{NF} - k^{nom}\omega_{em}) \end{aligned} \quad (6.5)$$

where T_{em}^{eq3} is the delivered torque from the machine given by (6.3), and $T_{em}^{eq3,NF}$ is the delivered torque in the fault free case that also is computed using (6.3), but with the nominal values of the parameters in the machine. The parameters k and R_{em} , and the voltage U_{em} used to calculate T_{em}^{eq3} , include models for the faults according to (6.2).

The voltage U_{em}^{ctrl} needs to be calculated to find U_{em} and U_{em}^{NF} used in (6.5). The voltage is not modeled in the map based model, and is therefore computed using `electricmotor_quasistatic3`. The angular speed and the requested torque is used in the expression, that is based on (6.3)

$$U_{em}^{ctrl} = \left(\frac{T_{em,req}}{k^{nom}} + \frac{c_{em,f}}{k^{nom}} \omega_{em} \right) R_{em}^{nom} + k^{nom} \omega_{em} \quad (6.6)$$

The delivered torque from the machine is not known in the controller of the machine, where U_{em}^{ctrl} is set, and therefore the requested torque in the map based model is used in (6.6). For the same reason R_{em} and k in the expression are the nominal values even if there is a fault in the machine affecting these parameters.

6.2.2 Finding an expression for $\Delta P_{em,l}$

The expression for the power losses in `electricmotor_quasistatic3` given in (3.17) is recalled here

$$P_{em,l}^{eq3} = R_{em} \left(\frac{T_{em}^2}{k^2} + \frac{2c_{em,f}}{k^2} \omega_{em} T_{em} + \frac{c_{em,f}^2}{k^2} \omega_{em}^2 \right) + c_{f,em} \omega_{em}^2 \quad (6.7)$$

The expression states that $f_{em,k}$ and $f_{em,R}$ affect the power losses in the model. The losses in the map based model are modeled as

$$\tilde{P}_{em,l}^{map} = P_{em,l}^{map} + \Delta P_{em,l} \quad (6.8)$$

where $P_{em,l}^{map}$ is the original map and $\Delta P_{em,l}$ are computed using the model `electricmotor_quasistatic3`

$$\begin{aligned}
\Delta P_{em,l} &= P_{em,l}^{eq3} - P_{em,l}^{eq3,NF} \\
&= R_{em} \left(\frac{T_{em}^2}{k^2} + \frac{2c_{em,f}}{k^2} \omega_{em} T_{em} + \frac{c_{em,f}^2}{k^2} \omega_{em}^2 \right) + c_{f,em} \omega_{em}^2 - \\
&\quad - \left[R_{em}^{nom} \left(\frac{T_{em}^2}{(k^{nom})^2} + \frac{2c_{em,f}}{(k^{nom})^2} \omega_{em} T_{em} + \frac{c_{em,f}^2}{(k^{nom})^2} \omega_{em}^2 \right) + c_{f,em} \omega_{em}^2 \right] \\
&= \left(\frac{R_{em}}{k^2} - \frac{R_{em}^{nom}}{(k^{nom})^2} \right) (T_{em}^2 + 2c_{em,f} \omega_{em} T_{em} + c_{em,f}^2 \omega_{em}^2) \quad (6.9)
\end{aligned}$$

where $P_{em,l}^{eq3}$ is the losses in `electricmotor_quasistatic3` given in (6.7), and $P_{em,l}^{eq3,NF}$ the losses in the same model when the nominal values of the parameters R_{em} and k are used. The torque used in the expression is the delivered torque T_{em} from the machine in the map based model, see Figure 6.2.

6.3 Maximum fault isolability performance

The best fault isolability performance that is possible to achieve in a diagnosis system monitoring the fault modes in (6.2) is investigated. In Section 6.3.1 this is done only using a fault free model of the electric machine in the diagnosis system. In Section 6.3.2 a model including fault models is considered.

6.3.1 Model for correct behavior

There are three fault modes to be monitored in the diagnosis system, and a single fault assumption is made. The fault modes affect the equation describing the delivered torque of the machine given in (6.4) and (6.5), and the power losses given in (6.8) and (6.9). All faults affect the delivered torque

$$T_{em} = g_1(f_{em,k}, f_{em,R}, f_{pe}) \quad (6.10)$$

while the power losses only depend on the fault modes in the electric machine

$$P_{em,l} = g_2(f_{em,k}, f_{em,R}) \quad (6.11)$$

The faults $f_{em,k}$ and $f_{em,R}$ are included in the same model equations and can therefore not be isolated from each other without using information about how the faults affect T_{em} or $P_{em,l}$. When the equation for $P_{em,l}$ is not consistent, this can only be explained by either $f_{em,k}$ or $f_{em,R}$, since f_{pe} does not affect the power losses. The fault in the power electronics affects the equation for T_{em} , where also $f_{em,k}$ and $f_{em,R}$ are included. If the equation for T_{em} is inconsistent, this can be explained with any of the faults. Therefore a fault in the

electric machine can be isolated from a fault in the power electronics, but not vice versa. Further, it is not possible to isolate the fault modes in the electric machine from each other when no fault models are used. These results are due to the structure of the model, and no sensor configuration can improve the fault isolability performance without using models for the faults.

If diagnosis aspects are considered when designing the model, it is possible to construct the model in a way that the different fault modes affect different parts of the model. By doing so it is possible to isolate the faults only using models for the correct behavior of the component.

6.3.2 Model for correct and faulty behavior

As stated above, fault models are required to isolate the fault modes from each other in the diagnosis system. Here the faults' influence on ΔT_{em} and $\Delta P_{em,l}$ described in (6.5) and (6.9) are used in the diagnosis system, and it is assumed that the faults are constant, i.e. $\dot{f} = 0$. Full isolability can possibly be achieved only using information about how T_{em} is modified when there is fault in the machine using (6.5). This is since the parameters k and R_{em} , and the voltage U_{em} are included in the expression for T_{em} . This information in combination with the knowledge of how the faults affect the parameters and the voltage in (6.2), can be used to isolate the faults from each other. One disadvantage of doing so is that the information about the faults' impact on $\Delta P_{em,l}$ in (6.9) will not be used. To use information from both the expressions for ΔT_{em} and $\Delta P_{em,l}$, the faults are estimated using observers.

6.4 Transforming the model from DAE to ODE

The model used in the observers, that are the basis in the diagnosis system, is summarized below. In its original form it is given as a DAE of index one, but is reformulated as an ODE to be able to use standard observer techniques in Section 6.5. The model of the electric machine used in the diagnosis system is based on the map based model described in Section 3.5.2, `electricmotor_quasistatic3` described in Section 3.5.4, and the fault models described in (6.2). The model is given in the form

$$\dot{x}_1 = 0 \tag{6.12a}$$

$$0 = g(x_1, x_2, u) \tag{6.12b}$$

$$y = h(x_1, x_2, u) \tag{6.12c}$$

where x_1 is the vector of faults, x_2 is the vector of algebraic variables, and u is the vector of known signals. The expression $g(x_1, x_2, u)$ includes the model equations, and the algebraic variables x_2 can be computed from $g(x_1, x_2, u)$ by

$$x_2 = g^{-1}(x_1, u) = G(x_1, u) \tag{6.13}$$

leading to the ODE

$$\dot{x}_1 = 0 \quad (6.14a)$$

$$y = h(x_1, G(x_1, u), u) \quad (6.14b)$$

which has the same solution set as (6.12). The algebraic variables x_2 and $G(x_1, u)$ are given by

$$\underbrace{\begin{bmatrix} k \\ R_{em} \\ U_{em}^{ctrl} \\ U_{em} \\ U_{em}^{NF} \\ \Delta T_{em} \\ T_{em,req}^{map} \\ T_{em,lim} \\ P_{em,m} \\ \Delta P_{em,l} \\ P_{em,l}^{map} \\ P_{em,e} \end{bmatrix}}_{x_2} = \underbrace{\begin{bmatrix} k^{nom}(1 + f_{em,k}) \\ R_{em}^{nom}(1 + f_{em,R}) \\ \frac{R_{em}^{nom}}{k^{nom}}(T_{em,req} + c_{em,f}\omega_{em}) + k\omega_{em} \\ U_{em}^{ctrl}(1 + f_{pe}) \\ U_{em}^{ctrl} \\ \frac{k}{R_{em}}[U_{em} - k\omega_{em}] - \frac{k^{nom}}{R_{em}^{nom}}[U_{em}^{NF} - k^{nom}\omega_{em}] \\ T_{em,req} + \Delta T_{em} \\ \min\{\max\{T_{em,min}, T_{em,req}^{map}\}, T_{em,max}\} \\ T_{em,lim}\omega_{em} \\ \left(\frac{R_{em}}{k^2} - \frac{R_{em}^{nom}}{(k^{nom})^2}\right)(T_{em}^2 + 2c_{em,f}\omega_{em}T_{em} + c_{em,f}^2\omega_{em}^2) \\ f(T_{em,lim}, \omega_{em}, U_b) \\ P_{em,m} + P_{em,l}^{map} + \Delta P_{em,l} \end{bmatrix}}_{G(x_1, u)} \quad (6.15)$$

The known signals are the requested torque, angular speed, and the battery voltage. Of these the angular speed and battery voltage are sensor signals

$$u = \begin{bmatrix} T_{em,req} \\ \omega_{em} \\ U_b \end{bmatrix} \quad (6.16)$$

The output signals are the delivered torque and the battery current, that are calculated in (6.12c) and are given by

$$h(x_1, x_2, u) = \begin{bmatrix} T_{em,lim} \\ \frac{P_{em,e}}{U_b} \end{bmatrix} \quad (6.17)$$

6.5 Design of residual generators

The residual generators used in the diagnosis system are based on the estimated faults computed in observers using the model presented in Section 6.4. One way to estimate the fault modes to be monitored is to design an observer estimating the three faults. This is not possible, since the faults are not observable when all faults are estimated using one observer. Instead three observers are used, where each observer estimates one fault, and assumes that the other faults are zero. The three observers estimating $f_{em,k}$, $f_{em,R}$, and f_{pe} , are denoted $\mathcal{O}_{em,k}$, $\mathcal{O}_{em,R}$, and \mathcal{O}_{pe} respectively.

To illustrate how the residual generators are constructed an example is used. When a constant fault has occurred in the power electronics resulting in that $U_{em} \neq U_{em}^{ctrl}$, \hat{f}_{pe} is constant, but the estimated faults $\hat{f}_{em,k}$ and $\hat{f}_{em,R}$ calculated in $\mathcal{O}_{em,k}$ and $\mathcal{O}_{em,R}$, are dependent on the operating point of the electric machine. This is to estimate the correct values of ΔT_{em} and $\Delta P_{em,l}$, and is illustrated below using the expression for ΔT_{em} in (6.5). It is only T_{em}^{eq3} and not $T_{em}^{eq3,NF}$ that is affected when there is a fault in the component. Combining (6.2) and (6.3) leads to

$$T_{em}^{eq3} = k^{nom}(1+f_{em,k}) \left(\frac{U_{em}^{NF}(1+f_{pe})}{R_{em}^{nom}(1+f_{em,R})} - \frac{k^{nom}(1+f_{em,k})}{R_{em}^{nom}(1+f_{em,R})} \omega_{em} \right) - c_{em,f} \omega_{em} \quad (6.18)$$

A fault in the resistance is e.g. included in two terms in the expression, one that is proportional to U_{em}^{NF} and one that is proportional to ω_{em} . The fault in the power electronics is only included in the term that is proportional to the voltage. This leads to that when there is a constant fault in the power electronics, the value of $\hat{f}_{em,R}$ varies with ω_{em} to achieve the same value for T_{em}^{eq3} as f_{pe} does. This information is used to construct residual generators in the diagnosis system.

The estimated faults are used in the residual generators, and it is only one of the three estimated faults in the observers that estimates a correct value of the fault. Three residual generators are created and these are equal to the variation in the estimated faults.

6.5.1 Observers

The observers estimating the faults used in the residual generators are designed using discrete Extended Kalman Filters (EKF) (Kailath et al., 2000). All three observers use the same model equations, except for which fault that is to be estimated, and the used model equations are given in (6.15). Note that two faults in (6.15) are assumed to be zero in the observers, and x_1 in (6.14a) only includes the fault that is to be estimated in the observer.

The system given in (6.14) is time discretized in the observers. This is trivial to do since the only dynamics in the model is $\dot{x}_1 = 0$. Adding the process noise ω results in

$$x_{1,t+1} = x_{1,t} + \omega_t \quad (6.19)$$

and the covariance of ω_t is denoted Q_t . The sensors assumed available in the diagnosis system are a torque sensor and a current sensor

$$y = \begin{bmatrix} T_{em,sens} \\ I_{b,sens} \end{bmatrix} \quad (6.20)$$

The torque sensor is used for simplicity, but if it is not available it is possible to use other sensors, as in Diagnosis system 2 and Diagnosis system 3 in Chapter 4.

The equations in the EKF can be divided into a measurement update phase and a time update phase. The measurement update phase is given by

$$\hat{x}_{1,t|t} = \hat{x}_{1,t|t-1} + K_t \left(y_t - \underbrace{h(\hat{x}_{1,t|t-1}, G(\hat{x}_{1,t|t-1}, u_t), u_t)}_{\hat{y}_t} \right) \quad (6.21)$$

where the observer gain K is calculated by

$$K_t = P_{t|t-1} H_t^T (H_t P_{t|t-1} H_t^T + R_t) \quad (6.22)$$

where R is the covariance of the sensor noise and P is given by

$$P_{t|t} = (I - K_t H_t) P_{t|t-1} \quad (6.23)$$

The matrix H used in (6.22) and (6.23) is calculated by

$$H_t = \left. \frac{dh}{dx_1} \right|_{x_1=\hat{x}_{1,t|t-1}} = \underbrace{\frac{\partial h}{\partial x_1}}_{=0} + \frac{\partial h}{\partial x_2} \frac{\partial G}{\partial x_1} \bigg|_{x_1=\hat{x}_{1,t|t-1}} \quad (6.24)$$

where

$$\frac{\partial h}{\partial x_2} = \begin{bmatrix} 0 & 0 & 0 & 0 & 0 & 0 & 0 & 0 & 1 & 0 & 0 & 0 & 0 \\ 0 & 0 & 0 & 0 & 0 & 0 & 0 & 0 & 0 & 0 & 0 & 0 & \frac{1}{U_b} \end{bmatrix} \quad (6.25)$$

and $\left. \frac{\partial G}{\partial x_1} \right|_{x_1=\hat{x}_{1,t|t-1}}$ is numerically estimated using the central difference

$$\left. \frac{\partial G(x_1, u)}{\partial x_1} \right|_{x_1=\hat{x}_{1,t|t-1}} \approx \frac{G(\hat{x}_1 + \frac{\varepsilon}{2}, u) - G(\hat{x}_1 - \frac{\varepsilon}{2}, u)}{\varepsilon} \quad (6.26)$$

where ε is a small value. The time update phase is given by

$$\hat{x}_{1,t+1|t} = \hat{x}_{1,t|t} \quad (6.27)$$

since $x_{1,t+1} = x_{1,t}$. The P matrix is updated using

$$P_{t+1|t} = P_{t|t} + Q_t \quad (6.28)$$

6.5.2 Residual generators and decision structure

As stated above, three residual generators are constructed based on the change in the estimated faults in the observers between two time steps. An expression for this is found in (6.21)

$$r_t = \hat{x}_{1,t|t} - \hat{x}_{1,t|t-1} = K_t (y_t - \hat{y}_t) \quad (6.29)$$

The test quantities are post processed using the CUSUM algorithm described in Section 4.1.2. The decision structure is shown in Table 6.1, where T_1 , T_2 , and T_3 are based on $\mathcal{O}_{em,k}$, $\mathcal{O}_{em,R}$, and \mathcal{O}_{pe} respectively.

Table 6.1: Decision structure for the diagnosis system including fault models. Full isolability is structurally achieved, since a unique set of tests ideally react for each fault.

	$f_{em,k}$	$f_{em,R}$	f_{pe}
T1		X	X
T2	X		X
T3	X	X	

6.6 Results

Simulations are carried out to investigate the performance of the designed diagnosis system. The faults are induced one by one in the model, and the driving cycle used is FTP75. The faults induced in the model are $f_{em,k} = -0.03$, $f_{em,R} = -0.03$, and $f_{pe} = -0.01$, respectively. The faults are smaller compared to the induced faults in Chapters 4 and 5, where a fault has resulted in that a parameter value is half of its nominal value according to Table 4.1.

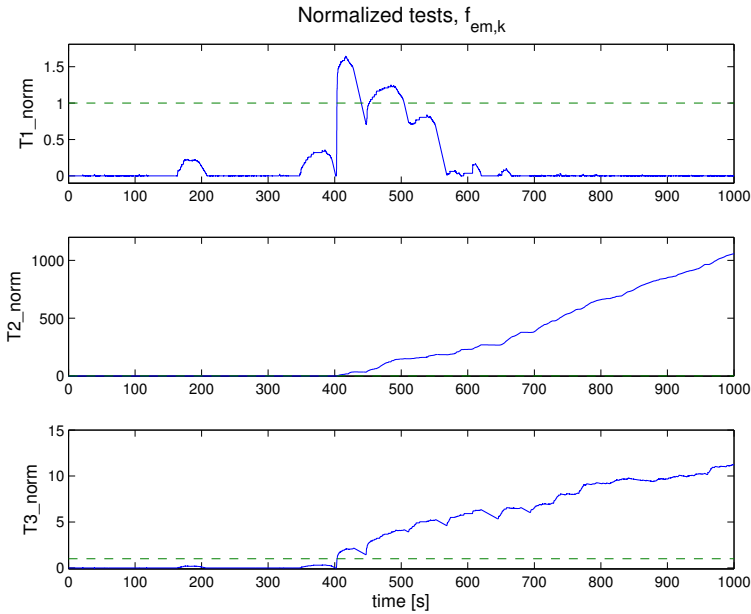


Figure 6.3: The normalized test quantities when $f_{em,k}$ has occurred after 400 seconds in FTP75. Test 2 and Test 3 are supposed to react on the fault and do so. Test 1 reacts for a short period immediately after the fault is induced. This can be explained with that the assumption $\dot{f} = 0$ is not fulfilled when the fault occurs.

The tests are well below the thresholds in the fault free case, and all monitored faults in the diagnosis system are detected and fully isolated. Figure 6.3 shows the normalized test quantities (see Section 4.7 for the definition) when $f_{em,k}$ is induced in the model after 400 seconds. According to the decision structure in Table 6.1, Test 2 and Test 3 are supposed to react on this fault. In Figure 6.3 it can be shown that also Test 1 reacts on the fault for a short time. The reason for this is that when the fault is induced, the assumption $\dot{f} = 0$ is no longer valid. The residual is non-zero since $\hat{f}_{em,k}$ in $\mathcal{O}_{em,k}$ has not converged to the value of the fault. This can be solved by e.g. adding a constraint that a test has to be above the threshold a predefined time before the test alarms.

The estimated faults in the three observers when $f_{em,k}$ is induced in the vehicle model, are presented in Figure 6.4. It can be seen that $\hat{f}_{em,k}$ converges fast to the correct value. It can also be seen that \hat{f}_{pe} does not vary as much as $\hat{f}_{em,R}$ when $f_{em,k}$ is induced. This can be explained by that U_{em} and $k\omega_{em}$ in (6.5) are of the same order of magnitude in most operating points. An increase in ΔT_{em} can e.g. be achieved by increasing U_{em} or decreasing $k\omega_{em}$. When large torques are delivered by the electric machine, the difference between U_{em} and $k\omega_{em}$ is larger, and the term $\frac{k}{R_{em}}$ in (6.5) has larger influence on ΔT_{em} . Therefore it is possible to isolate the faults f_{pe} and $f_{em,k}$ from each other.

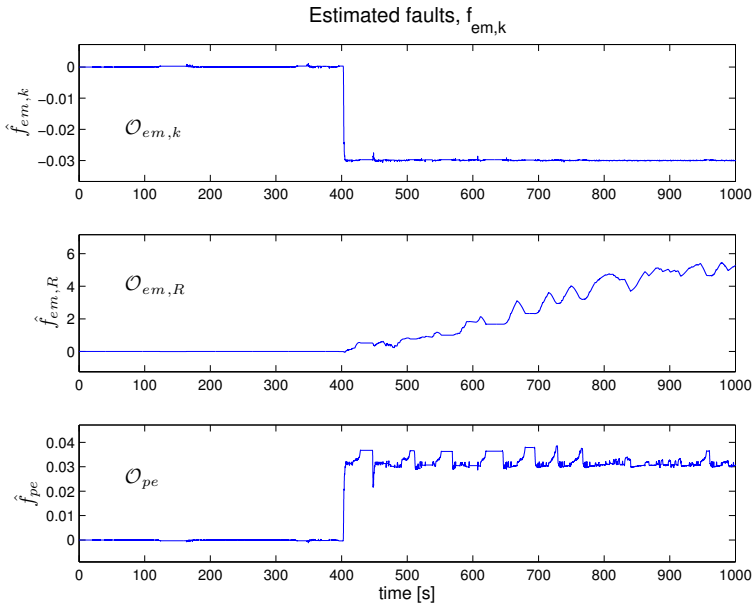


Figure 6.4: The estimated faults in the three observers when $f_{em,k} = -0.03$ after 400 seconds in FTP75. The estimated fault $\hat{f}_{em,k}$ converges fast to the value of $f_{em,k}$, and especially $\hat{f}_{em,R}$ varies significantly.

6.7 Conclusions

A diagnosis system monitoring the electric machine and the power electronics has been designed using a map based model. Such models are generally accurate and are therefore beneficial to use to detect faults in a diagnosis system. As a consequence of the structure of the model used, it is shown that full fault isolability is not possible to achieve only using the model for correct behavior of the machine. To obtain isolability fault models are therefore introduced. In this work a methodology including two models of the electric machine is used in the design of the diagnosis system. A parametrized model based on an equivalence circuit is used to model how the faults affect the machine, and the map based model is used to model the fault free behavior of the component. The advantage of this design methodology is that it is possible to isolate the faults, and the performance of the diagnosis system increases compared to a diagnosis system only using the equivalence circuit model.

The model including the faults is given as a DAE and is reformulated as an ODE. Based on the model, three observers are used to estimate the size of the faults in the machine, and this is possible to do since fault models are used in the diagnosis system. In the simulation study, the tests that are supposed to react on the induced faults react. This results in that the diagnosis system isolates the faults in the simulations, even though the induced faults are small. One test that is not supposed to react do so for a short period. The reason for this is that the assumption that the faults in the monitored system are constant is not valid when the fault is induced in the machine. Finally, the size of the faults are accurately estimated in the observers.

CONCLUSIONS

When designing a diagnosis system on vehicle level for a hybrid powertrain, it is crucial to understand how the sensor configuration, energy management, and design of the diagnosis system affect the diagnosis performance, and design and computational complexity of the system. To investigate these aspects, several diagnosis systems have been analyzed and explored by designing and evaluating the systems using a simulation model of a long haulage truck.

Three diagnosis systems based on fault free models of the vehicle and different sensor configurations were designed and evaluated in Chapter 4. Two sensor configurations include the same number of sensors, but in one of these systems the sensors are placed closer, in model sense, to the components to be monitored. The third sensor configuration uses a minimal set of sensors to structurally achieve full fault isolability in the diagnosis system. The diagnosis systems are evaluated, and the performance is good, even though no models for the faults are used in the systems. One benefit of not using fault models is that the designer of the diagnosis system does not need to know how a fault will affect the monitored system, except from which model equations that are affected of the fault. It is shown that the performance of the diagnosis systems generally is increased if several sensors are available, and the sensors measure signals leading to that a small part of the vehicle model is used in the diagnosis. There is no major difference in the design complexity of the three diagnosis systems, but in the diagnosis system based on a minimal set of sensors, the residual generators are larger and therefore slightly more computational demanding than the other two systems. The performance of the diagnosis is dependent on the operating points of the vehicle and if this is considered when the energy management is

designed, a pattern of operating points of the vehicle that positively affect the diagnosis performance can be used.

The selection of consistency relation in a set of equations to be used in a residual generator affects the diagnosis performance, which is illustrated in a realistic example in Chapter 5. It is shown that it is possible to uniquely compute the unknown variables in the residual generators for some selections of consistency relations, but not for others, given an overdetermined set of equations to be used. Using a permanent magnet synchronous machine the selection of consistency relation either results in uniqueness of the variables in the residual generators or not, but when a series wound machine was used it was no longer possible to find a unique residual generator for the corresponding set of equations. There are many possible residual generators to be used in a diagnosis system and to find good alternatives among all possible residual generators in large systems, systematic methods investigating the properties in the residual generator candidates are valuable. In e.g. the diagnosis system designed in Chapter 5, only two of approximately 30 equations can be selected to be consistency relations to achieve unique residuals and integral causality in the computational sequences in the residual generators. Thus, the value of using systematic methods to analyze the residual generator candidates is reinforced. A diagnosis system where unique residual and integral causality is used is compared with a diagnosis system using the same sensor configuration designed in Chapter 4. The systems are based on the same MSOs, but the performance is better in the system designed with respect to the constraints in the residual generators.

Map based models are common in automotive systems and a diagnosis system is designed using such a model. One benefit of using a map based model in a diagnosis system is that the model is based on measurements and the accuracy of the model is high, which generally leads to that the possibility to detect faults is high in the diagnosis system. As a consequence of the structure of the map based model used in Chapter 6, fault models are required to achieve full fault isolability since the faults affect the same model equations. The faults' impact on the machine were modeled using an equivalence circuit model of the machine, and the model used was developed to capture the qualitative behavior of the machine. By using both the map based model and the model based on the equivalence circuit in the diagnosis system, it is possible to isolate the faults, and the size of the faults are accurately estimated in the observers.

It is indicated throughout the thesis that the performance of the diagnosis system is affected by the sensor configuration, design of the energy management, and the design of the diagnosis system. If the interaction between the operating points of the components in the powertrain, design of the diagnosis system, and the diagnosis performance is understood, it may be possible to reduce the number of sensors required in the diagnosis, and thereby reduce cost.

REFERENCES

Armengol, J., Bregon, A., Escobet, T., Gelso, E. R., Krysander, M., Nyberg, M., Olive, X., Pulido, B., and Trave-Massuyes, L. (2009). Minimal structurally overdetermined sets for residual generation: A comparison of alternative approaches. In *Proceedings of IFAC Safeprocess'09*, Barcelona, Spain.

Blanke, M., Kinnaert, M., Lunze, J., and Staroswiecki, M. (2006). *Diagnosis and Fault-Tolerant Control*. Springer, 2nd edition.

Borhan, H. A., Vahidi, A., Phillips, A. M., Kuang, M. L., and Kolmanovsky, I. V. (2009). Predictive energy management of a power-split hybrid electric vehicle. In *Proceedings of the 2009 conference on American Control Conference*, pages 3970–3976, Piscataway, USA. IEEE Press.

Brenan, K. E., Campbell, S. L., and Petzold, L. R. (1996). *Numerical Solution of Initial-Value Problems in Differential-Algebraic Equations*. Siam.

CAPSim (2009). <http://www.capsim.se>.

Cassar, J. and Staroswiecki, M. (1997). A structural approach for the design of failure detection and identification systems. In *Proceedings of IFAC Control of Industrial Systems*, Belfort, France.

Chau, K., Chan, C., and Liu, C. (2008). Overview of permanent-magnet brushless drives for electric and hybrid electric vehicles. *Industrial Electronics, IEEE Transactions on*, 55(6):2246–2257.

- de Flaugergues, V., Cocquempot, V., Bayart, M., and Pengov, M. (2009). Structural analysis for fdi: a modified, invertibility-based canonical decomposition. In *Proceedings of the 20th International Workshop on Principles of Diagnosis*, pages 59–66.
- de Kleer, J., Mackworth, A., and Reiter, R. (1992). Characterizing diagnoses and systems. *Artificial Intelligence*, 56(2-3):197–222.
- de Kleer, J. and Williams, B. C. (1987). Diagnosing multiple faults. *Artificial Intelligence*, 32:97–130.
- Dulmage, A. and Mendelsohn, N. (1958). Coverings of bipartite graphs. *Canadian Journal of Mathematics*, 10:517–534.
- Dustegör, D., Frisk, E., Coquempot, V., Krysander, M., and Staroswiecki, M. (2006). Structural analysis of fault isolability in the DAMADICS benchmark. *Control Engineering Practice*, 14(6):597–608.
- Fitzgerald, A., Charles Kingsley, J., and Umans, S. D. (2003). *Electric Machinery*. McGraw - Hill, Singapore, 6th edition.
- Frisk, E., Bregon, A., Åslund, J., Krysander, M., Pulido, B., and Biswas, G. (2010). Diagnosability analysis considering causal interpretations for differential constraints. 21st International Workshop on Principles of Diagnosis (DX-10), Portland, Oregon, USA.
- Frisk, E. and Nyberg, M. (2001). A minimal polynomial basis solution to residual generation for fault diagnosis in linear systems. *Automatica*, 37(9):1417–1424.
- Gerhardsson, D. (2010). Starter motor protection. Master’s thesis, LiTH-ISY-EX-10/4405--SE, Linköping University.
- Guzzella, L. and Amstutz, A. (1999). CAE tools for quasi-static modeling and optimization of hybrid powertrains. *Vehicular Technology, IEEE Transactions on*, 48(6):1762 –1769.
- Guzzella, L. and Onder, C. H. (2004). *Introduction to Modeling and Control of Internal Combustion Engine Systems*. Springer Verlag, Zürich.
- Guzzella, L. and Sciarretta, A. (2007). *Vehicle Propulsion System, Introduction to Modelling and Optimization*. Springer Verlag, Zürich, 2nd edition.
- Hambley, A. R. (2005). *Electrical Engineering, principles and applications*. Pearson Education, Upper Sadle River, 3rd edition.
- Inhelder, J. (1996). *Verbrauchs- und schadstoffoptimiertes Ottomotor-Aufladekonzept*. PhD thesis, Eidgenössische Technische Hochschule.

- Kailath, T., Sayed, A. H., and Hassibi, B. (2000). *Linear Estimation*. Prentice Hall.
- Krysander, M., Åslund, J., and Nyberg, M. (2008). An efficient algorithm for finding minimal over-constrained sub-systems for model-based diagnosis. *IEEE Transactions on Systems, Man, and Cybernetics – Part A: Systems and Humans*, 38(1).
- Krysander, M. and Frisk, E. (2008). Sensor placement for fault diagnosis. *IEEE Transactions on Systems, Man, and Cybernetics – Part A: Systems and Humans*, 38(6):1398–1410.
- Lin, C.-C., Peng, H., Grizzle, J., and Kang, J.-M. (2003). Power management strategy for a parallel hybrid electric truck. *Control Systems Technology, IEEE Transactions on*, 11(6):839 – 849.
- Mellor, P. (1999). High efficiency drive-trains for electric and hybrid vehicles. In *Electrical Machine Design for All-Electric and Hybrid-Electric Vehicles (Ref. No. 1999/196)*, *IEE Colloquium on*, pages 8/1 –8/7.
- Page, E. (1954). Continuous inspection schemes. *Biometrika*, 41:100–115.
- Peterson, S. B., Apt, J., and Whitacre, J. (2010). Lithium-ion battery cell degradation resulting from realistic vehicle and vehicle-to-grid utilization. *Journal of Power Sources*, 195(8):2385 – 2392.
- Pulido, B. and Gonzalez, C. (2004). Possible conflicts: a compilation technique for consistency-based diagnosis. *Systems, Man, and Cybernetics, Part B: Cybernetics, IEEE Transactions on*, 34(5):2192 –2206.
- Sciarretta, A. and Guzzella, L. (2007). Control of hybrid electric vehicles. *IEEE CONTROL SYSTEMS MAGAZINE*, 27(2):60–70.
- Sivertsson, M. J., Sundström, C., and Eriksson, L. (2011). Fuel consumption minimization in a two axle hybrid with adaptive ECMS. Accepted for publication in IFAC Word Congress, Milano, Italy.
- Struss, P. and Dressier, O. (1989). "physical negation": integrating fault models into the general diagnostic engine. In *Proceedings of the 11th international joint conference on Artificial intelligence - Volume 2*, pages 1318–1323, San Francisco, CA.
- Sundström, C., Frisk, E., and Nielsen, L. (2010a). Overall monitoring and diagnosis for hybrid vehicle powertrains. In *6th IFAC Symposium on Advances in Automotive Control*, Munich, Germany.
- Sundström, C., Frisk, E., and Nielsen, L. (2010b). A platform for overall monitoring and diagnosis for hybrid vehicle powertrains. Technical Report LiTH-R-2925, Department of Electrical Engineering, Linköpings Universitet, Sweden.

- Sundström, C., Frisk, E., and Nielsen, L. (2011). Residual generator selection for fault diagnosis of hybrid vehicle powertrains. Accepted for publication in IFAC World Congress, Milano, Italy.
- Svärd, C. and Nyberg, M. (2010). Residual generators for fault diagnosis using computation sequences with mixed causality applied to automotive systems. *IEEE Transactions on Systems, Man, and Cybernetics – Part A: Systems and Humans*, 40(6):1310–1328.
- Valøen, L. O. and Shoesmith, M. I. (2007). The effect of PHEV and HEV duty cycles on battery and battery pack performance. In *Proceedings in 2007 Plug-in Highway Electric Vehicle Conference*, Manitoba, Canada.
- Wallmark, O. (2006). *Control of Permanent-Magnet Synchronous Machines in Automotive Applications*. PhD thesis, Chalmers tekniska högskola.
- Zhu, G., Dessaint, L.-A., Akhrif, O., and Kaddouri, A. (2000). Speed tracking control of a permanent-magnet synchronous motor with state and load torque observer. *Industrial Electronics, IEEE Transactions on*, 47(2):346–355.
- Zhu, Z. and Howe, D. (2007). Electrical machines and drives for electric, hybrid, and fuel cell vehicles. *Proceedings of the IEEE*, 95(4):746–765.

MODEL EQUATIONS

The model equations used in the simulation environment for the vehicle driver, control and energy management, and vehicle components are summarized in this appendix. Some of the equations are already presented in Chapter 2 and 3. The model equations of two electric machine models are presented. It is `electricmotor_quasistatic2` and the map based model, since both these models are used in the diagnosis systems described in Chapters 4-6. The models for the engine and one of the electric machines include a controller, that converts the requested torque from the energy management to a signal related to the amount of fuel to be injected, and the voltage to be applied on the machine, respectively. These controllers are below denoted local controllers. There is a local controller in the buffer that estimates the *SoC*, and this signal is used in the energy management.

A.1 Vehicle driver

$$\begin{aligned}
 e &= v_{ref} - v \\
 u_{vd} &= \begin{cases} -1, & K_p e + K_i \int edt < -1 \\ K_p e + K_i \int edt, & -1 \leq K_p e + K_i \int edt < 1 \\ 1, & K_p e + K_i \int edt \geq 1 \end{cases} \\
 accPed &= \max \{u_{vd}, 0\} \\
 brakePed &= -\min \{u_{vd}, 0\} \\
 gear &= f(v, v_{ref}), \quad gear \in \{0, 1, \dots, 12\} \\
 clutchPed(t) &= \begin{cases} 0, & gear(t) \neq gear(t - \Delta) \\ 1, & gear(t) = gear(t - \Delta) \end{cases}
 \end{aligned}$$

A.2 Control and energy management

The requested retardation torque, T_r , and traction torque, T_t , from the driver are calculated as a function of the pedal positions

$$\begin{aligned}
 T_r &= f(brakePed, \omega_e) \\
 T_t &= f(accPed, \omega_e)
 \end{aligned}$$

and the overall requested torque is

$$T_{req} = T_t - T_r \quad (\text{A.1})$$

The torques $T_{e,req}$, $T_{em,req}$ and $T_{b,req}$ are determined by

```

if Treq < 0
  if soc > socUpperLimit
    Tem = 0;
    Tbrake = Treq;
  else
    if -maxEMBrakeTorque < Treq
      if gear == 0
        Tem=0;
        Tbrake = Treq*Gr;
      else
        Tem = Treq/uem;
        Tbrake = 0;
      end
    else
      if gear == 0
        Tem = 0;
        Tbrake = Treq;
      else
        Tem = -maxEMBrakeTorque;
        Tbrake = (Treq + maxEMBrakeTorque)*Gr;
      end
    end
  end

```

```

        end
    end

else
    if socDiff > 0
        if socDiff < 0.02
            maxEMTorqueLocal = 50*(socDiff)*maxEMTorque;
        else
            maxEMTorqueLocal = maxEMTorque;
        end
    elseif socDiff < -0.05
        if socDiff > -0.07
            maxEMTorqueLocal = 50*(socDiff+0.05)*maxEMTorque;
        else
            maxEMTorqueLocal = -maxEMTorque;
        end
    else
        maxEMTorqueLocal = 0;
    end

    if connected == 0
        if gear == 0
            Tem = 0;
            Tice = 0;
        else
            if Treq < maxEMTorqueLocal
                Tem = Treq;
                Tice = 0;
            else
                Tem = maxEMTorqueLocal;
                Tice = 0;
            end
        end
    else
        if gear == 0
            Tem = 0;
            Tice = 0;
        else
            if Treq < 0.7*maxEMTorqueLocal
                Tem = Treq*1/uem;
                Tice = 0;
            else
                Tem = 0.7*maxEMTorqueLocal;
                Tice = Treq - Tem*uem;
            end
        end
    end
end

TeReq1 = Tice;
TemReq1 = Tem;
TbReq1 = Tbrake;

```

$$\begin{aligned}
T_{e,req} &= \frac{1}{\tau_{ctrl}S + 1} T_{e,req1} \\
T_{em,req} &= \frac{1}{\tau_{ctrl}S + 1} T_{em,req1} \\
T_{b,req} &= \frac{1}{\tau_{ctrl}S + 1} T_{b,req1}
\end{aligned}$$

A.3 Vehicle

A.3.1 Fuel tank

$$\begin{aligned}
m_f &= \int -\max\{0, \dot{m}_f\} dt + m_{f,0} \\
m_{f,r} &= \int \max\{0, \dot{m}_f\} dt
\end{aligned}$$

A.3.2 Engine

Local controller:

$$ice_{ctrl} = p_{mf} V_d = \underbrace{\left(T_{e,req} \frac{16}{SB^2 N_{cyl}} + p_{me0,f} + p_{me0,g} \right)}_{p_{mf} \eta_{e,i}} \frac{N_{cyl} \pi SB^2}{4 \eta_{e,i}}$$

$$p_{me0,f} = k_1 (k_2 + k_3 S^2 \omega_{e,sens}^2) \Pi_{bl} \sqrt{\frac{k_A}{B}}$$

engine:

$$\dot{m}_f = ice_{ctrl} \frac{\omega_e}{4 \pi Q_{LHV}}$$

$$T_e = \left(ice_{ctrl} \frac{4 \eta_{e,i}}{N_{cyl} \pi SB^2} - p_{me0,f} - p_{me0,g} \right) N_{cyl} \frac{SB^2}{16}$$

$$p_{me0,f} = k_1 (k_2 + k_3 S^2 \omega_e^2) \Pi_{bl} \sqrt{\frac{k_A}{B}}$$

A.3.3 Buffer

Local controller:

$$SoC_{ctrl} = \int -\frac{I_{b,sens}}{Q_b} dt$$

Buffer:

$$\begin{aligned} SoC &= \int -\frac{I_b}{Q_b} dt \\ U_{oc} &= f(SoC) \\ U_b &= nU_{oc} - nR_b I_b \end{aligned}$$

A.3.4 Electric Machine - electricmotor_quasistatic2

Local controller:

$$U_{limit,upper} = \left(P_{em,max} + \frac{k_a k_i}{R_{em}} \omega_{em,sens}^2 \right) \frac{R_{em}}{k_i \omega_{em,sens}} \quad (A.2)$$

$$U_{limit,lower} = - \left(P_{em,max} + \frac{k_a k_i}{R_{em}} \omega_{em,sens}^2 \right) \frac{R_{em}}{k_i \omega_{em,sens}} \quad (A.3)$$

$$U_{unlimit} = T_{em,req} \frac{R_{em}}{k_a} + \frac{k_i}{R_{em}} \omega_{em,sens}$$

$$U_{em,ctrl} = \begin{cases} U_{limit,lower}, & U_{unlimit} < U_{limit,lower} \\ U_{unlimit}, & U_{limit,lower} \leq U_{unlimit} < U_{limit,upper} \\ U_{limit,upper}, & U_{unlimit} \geq U_{limit,upper} \end{cases}$$

Remark: There is a bug in the CAPSim implementation of equations (A.2) and (A.3), and the equations above are the corrected ones.

Electric machine:

$$\begin{aligned} \tilde{U}_{em} &= \frac{1}{\tau_{em}s + 1} U_{em,ctrl} \\ T_{em} &= \frac{\tilde{U}_{em} k_a}{R_{em}} - \frac{\omega_{em} k_a k_i}{R_{em}} \\ I_b &= \underbrace{\frac{T_{em}}{k_a}}_{I_{em}} \frac{\tilde{U}_{em}}{U_b} \end{aligned}$$

A.3.5 Electric Machine - Map based model

$$\begin{aligned}
 T_{em,min} &= f(\omega_{em}, U_b) \\
 T_{em,max} &= f(\omega_{em}, U_b) \\
 T_{em,lim} &= \begin{cases} T_{em,min}, & T_{em,req} < T_{em,min} \\ T_{em,req}, & T_{em,min} \leq T_{em,req} < T_{em,max} \\ T_{em,max}, & T_{em,req} \geq T_{em,max} \end{cases} \\
 T_{em} &= \frac{1}{\tau_{em}s + 1} T_{em,lim} \\
 P_{em,l} &= f(T_{em}, \omega_{em}, U_b) \\
 P_{em,m} &= T_{em} \omega_{em} \\
 P_{em,e} &= P_{em,m} + P_{em,l} \\
 I_b &= \frac{P_{em,e}}{U_b}
 \end{aligned}$$

A.3.6 Clutch

$$\begin{aligned}
 T_c &= T_e, & \text{clutchPed} \geq 0.1 \wedge |\Delta\omega| < 1 \text{rad/s} \\
 \omega_c &= \omega_e, & \text{clutchPed} \geq 0.1 \wedge |\Delta\omega| < 1 \text{rad/s}
 \end{aligned}$$

A.3.7 Mechanical joint

$$\begin{aligned}
 T_{mj} &= T_{em} u_{em} + T_c \\
 J_{mj} &= J_{em} u_{em}^2 + J_c + J_e \\
 \omega_{em} &= \frac{1}{u_{em}} \omega_{mj} \\
 \omega_c &= \omega_{mj}
 \end{aligned}$$

A.3.8 Gearbox

$$\begin{aligned}
 J_{gb} &= f(\text{gear}) \\
 u_{gb} &= f(\text{gear}) \\
 \eta_{gb} &= \begin{cases} \eta_{pos}, & T_{mj} > T_{gb,l} \\ \eta_{neg}, & T_{mj} \leq T_{gb,l} \end{cases} \\
 T_{gb,l} &= f(\text{gear}, \omega_e) \\
 T_{gb} &= (T_{mj} - T_{gb,l}) \eta_{gb} u_{gb} \\
 J_{tot} &= (J_{gb} + u_{gb}^2 J_{mj}) \\
 \omega_{mj} &= \frac{1}{u_{gb}} \omega_{gb}
 \end{aligned}$$

A.3.9 Chassis

$$\begin{aligned}
 m_v &= m_{v,0} - m_{f,r} \\
 T_d &= \frac{1}{2} \rho C_d A_f \omega_w^2 r_w^3 \\
 T_r &= \begin{cases} m_v g C_r r_w, & 1000 \omega_w > m_v g C_r r_w \\ 1000 \omega_w, & -m_v g C_r r_w \leq 1000 \omega_w < m_v g C_r r_w \\ -m_v g C_r r_w, & 1000 \omega_w \leq -m_v g C_r r_w \end{cases} \\
 T_g &= m_v g r_w \sin \alpha \\
 T_b &= T_{b,ctrl} \\
 T_{net} &= T_{gb} u_f - T_d - T_b - T_r - T_g \\
 \dot{\omega}_w &= \frac{T_{net}}{J_{tot} u_f^2 + m_v r_w^2} \\
 v &= \omega_w r_w \\
 s &= r_w \int \omega_w dt \\
 \omega_{gb} &= \omega_w u_f
 \end{aligned}$$

RESIDUAL GENERATORS USED IN CHAPTER 4

Five residual generators used in Diagnosis system 2 and Diagnosis system 3 are presented in this appendix. All these residual generators include dynamics, and the same consistency relation is used in all residual generators. It is the same consistency relation that is used in Test 3 in Diagnosis system 2, given in (4.6), and is recalled

$$\tilde{r} = \underbrace{\frac{1}{u_{em}} \left(J_{tot} + \frac{1}{u_f^2} m_v r_w^2 \right)}_a \dot{\omega}_{gb} + \underbrace{\frac{1}{u_{em} u_f} (T_d + T_r + T_b) + \frac{u_{gb} \eta_{gb}}{u_{em}} (T_{gb,l} - T_e) - (u_{gb} \eta_{gb}) T_{em}}_b$$

The variables are differently computed in the residual generators, and the tests are therefore sensitive for different fault modes in the vehicle. The equations used in Test 4 in Diagnosis system 2 are given in Section B.1, and the equations used in Tests 3-6 in Diagnosis system 3 are presented in Sections B.2-B.5.

B.1 Diagnosis system 2 - Test 4

$$\begin{aligned}
u_{gb} &= f(\text{gear}) \\
\dot{m}_f &= \text{ice}_{ctrl} \frac{\omega_e}{4\pi q_{LHV}} \\
m_{f,r} &= \int \dot{m}_f dt \\
m_v &= m_{v,0} - m_{f,r} \\
\eta_{gb} &= \begin{cases} \eta_{pos}, & T_{mj} > T_{gb,l} \\ \eta_{neg}, & T_{mj} \leq T_{gb,l} \end{cases} \\
T_{mj} &= u_{em} T_{em} + T_c \\
T_c &= T_e, \text{ when clutch engaged} \\
J_{tot} &= (J_{gb} + J_{mj}) u_{gb}^2 \\
J_{gb} &= f(\text{gear}) \\
J_{mj} &= J_{em} u_{em}^2 + J_c + J_e \\
T_d &= \frac{1}{2} \rho C_d A_f \omega_w^2 r_w^3 \\
T_r &= \begin{cases} m_v g C_r r_w, & 1000 \omega_w > m_v g C_r r_w \\ 1000 \omega_w, & -m_v g C_r r_w \leq 1000 \omega_w < m_v g C_r r_w \\ -m_v g C_r r_w, & 1000 \omega_w \leq -m_v g C_r r_w \end{cases} \\
T_b &= T_{b,ctrl} \\
\omega_w &= \frac{\omega_{gb}}{u_f} \\
T_e &= \left(\text{ice}_{ctrl} \frac{4\eta_{e,i}}{N_{cyl} \pi S B^2} - p_{me0,f} - p_{me0,g} \right) N_{cyl} \frac{S B^2}{16} \\
p_{me0,f} &= k_1 (k_2 + k_3 S^2 \omega_e^2) \Pi \sqrt{\frac{k_4}{B}} \\
T_g &= m_v g r_w \sin \alpha \\
T_{em} &= I_{em} k_a \\
I_{em} &= \frac{I_b U_b}{\tilde{U}_{em}} \\
\tilde{U}_{em} &= \frac{1}{\tau_{em} s + 1} U_{em} \\
U_b &= n U_{oc} - n R_b I_b \\
U_{oc} &= f(\text{SoC}) \\
\text{SoC} &= \int \dot{\text{SoC}} dt \\
\dot{\text{SoC}} &= -\frac{I_b}{Q_b} \\
\omega_e &= \omega_{e,sens} \\
\omega_{gb} &= \omega_{gb,sens} \\
U_{em} &= U_{em,sens} \\
I_b &= I_{b,sens}
\end{aligned} \tag{B.1}$$

B.2 Diagnosis system 3 - Test 3

$$\begin{aligned}
u_{gb} &= f(\text{gear}) \\
m_v &= m_{v,0} - m_{f,r} \\
m_{f,r} &= \int \dot{m}_f dt \\
\dot{m}_f &= \text{ice}_{ctrl} \frac{\omega_e}{4\pi q_{LHV}} \\
\eta_{gb} &= \begin{cases} \eta_{pos}, & T_{mj} > T_{gb,l} \\ \eta_{neg}, & T_{mj} \leq T_{gb,l} \end{cases} \\
J_{tot} &= (J_{gb} + J_{mj}) u_{gb}^2 \\
J_{gb} &= f(\text{gear}) \\
J_{mj} &= J_{em} u_{em}^2 + J_c + J_e \\
T_r &= \begin{cases} m_v g C_r r_w, & 1000\omega_w > m_v g C_r r_w \\ 1000\omega_w, & -m_v g C_r r_w \leq 1000\omega_w < m_v g C_r r_w \\ -m_v g C_r r_w, & 1000\omega_w \leq -m_v g C_r r_w \end{cases} \\
T_b &= T_{b,ctrl} \\
T_{gb,l} &= f(\text{gear}, \omega_e) \\
\omega_w &= \frac{\omega_{gb}}{u_f} \\
T_e &= \left(\text{ice}_{ctrl} \frac{4\eta_{e,i}}{N_{cyl} \pi S B^2} - p_{me0,f} - p_{me0,g} \right) N_{cyl} \frac{S B^2}{16} \\
p_{me0,f} &= k_1 \left(k_2 + k_3 S^2 \omega_e^2 \right) \Pi \sqrt{\frac{k_4}{B}} \\
\omega_e &= \omega_{mj} \\
\omega_{mj} &= u_{gb} \omega_{gb} \\
T_{em} &= \frac{\tilde{U}_{em} k_a - \omega_{em} k_a k_i}{R_{em}} \\
\tilde{U}_{em} &= \frac{1}{\tau_{em} s + 1} U_{em} \\
U_{em} &= U_{em,ctrl} \\
\omega_{gb} &= \omega_{gb,sens}
\end{aligned}$$

B.3 Diagnosis system 3 - Test 4

$$\begin{aligned}
u_{gb} &= f(\text{gear}) \\
m_v &= m_{v,0} - m_{f,r} \\
m_{f,r} &= \int \dot{m}_f dt \\
\dot{m}_f &= \text{ice}_{ctrl} \frac{\omega_e}{4\pi Q_{LHV}} \\
\eta_{gb} &= \begin{cases} \eta_{pos}, & T_{mj} > T_{gb,l} \\ \eta_{neg}, & T_{mj} \leq T_{gb,l} \end{cases} \\
J_{tot} &= (J_{gb} + J_{mj}) u_{gb}^2 \\
J_{gb} &= f(\text{gear}) \\
J_{mj} &= J_{em} u_{em}^2 + J_c + J_e \\
T_{mj} &= u_{em} T_{em} + T_c \\
T_c &= T_e, \text{ when clutch engaged} \\
T_d &= \frac{1}{2} \rho C_d A_f \omega_w^2 r_w^3 \\
T_r &= \begin{cases} m_v g C_r r_w, & 1000 \omega_w > m_v g C_r r_w \\ 1000 \omega_w, & -m_v g C_r r_w \leq 1000 \omega_w < m_v g C_r r_w \\ -m_v g C_r r_w, & 1000 \omega_w \leq -m_v g C_r r_w \end{cases} \\
T_b &= T_{b,ctrl} \\
\omega_w &= \frac{\omega_{gb,sens}}{u_f} \\
T_e &= \left(\text{ice}_{ctrl} \frac{4\eta_{e,i}}{N_{cyl} \pi S B^2} - p_{me0,f} - p_{me0,g} \right) N_{cyl} \frac{S B^2}{16} \\
p_{me0,f} &= k_1 \left(k_2 + k_3 S^2 \omega_e^2 \right) \Pi \sqrt{\frac{k_4}{B}} \\
\omega_e &= \omega_{mj} \\
\omega_{mj} &= u_{gb} \omega_{gb} \\
T_{em} &= I_{em} k_a \\
I_{em} &= \frac{\tilde{U}_{em} - \omega_{em} k_i}{R_{em}} \tag{B.2} \\
\tilde{U}_{em} &= \frac{I_b U_b}{I_{em}} \tag{B.3} \\
I_b &= \frac{1}{R_b} \left(U_{oc} - \frac{U_b}{n} \right) \\
U_{oc} &= f(\text{SoC}) \\
\text{SoC} &= \int \dot{\text{SoC}} dt \\
\dot{\text{SoC}} &= -\frac{I_b}{Q_b} \\
\omega_{em} &= u_{em} \omega_{mj} \\
U_b &= U_{b,sens,a} \\
\omega_{gb} &= \omega_{gb,sens}
\end{aligned}$$

B.4 Diagnosis system 3 - Test 5

$$\begin{aligned}
u_{gb} &= f(\text{gear}) \\
m_v &= m_{v,0} - m_{f,r} \\
m_{f,r} &= \int \dot{m}_f dt \\
\dot{m}_f &= \text{ice}_{ctrl} \frac{\omega_e}{4\pi q_{LHV}} \\
\eta_{gb} &= \begin{cases} \eta_{pos}, & T_{mj} > T_{gb,l} \\ \eta_{neg}, & T_{mj} \leq T_{gb,l} \end{cases} \\
J_{tot} &= (J_{gb} + J_{mj}) u_{gb}^2 \\
J_{gb} &= f(\text{gear}) \\
J_{mj} &= J_{em} u_{em}^2 + J_c + J_e \\
T_{mj} &= u_{em} T_{em} + T_c \\
T_c &= T_e, \text{ when clutch engaged} \\
T_d &= \frac{1}{2} \rho C_d A_f \omega_w^2 r_w^3 \\
T_r &= \begin{cases} m_v g C_r r_w, & 1000\omega_w > m_v g C_r r_w \\ 1000\omega_w, & -m_v g C_r r_w \leq 1000\omega_w < m_v g C_r r_w \\ -m_v g C_r r_w, & 1000\omega_w \leq -m_v g C_r r_w \end{cases} \\
T_b &= T_{b,ctrl} \\
\omega_w &= \frac{\omega_{gb}}{u_f} \\
T_e &= \left(\text{ice}_{ctrl} \frac{4\eta_{e,i}}{N_{cyl} \pi S B^2} - p_{me0,f} - p_{me0,g} \right) N_{cyl} \frac{S B^2}{16} \\
p_{me0,f} &= k_1 (k_2 + k_3 S^2 \omega_e^2) \Pi \sqrt{\frac{k_4}{B}} \\
\omega_e &= \omega_{mj} \\
\omega_{mj} &= u_{gb} \omega_{gb} \\
T_{em} &= I_{em} k_a \\
I_{em} &= \frac{I_b U_b}{\tilde{U}_{em}} \\
I_b &= \frac{n U_{oc} - U_b}{n R_b} \\
U_{oc} &= f(\text{SoC}) \\
\text{SoC} &= \int \dot{\text{SoC}} dt \\
\dot{\text{SoC}} &= -\frac{I_b}{Q_b} \\
\tilde{U}_{em} &= \frac{1}{\tau_{em} s + 1} U_{em} \\
U_{em} &= U_{em,ctrl} \\
U_b &= U_{b,sens,b} \\
\omega_{gb} &= \omega_{gb,sens}
\end{aligned}$$

B.5 Diagnosis system 3 - Test 6

$$\begin{aligned}
u_{gb} &= f(\text{gear}) \\
m_v &= m_{v,0} - m_{f,r} \\
m_{f,r} &= \int \dot{m}_f dt \\
\dot{m}_f &= \text{ice}_{ctrl} \frac{\omega_e}{4\pi Q_{LHV}} \\
\eta_{gb} &= \begin{cases} \eta_{pos}, & T_{mj} > T_{gb,l} \\ \eta_{neg}, & T_{mj} \leq T_{gb,l} \end{cases} \\
J_{tot} &= (J_{gb} + J_{mj}) u_{gb}^2 \\
J_{gb} &= f(\text{gear}) \\
J_{mj} &= J_{em} u_{em}^2 + J_c + J_e \\
T_{mj} &= u_{em} T_{em} + T_c \\
T_c &= T_e, \text{ when clutch engaged} \\
T_d &= \frac{1}{2} \rho C_d A_f \omega_w^2 r_w^3 \\
T_r &= \begin{cases} m_v g C_r r_w, & 1000 \omega_w > m_v g C_r r_w \\ 1000 \omega_w, & -m_v g C_r r_w \leq 1000 \omega_w < m_v g C_r r_w \\ -m_v g C_r r_w, & 1000 \omega_w \leq -m_v g C_r r_w \end{cases} \\
T_b &= T_{b,ctrl} \\
T_e &= \left(\text{ice}_{ctrl} \frac{4\eta_{e,i}}{N_{cyl} \pi S B^2} - p_{me0,f} - p_{me0,g} \right) N_{cyl} \frac{S B^2}{16} \\
p_{me0,f} &= k_1 (k_2 + k_3 S^2 \omega_e^2) \Pi \sqrt{\frac{k_4}{B}} \\
\omega_w &= \frac{\omega_{gb}}{u_f} \\
\omega_{gb} &= \frac{\omega_{mj}}{u_{gb}} \\
\omega_{mj} &= \frac{\omega_{em}}{u_{em}} \\
\omega_{em} &= \frac{\tilde{U}_{em} - I_{em} R_{em}}{k_i} \\
\omega_e &= \omega_{mj} \\
\tilde{U}_{em} &= \frac{1}{\tau_{em} s + 1} U_{em} \\
U_{em} &= U_{em,ctrl} \\
I_{em} &= \frac{U_b I_b}{\tilde{U}_{em}} \\
I_b &= \frac{n U_{oc} - U_b}{n R_b} \\
U_{oc} &= f(\text{SoC})
\end{aligned}$$

$$SoC = \int \dot{SoC} dt$$

$$\dot{SoC} = -\frac{I_b}{Q_b}$$

$$T_{em} = I_{em} k_a$$

$$U_b = U_{b,sens,b}$$